“GnRH and testosterone treatment generate GnRH neurons in the hypothalamus of adult zebrafish (*Danio rerio*)”

Tesis entregada a la

UNIVERSIDAD DE VALPARAíSO

En Cumplimiento Parcial de los requisitos para optar al grado de

Doctor en Ciencias con Mención en Neurociencia

Facultad de Ciencias

por

RICARDO ANDRÉS CERIANI FERNANDEZ

Julio, 2019

Tesis dirigida por

Dra. KATHLEEN WHITLOCK

FACULTAD DE CIENCIAS

UNIVERSIDAD DE VALPARAÍSO

INFORME DE APROBACION DE TESIS DE DOCTORADO

Se informa a la Facultad de Ciencias que la Tesis de Doctorado presentada por:

Ricardo Andrés Ceriani Fernandez

Ha sido aprobada por la comisión de Evaluación de la tesis como requisito para optar al grado de Doctor en Ciencias con mención en Neurociencia, en el examen de Defensa de Tesis rendido el 26 de julio de 2019.

Directora de Tesis

Dra. Kathleen Whitlock ……

Comisión de Tesis

Dr. Agustín Martínez (Presidente) ……

Dr. John Ewer (Evaluador interno) ……

Dra. Verónica Palma (Evaluadora Externa) ……

Funding

Este proyecto fue realizado con el siguiente financiamiento:

- Beca de doctorado Nacional otorgada por CONICYT (21130469).
- FONDECYT-1111046.
- Proyecto Instituto Milenio PO9-022-F.

A mi esposa Carmen Gloria y a mis hijos Diego y Martin

ACKNOWLEDGMENTS

Esta tesis no la pude haber realizado solo, por lo que quiero agradecer infinitamente a todos los que directa o indirectamente colaboraron para su realización. Primeramente, quiero agradecer a mi tutora Dra. Kate Whitlock, siendo un pilar fundamental en este proceso, siempre brindándome toda su ayuda y confianza.

Además, quisiera hacer un especial agradecimiento al profesor Donald Brown, ya que amablemente me facilito las instalaciones de su laboratorio para realizar mi estudio.

También quiero agradecer a mi comisión: Dra. Verónica Palma, Dr. Agustín Martínez y especialmente al Dr. John Ewer, por sus comentarios y críticas constructivas.

Quisiera agradecer a mis compañeros de laboratorio los pescadólogos y moscólogos: Cristian, Fernanda, Andrea, Eugene, Pablo, Trinidad, Angelina, Javier (grande), Javier (chico), Justin, Lily, Catalina y Valeria por su apoyo y por crear un ambiente muy agradable de trabajo.

Adicionalmente, quisiera agradecer a mis antiguos amigos del CINV: Jaime, Oscar, Carola, Cote y Carolina por su gran apoyo y risas y por todos los momentos muy agradables que hemos vivido.

Finalmente, y no menos importante quiero agradecer ampliamente a mi familia y especialmente a mi esposa Carmen Gloria por todo su apoyo y contención y a mis hijos Diego y Martin y a mi madre, ellos sin duda me fortalecen día a día.

TABLE OF CONTENTS

Index of Tables

CHAPTER 2:

CHAPTER 3:

Index of Figures

CHAPTER 2:

Abbreviations

AcLysine: Acetylated lysine.

AdH: Adenohypophysis.

Agrp1: Agouti-related peptide 1

ARN: Arcuate nuclei.

BrdU: 5-bromo-2´-deoxyuridine.

Cantd: Anterior commissure, *pars dorsalis.*

Cantv: Anterior commissure, *pars ventralis.*

chd7: chromodomain helicase DNA binding protein 7.

Ck: Cytokeratin.

DIL: Dorsal zones of periventricular hypothalamus.

DiV: Diencephalic ventricle.

E2: 17β-estradiol.

fezf2: fez Family zinc finger 2.

fgf8: Fibroblast growth factor 8.

fgfr1: Fibroblast growth factor receptor 1.

FSH: Follicle-stimulating hormone.

GAP: GnRH-associated peptide.

GFP: Green fluorescent protein.

GFAP: *Glial fibrillary acidic protein*.

GnRH: Gonadotropin-releasing hormone.

GnRH-LIR: Gonadotropin-releasing hormone like immunoreactivity.

GnRH-R: Gonadotropin-releasing hormone Receptor.

Gpr173: Orphan G protein-coupled receptor.

FSH: Follicle-stimulating hormone.

gh: growth hormone.

ghr1: growth hormone receptor 1.

ghr2: growth hormone receptor 2.

HPZ: Hypothalamic proliferating zone.

HVZ: Hypothalamic ventricular zone.

Hpf: Hour post-fertilization.

HRP: Horseradish Peroxidase.

HC: Caudal zones of periventricular hypothalamus.

IHH: Congenital idiopathic hypogonadotropic hypogonadism.

KS: Kallmann Syndrome.

Kiss: Kisspeptin.

Kiss-R: Kisspeptin receptor.

LH: luteinizing hormone.

MALDI TOF: Matrix-Assisted Laser Desorption/Ionization.

NPO: Pre-optic neurosecretory area.

NeH: Neurohypophysis.

NSC: Neural stem cell.

ON: Optic nerve.

Otp: Orthopedia transcriptor factor.

OB: Olfatory Bulb.

pacap1: pituitary adenylate cyclase-activating peptide 1.

PCNA: *Proliferating cell nuclear antigen*.

POA: Preoptic area.

prok2: prokineticin 2.

prokr2: prokineticin receptor 2.

PNX: Phoenixin.

PPa: Anterior parvocelullar preoptic nucleus.

PM: Magnocelullar nucleus.

PPp: Parvocellular nucleus posterior part.

Sox2: Sex determining region Y-box 2.

SVZ: Subventricular zone.

SC: Suprachiasmatic nucleus.

scg2: secretogranin 2

SMIM20: Small integral membrane protein 20.

TelV: Ventricle telencephalon.

tac3a: tachykinin 3a.

TeO: Tectum opticum.

Tel: Telencephalon.

TAC3: Tachykinin-3

TACR3: Tachykinin Receptor 3

Vim: Vimentin.

WT: Wild-type

SUMMARY

Gonadotropin-releasing hormone (GnRH) is an essential in the control of reproduction of vertebrates. A decrease in the secretion of GnRH causes reproductive disorders called congenital idiopathic hypogonadotropic hypogonadism (IHH), which is characterized by absence of puberty. Once diagnosed, IHH patients can be treated with reproductive hormone therapy to restore the disease. Interestingly, studies have documented a reversion of the disease after discontinuation of hormone treatment, which improves the reproductive capacities. We suggest the hormone treatment stimulate the neurogenesis of GnRH neurons in the hypothalamus in such a way to produce reversion in IHH patients. Here, we characterized the neurogenesis in the preoptic area (POA) of adult zebrafish. Our results showed that GnRH and not testosterone treatment, significantly increased the neurogenesis in the POA. In addition, results obtained by *in situ* hybridization to *gnrh3* and MALDI TOF, did not detect any GnRH isoform in the hypothalamus. Therefore, our results and recent publications show that GnRH does not affect the control of reproduction in zebrafish. In order to find a potential candidate to replace GnRH, we cloned and characterized *phoenixin*/*smim20* expression, which has a reproductive role in mammals. *phoenixin*/*smim20* is widely expressed in the brain especially in the hypothalamus of adult zebrafish.

ABSTRACT

Gonadotropin-releasing hormone (GnRH) is an essential decapeptide in the control of reproduction of vertebrates. It is secreted by GnRH neurons that reside in the preoptic area (POA) of the hypothalamus. A decrease in the secretion of GnRH causes reproductive disorders called congenital idiopathic hypogonadotropic hypogonadism (IHH), which is characterized by incomplete or absence of puberty. Once diagnosed, male IHH patients can be treated with reproductive hormone therapy like testosterone or GnRH to restore reproductive capacities. Interestingly, studies have documented a reversion of the disease after discontinuation of hormone treatment, which improves gametogenesis and the appearance of secondary sex characteristics. Therefore, here we suggest that reversion occurs due to neurogenesis of GnRH neurons in the adult hypothalamus caused by hormonal treatment. By immunofluorescence technique in paraffin sections of hypothalamus of adult zebrafish, we characterized the neurogenesis in the POA using neurogenic markers: vimentin, GFAP, Sox2 and proliferative marker: BrdU and PCNA. We identified proliferative cell positive to BrdU, PCNA and Sox2 in the wall of the POA, these cells are negative to Vimentin and GFAP. Moreover, in the neurosecretory region of the POA, we detected cytoplasmic Sox2 positive cells that also express *fezf2:gfp*, a transcription factor related to neuroendocrine cells specification. Intraperitoneal injection of GnRH or testosterone were performed in adult male zebrafish to assess the effect of hormonal treatment on neurogenesis. While the testosterone treatment showed no significant changes in the neurogenesis, GnRH

treatment increased significant the number of BrdU-labeled cells and cytoplasmic Sox2 cells.

A recent study confirmed that *gnrh1* (hypothalamic isoform) is not express in zebrafish, this suggests that GnRH3 (isoform found only in teleost fish) would replace its function in the hypothalamus. Therefore, we determine whether *gnrh3* isoform is located in the hypothalamus. By using three *gnrh3* probes previously published, we confirmed that *gnrh3* is not expressed in the POA of developing 3dpf and fertile male adult zebrafish. In addition, we used MALDI-TOFF analysis in hypothalamus of fertile adult male zebrafish and we did not identified any GnRH isoforms in the hypothalamus. Therefore, these results agree with recent publications showing that the GnRH does not control the reproduction and suggest that another mechanism independent of GnRH exists for the control of reproduction in zebrafish. In order to find a potential candidate to replace GnRH, we studied the expression of *phoenixin/smim20* in zebrafish brain, because this peptide regulate the reproduction in mammals and is highly conserved in vertebrates. Here, we described the expression of *phoenixin/smim20* in developing and adult zebrafish. In the adult brain *phoenixin/smim20* is expressed in a variety of brain structures, including the hypothalamus. Thus, these results are consistent with the potential role in regulating fertility and reproduction in zebrafish.

CHAPTER 1: INTRODUCTION

Gonadotropin-releasing hormone: Location and role.

Gonadotropin-releasing hormone (GnRH) is an essential decapeptide in the control of reproduction (reviewed in Stevenson *et al*., 2013). According to their sequence and location in the brain, at least three GnRH isoforms (GnRH 1-3) have been described in vertebrates: the hypothalamic form is GnRH1, the midbrain form is GnRH2, and the nervus terminalis–telencephalic form is GnRH3 (reviewed by Whitlock, 2005). In most vertebrates, GnRH1 is the hypophysiotropic form that controls reproduction. It is secreted by GnRH neurons that form a network of approximately 1,300 neurons that reside predominantly in the medial preoptic area (Wray and Hoffman 1986). In mammals, the GnRH neurons project their axons to the median eminence, and the peptide is mobilized to the pituitary via portal vessels. By contrast, in teleost fish, the hypothalamic GnRH neurons directly innervate the pituitary (Yamamoto *et al.,* 1998). The release of GnRH1 allows the synthesis and secretion of two gonadotropic hormones: luteinizing hormone (LH) and follicle-stimulating hormone (FSH) in the anterior pituitary. Both LH and FSH stimulate gametogenesis as well as gonadal steroid hormones production such as; testosterone in testes, and 17β-estradiol (E2) and progesterone in ovaries (rewieved in Hrabovszky and Liposits 2013).

In mammals, the secretion of GnRH from the hypothalamus starts during the late embryonic stages and continues until the early neonatal period. It becomes quiescent during childhood (Waldhauser *et al.,* 1981). Puberty is initiated by an increase in GnRH levels as well as the initiation of pulsatile release (Plant, Gay, Marshall, & Arslan, 1989; Ohkura *et al*., 2009); this process is essential for maintaining the GnRH sensitivity of the pituitary gland and is indispensable for normal reproduction.

Congenital idiopathic hypogonadotropic hypogonadism

A decrease in the secretion of GnRH causes reproductive disorders called congenital idiopathic hypogonadotropic hypogonadism (IHH), which is characterized by incomplete or absence of puberty accompanied by a low levels of gonadotropins and sex steroids hormones (Hoffman and Crowley, 1982). A specific form of IHH, associated with anosmia (loss of the sense of smell) is known as Kallmann Syndrome (KS). KS affects 1 in 8000 males and 1 in 40,000 females (rewieved in Dodé and Hardelin 2009). The patients have hypoplasia or aplasia of the olfactory bulbs and tract. Additional phenotypes include disorders such as synkinesia, eye movement abnormalities, cerebellar ataxia, evoked horizontal nystagmus, microphtalmia spatial attentional abnormalities, spastic paraplegia, mental retardation, pes cavus, unilateral renal agenesis and cleft lip and palate (rewieved in Hu *et al.*, 2003).

KS is a genetically heterogeneous disease, which is principally generated by sporadic cases (60%), although some cases exhibit three modes of familial inheritance, namely X chromosome linked, autosomal dominant, and autosomal recessive (Oliveira et al., 2001). Several genes have been implicated in KS, such as *kal1, prok2, prokr2, fgfr1 (kal2), fgf8,* and *chd7* (rewieved in Raivio et al., 2012). Mutations in *kal1, prok2, prokr2, fgfr1,* or *fgf8,* are associated with an impairment of GnRH neurons in the hypothalamus and a reduced size of the olfactory bulb (Schwanzel-Fukuda *et al*,. 1989;Dodé et al., 2003; rewieved in Dodé and Rondard 2013). Mutations in *chd7* multisystem disorders (CHARGE syndrome) that affects KS-relevant tissues such as the olfactory epithelium, hypothalamus and pituitary (Kim *et al.,* 2008). In contrast to KS, patients with normosmic idiopathic hypogonadotropic hypogonadism (nIHH) exhibit a loss of pulsatile GnRH, but have a normal sense of smell (Lisa *et al.,* 1997). This alteration is produced by mutations that affect peptides and/or ligands related with to

GnRH release (GNRH1/GNRHR, KISS1/KISS1R and TAC3/TACR3) (rewieved in Semple and Topaloglu 2010).

Hypothalamic neurogenesis

In mammals, adult neurogenesis occurs in the hippocampal dentate gyrus and the subependymal layer of the subventricular zone (reviewed in Cheng, 2013). However it is not limited to these areas of the brain since adult neurogenesis has been reported in the hypothalamus (Xu et al., 2005). Here, two neurogenic stem cell niches have been distinguished: hypothalamic ventricular zone (HVZ), located in lateral walls of the third ventricle at the level of paraventricular and arcuate nuclei and hypothalamic proliferating zone (HPZ), located in the ventral region of the third ventricle in median eminence region (Kokoeva *et al.,* 2007). These regions are composed of a specialized radial glial-like cell called tanycytes (reviewed in Rodríguez et al., 2005), which are a stem cell population (Pérez-Martín et al., 2010). Tanycytes are characterized by have a long process that projects to the brain parenchyma, including one or two apical cilia. These cells express radial glia markers such as vimentin, nestin, GFAP and Sox2 (Pellegrino et al., 2018). Tanycytes have been classified into four subtypes according to their location, morphology, and gene expression (Rodriguez 2005): α1, α2, β1 and β2. However, only α2 localized to the arcuate nuclei (ARN) has neurogenic capacity in the adult (Robins et al., 2013). The α2 tanycytes express GFAP (Robins et al., 2013), a typical marker of neural progenitors in adult neurogenesis (Garcia et al., 2004).

Reversion of IHH

Once diagnosed, male IHH and KS patients can be treated with hormone therapy (includes testosterone, GnRH and gonadotropins) to restore reproductive capacities (Raivio et al., 2007). Interestingly, studies have documented a reversion of the disease after discontinuation of hormone treatment in 14 % of the patients (Pitteloud et al., 2005; Ribeiro et al., 2007; Sidhoum et al., 2014; Raivio et al., 2007), increasing the levels of reproductive hormones, which improves gametogenesis and the appearance of secondary sex characteristics (Raivio et al., 2007; Sidhoum et al., 2014). This suggests that testosterone and GnRH could stimulate the neurogenesis of GnRH neurons in hypothalamus of adult humans. Until now, there is evidence for hypothalamic GnRH neurogenesis in ring dove (Cheng et al., 2011). Additionally, our lab has demonstrated that the hypothalamic-derived neurospheres of adult zebrafish are capable of differentiating into GnRH neurons in culture (Cortes-Campos *et al*., 2015). Furthermore, when the neurospheres were exposed to either testosterone or GnRH, the number of differentiated GnRH cells increased (Cortes-Campos *et al*., 2015). These results suggest that testosterone or GnRH can stimulate the generation of new GnRH neurons from hypothalamic neural progenitors in the adult.

It has been proposed that zebrafish is a good model to study neurogenesis and is becoming more popular to address issues of adult neural stem cell (NSC) biology and regeneration (Than-Trong and Bally-Cuif, 2015). Similar to mammals, zebrafish also exhibit proliferation zones in the hypothalamus, specifically the preoptic zone, including the ventricular zone along the ventral part of the anterior parvocellular preoptic nucleus (Grandel et al., 2006). In this thesis, we use zebrafish as an animal model to study the generation of GnRH neurons through the treatment with GnRH or testosterone, to study whether the treatment with GnRH or testosterone causes neurogenesis in the

hypothalamus as we demonstrated previously in vitro (Cortes-Campos *et al*., 2015), and thus explain the reversion in IHH patients.

REFERENCES

1. **Stevenson TJ, Hahn TP, MacDougall-Shackleton SA and BG.** Gonadotropin-releasing hormone plasticity: A comparative perspective. *Front Neuroendocr.* 2013;33(3):287–300.
2. **Whitlock KE.** Origin and development of GnRH neurons. *Trends Endocrinol. Metab.* 2005;16(4):145–51.
3. **S. Wray GH.** A developmental study of the quantitative distribution of LHRH neurons within the central nervous system of postnatal male and female rats. *J. Comp. Neurol.* 1986;531:522–531.
4. **Yamamoto N, Parhar IS, Sawai N, Oka Y, Ito H.** Preoptic gonadotropin-releasing hormone (GnRH) neurons innervate the pituitary in teleosts. *Neurosci. Res.* 1998;31(1):31–8.
5. **Hrabovszky E, Liposits Z.** Afferent Neuronal Control of Type-I Gonadotropin Releasing Hormone Neurons in the Human. *Front. Endocrinol. (Lausanne).* 2013;4(September):130.
6. **F. Waldhauser, G. Weibenbacher, H. Frisch AP.** Pulsatile Secretion of Gonadotropins in Early Infancy. *Eur. J. Pediatr.* 1981:71–74.
7. **Plant TM, Gay VL, Marshall GR, Arslan M.** Puberty in monkeys is triggered by chemical stimulation of the hypothalamus. *Proc. Natl. Acad. Sci. U. S. A.* 1989;86(7):2506–10.
8. **Ohkura S, Takase K, Matsuyama S, Mogi K, Ichimaru T, Wakabayashi Y, Uenoyama Y, Mori Y, Steiner R a, Tsukamura H, Maeda K-I, Okamura H.** Gonadotrophin-releasing hormone pulse generator activity in the hypothalamus of the goat. *J. Neuroendocrinol.* 2009;21(10):813–21.
9. **Hoffman A, Crowley W.** Induction of Puberty in Men by Long-Term Pulsatile Administration of Low-Dose Gonadotropin-Releasing Hormone. *N Engl J Med* 1982;307(20):1237–1241.
10. **Dodé C, Hardelin J-P.** Kallmann syndrome. *Eur. J. Hum. Genet.* 2009;17(2):139–46.
11. **Hu Y, Tanriverdi F, MacColl GS, Bouloux P-MG.** Kallmann's syndrome: molecular pathogenesis. *Int. J. Biochem. Cell Biol.* 2003;35(8):1157–1162.

12. **Oliveira LM, Seminara SB, Beranova M, Hayes FJ, Valkenburgh SB, Schipani E, Costa EM, Latronico a C, Crowley WF, Vallejo M.** The importance of autosomal genes in Kallmann syndrome: genotype-phenotype correlations and neuroendocrine characteristics. *J. Clin. Endocrinol. Metab.* 2001;86(4):1532–8.
13. **Raivio T, Avbelj M, McCabe MJ, Romero CJ, Dwyer A a, Tommiska J, Sykiotis GP, Gregory LC, Diaczok D, Tziaferi V, Elting MW, Padidela R, Plummer L, Martin C, Feng B, Zhang C, Zhou Q-Y, Chen H, Mohammadi M, Quinton R, Sidis Y, Radovick S, Dattani MT, Pitteloud N.** Genetic overlap in Kallmann syndrome, combined pituitary hormone deficiency, and septo-optic dysplasia. *J. Clin. Endocrinol. Metab.* 2012;97(4):E694-9.
14. **Schwanzel-Fukuda M, Bick D, Pfaff DW.** Luteinizing hormone-releasing hormone (LHRH)-expressing cells do not migrate normally in an inherited hypogonadal (Kallmann) syndrome. *Brain Res. Mol. Brain Res.* 1989;6(4):311–26.
15. **Dodé C, Levilliers J, Dupont J-M, De Paepe A, Le Dû N, Soussi-Yanicostas N, Coimbra RS, Delmaghani S, Compain-Nouaille S, Baverel F, Pêcheux C, Le Tessier D, Cruaud C, Delpech M, Speleman F, Vermeulen S, Amalfitano A, Bachelot Y, Bouchard P, Cabrol S, Carel J-C, Delemarre-van de Waal H, Goulet-Salmon B, Kottler M-L, Richard O, Sanchez-Franco F, Saura R, Young J, Petit C, Hardelin J-P.** Loss-of-function mutations in FGFR1 cause autosomal dominant Kallmann syndrome. *Nat. Genet.* 2003;33(4):463–5.
16. **Dodé C, Rondard P.** PROK2/PROKR2 Signaling and Kallmann Syndrome. *Front. Endocrinol. (Lausanne).* 2013;4(April):19.
17. **Kim H-G, Kurth I, Lan F, Meliciani I, Wenzel W, Eom SH, Kang GB, Rosenberger G, Tekin M, Ozata M, Bick DP, Sherins RJ, Walker SL, Shi Y, Gusella JF, Layman LC.** Mutations in CHD7, encoding a chromatin-remodeling protein, cause idiopathic hypogonadotropic hypogonadism and Kallmann syndrome. *Am. J. Hum. Genet.* 2008;83(4):511–9.
18. **Lisa B. N Achitigall, M.D., Paul A. Bopple, M.D., F rancois P. P Ralong, M.D., and William F. Crowley, J R . M.** Adult-onset idiopathic hypogonadotropic hypogonadism — A treatable from of male infertility. 1997.

19. **Semple RK, Topaloglu a. K.** The recent genetics of hypogonadotrophic hypogonadism - novel insights and new questions. *Clin. Endocrinol. (Oxf).* 2010;72(4):427–435.
20. **Cheng M-F.** Hypothalamic neurogenesis in the adult brain. *Front. Neuroendocrinol.* 2013;34(3):167–78.
21. **Xu Y, Tamamaki N, Noda T, Kimura K, Itokazu Y, Matsumoto N, Dezawa M, Ide C.** Neurogenesis in the ependymal layer of the adult rat 3rd ventricle. *Exp. Neurol.* 2005;192(2):251–64.
22. **Kokoeva M V, Yin H, Flier JS.** Evidence for Constitutive Neural Cell Proliferation in the Adult Murine. 2007;220(September 2006):209–220.
23. **Rodríguez EM, Blázquez JL, Pastor FE, Peláez B, Peña P, Peruzzo B, Amat P.** Hypothalamic tanycytes: a key component of brain-endocrine interaction. *Int. Rev. Cytol.* 2005;247(05):89–164.
24. **Pérez-Martín M, Cifuentes M, Grondona JM, López-Ávalos MD, Gómez-Pinedo U, García-Verdugo JM, Fernández-Llebrez P.** IGF-I stimulates neurogenesis in the hypothalamus of adult rats. *Eur. J. Neurosci.* 2010;31(9):1533–1548.
25. **Pellegrino G, Trubert C, Terrien J, Pifferi F, Leroy D, Loyens A, Migaud M, Baroncini M, Maurage C-A, Fontaine C, Prévot V, Sharif A.** A comparative study of the neural stem cell niche in the adult hypothalamus of human, mouse, rat and gray mouse lemur (Microcebus murinus). *J. Comp. Neurol.* 2018;526(9):1419–1443.
26. **Robins SC, Stewart I, McNay DE, Taylor V, Giachino C, Goetz M, Ninkovic J, Briancon N, Maratos-Flier E, Flier JS, Kokoeva M V, Placzek M.** α-Tanycytes of the adult hypothalamic third ventricle include distinct populations of FGF-responsive neural progenitors. *Nat. Commun.* 2013;4(May):2049.
27. **Garcia a DR, Doan NB, Imura T, Bush TG, Sofroniew M V.** GFAP-expressing progenitors are the principal source of constitutive neurogenesis in adult mouse forebrain. *Nat. Neurosci.* 2004;7(11):1233–41.
28. **Raivio T, Falardeau J, Dwyer A, Quinton R, Hayes FJ, Hughes V a, Cole LW, Pearce SH, Lee H, Boepple P, Crowley WF, Pitteloud N.** Reversal of idiopathic hypogonadotropic hypogonadism. *N. Engl. J. Med.* 2007;357(9):863–73.
29. **Pitteloud N, Acierno JS, Meysing AU, Dwyer AA, Hayes FJ, Crowley WF.**

Reversible kallmann syndrome, delayed puberty, and isolated anosmia occurring in a single family with a mutation in the fibroblast growth factor receptor 1 gene. *J. Clin. Endocrinol. Metab.* 2005;90(3):1317–1322.

30. **Ribeiro RS, Vieira TC, Abucham J.** Reversible Kallmann syndrome: Report of the first case with a KAL1 mutation and literature review. *Eur. J. Endocrinol.* 2007;156(3):285–290.
31. **Sidhoum VF, Chan YM, Lippincott MF, Balasubramanian R, Quinton R, Plummer L, Dwyer A, Pitteloud N, Hayes FJ, Hall JE, Martin K a., Boepple P a., Seminara SB.** Reversal and relapse of hypogonadotropic hypogonadism: Resilience and fragility of the reproductive neuroendocrine system. *J. Clin. Endocrinol. Metab.* 2014;99(3):861–870.
32. **Cheng MF, Alexander K, Zhou S, Bonder E, Chuang LS.** Newborn GnRH neurons in the adult forebrain of the ring dove. *Horm. Behav.* 2011;60(1):94–104.
33. **Cortes-Campos C, Letelier J, Ceriani R, Whitlock KE.** Zebrafish adult-derived hypothalamic neurospheres generate gonadotropin-releasing hormone (GnRH) neurons. *Biol. Open* 2015:1–10.
34. **Than-Trong E, Bally-Cuif L.** Radial glia and neural progenitors in the adult zebrafish central nervous system. *Glia* 2015;63(8):1406–1428.
35. **Grandel H, Kaslin J, Ganz J, Wenzel I, Brand M.** Neural stem cells and neurogenesis in the adult zebrafish brain: origin, proliferation dynamics, migration and cell fate. *Dev. Biol.* 2006;295(1):263–77.

CHAPTER 2: CHARACTERIZATION OF NEUROGENIC PROGENITORS IN THE HYPOTHALAMUS OF THE ADULT ZEBRAFISH

Ricardo Ceriani and Kathleen E. Whitlock

Centro Interdisciplinario de Neurociencia de Valparaíso (CINV)

Instituto de Neurociencia, Facultad de Ciencias, Universidad de Valparaíso

Pasaje Harrington 269, Valparaíso, Chile

Telephone: 56-32-299-5510

FAX: 56-32-250-8027

Centro interdisciplinario de Neurociencia de Valparaíso

Universidad de Valparaíso,

Valparaíso, Chile

Correspondence to be sent to:

Kathleen Whitlock Instituto de Neurociencia, Universidad de Valparaíso, Pasaje Harrington 269, Valparaíso, Chile, e-mail: kathleen.whitlock@uv.cl

Key words: Tanycyte, GnRH, Pre-optic area.

ABSTRACT

Recently, it has been shown in adult mammals that the hypothalamus can generate new neurons in response to metabolic changes. These findings coupled with our recent studies showing that neurospheres generated from the hypothalamus of adult zebrafish increase neurogenesis in response to exogenously applied hormones, have led us to characterize hypothalamic neurogenesis in the adult zebrafish. Here we show that the preoptic region (POA) of the adult zebrafish has specific neurogenic domains characterized by the neurogenic markers vimentin, GFAP, Sox2, and PCNA. We found Vimentin/GFAP/Sox2 positive cells in the dorsal region lining the diencephalic ventricle (DiV), and cells are positive to Sox2, *nestin* and PCNA in the ventral regions of the DiV. Moreover, in the anterior/posterior parvocellular nucleus PPa/PPp and magnocellular preoptic nucleus (MP), we detected cytoplasmic Sox2 positive cells that also express *fezf2*, a transcription factor related to neuroendocrine cells specification. Finally, we study the effect of GnRH and testosterone treatment on neurogenesis in the POA by evaluating the number of BrdU-labeling, cytoplasmic Sox2, and GnRH-like immunoreactive cells in the hypothalamus. While the testosterone treated animals showed no significant changes in the number of BrdU-labeled, cytoplasmic Sox2 positive or GnRH-like immunoreactive cells, the GnRH treated animals increased significant the number of BrdU-labeled cells, and cytoplasmic Sox2 cells; however, the number of GnRH-like immunoreactive cells showed no significant change. In summary, we demonstrated that in the POA of zebrafish, the proliferative cells do not express radial glia markers such as Vimentin and GFAP, and that GnRH treatment increases neurogenesis.

INTRODUCTION

Adult neurogenesis plays an important role in the control of brain functions allowing the generation and maturation of new neurons and their integration into neural circuits (Cameron and Mckay, 2001; Kempermann et al., 2004). In mammals, neurogenesis is not limited to the hippocampal dentate gyrus, the olfactory bulb (Kaplan and Hinds, 1977), or the subventricular zone (SVZ) (Doetsch and Alvarez-Buylla, 1996). Indeed, other regions of the mammalian brain show neurogenesis including the thalamus (Pencea et al., 2001), the cerebellum (Klein et al., 2005), the neocortex (Gould et al., 1999) and the hypothalamus (Pencea et al., 2001)(Xu et al., 2005) Kokoeva *et al.,* 2007). The ventricular zone of the hypothalamus is composed of a specialized radial glial-like cell type called tanycytes, which is located in the wall of the third ventricle, where it contact the cerebrospinal fluid (Rodríguez et al., 2005). Tanycytes can be classified into four group (α1, α2, β1and β2), according on their location, morphology and gene expression (reviewed in Yoo and Blackshaw, 2018), but only the α2 tanycytes has neurogenic capacity (Robins et al., 2013).

Because the hypothalamus is involved in basic functions such as controlling metabolism, feeding, body temperature, circadian rhythms, and reproduction (Lévy et al., 2017), the possible role of neurogenesis in the control of these processes has acquired great relevance, especially in the development of stem-cells therapies for the treatment of neurological disorders (Lindvall and Kokaia, 2006).

Gonadotropin-releasing hormone (GnRH) is a decapeptide secreted by neurons that reside in the preoptic area of the hypothalamus (S. Wray, 1986) that, is essential for the control of reproduction. An increase in the production of the GnRH at puberty stimulates gametogenesis and the synthesis and secretion of the gonadal steroid

hormones, allowing the appearance of secondary sexual characteristics (Terasawa and Fernandez, 2001). The decrease in the secretion of GnRH causes a reproductive disorder known as Hypogonadotropic Hypogonadism (HH). The clinical manifestation of HH is expressed mainly at puberty, where the patients exhibit a lack of sexual development, identified by small testes and absent virilisation in males and the lack of breast development and primary amenorrhea in females (Dodé and Hardelin 2009). Interestingly, patients with HH subjected to hormone therapy using testosterone, GnRH, or both can show a reversion of HH accompanied by a restoration of pulsatile GnRH release that is maintained after removal of hormone treatment (Raivio et al., 2007; Sidhoum et al., 2014). While the mechanism that allows the restoration of GnRH level is unknown, this result suggests that testosterone and GnRH could stimulate the neurogenesis of GnRH neurons in hypothalamus of adult humans.

Several studies have documented the effect of these hormones on the regulation of neurogenesis (Ransome and Turnley, 2008; López-Juárez et al., 2012). In the case of GnRH, it increases neurogenesis in both the hypothalamus and the hippocampus of old mice (Zhang et al., 2013). Testosterone in some case also causes neurogenesis. Indeed recent studies have shown that testosterone can increase cell proliferation in the hippocampus (Galea et al., 2013) and the subventricular zone (SVZ) of the lateral ventricle (Farinetti et al., 2015). Our lab has demonstrated that hypothalamic-derived neurospheres of adult zebrafish are capable of differentiating into GnRH neurons in culture. Furthermore, when the cultures were exposed to either testosterone or GnRH, the number of GnRH cells increased (Cortes-Campos *et al*., 2015). These results suggest that testosterone or GnRH stimulate the generation of GnRH neurons from hypothalamic neural progenitors. Nevertheless, the effect of GnRH and testosterone in the generation of new GnRH neurons has not demonstrated *in vivo*.

Zebrafish is a good model to study neurogenesis because unlike mammals, it produces new neurons along the entire rostro-caudal brain axis throughout its life (Kizil et al., 2012). Zebrafish also exhibit proliferation zones in the hypothalamus, specifically the preoptic zone, including the ventricular zone along the ventral part of the anterior parvocellular preoptic nucleus (Grandel *et al*., 2006), but this zone has not been well characterized. Moreover, the expression of GnRH in the hypothalamus of embryos of 56 hpf (Whitlock et al., 2003) and of adult (Cortes-Campos *et al*., 2015) has been described. Studies in zebrafish with morpholinos to generate knockdown of kal1a and kal1b, which are homologues of *anosmin*, a gene involved in HH in humans, decreased the number of hypothalamic GnRH cells in the developing hypothalamus (Whitlock et al., 2005). These results indicate that zebrafish is a good model to study neurogenesis of GnRH.

Here, we characterized the neurogenesis in the preoptic area (POA) by neural progenitor marker, classifying different neurogenic domains within this region. In addition, adult fish were injected with testosterone and GnRH to study the effect on the neurogenesis. Our results showed that GnRH treatment and not testosterone treatment, significantly increases the number of $BrdU^+$ cells.

MATERIALS AND METHODS

Animals

Wild-type (WT) fish of the Cornell strain (derived from Oregon AB) were raised and maintained in Whitlock laboratory and maintained in a re-circulating system (Aquatic Habitats Inc, Apopka, FL) at 28°C under a light-dark cycle of 14 and 10 hours respectively. One-2-year-old male used. All protocols and procedures employed were reviewed and approved by the Institutional Committee of Bioethics for Research with Experimental Animals, University of Valparaiso (#BA084-2016). The *fezf2*:*gfp* line was gently provided for Dr. Su Guo (Berberoglu et al., 2009).

Histochemistry

Trichromic stain in paraffin sections

Once-2 years old male zebrafish 1- 2 years old were sacrificed and heads collected. The heads were fixed in Bouin's solution for 24 h at 4°C and decalcified in 0.2 Molar EDTA solution pH 7.6 for 7 days at 4°C. The heads were then rinsed in 70% ethanol dehydrated in an increasing ethanol series until 95% ethanol, cleared in butanol and embedded in Paraplast Plus (Sigma Chemical Co., St. Louis, MO, USA). Serial sections 5 µm thick of the POA were obtained with Leica RM 2155 microtome, mounted on slides, de-paraffinized and rehydrated. Sections processed for histology were stained with a trichromic stain (Hematoxylin/Erythrosine B-Orange G/Methyl blue) (Sigma Chemical Co, USA). The sections were then dehydrated and mounted with Entellan (107961- Merck Millipore).

Immunocytochemistry in paraffin sections.

One-2 year old male zebrafish were sacrificed and heads collected and fixed in 4% PFA with 7% saturated Picric Acid for 24 h at 4°C. The heads were decalcified in 0.2 Molar EDTA solution pH 7.6 for 7 days at 4°C. Similar to the trichromic stain protocols, heads were rinsed in 70% ethanol, dehydrated, cleared and embedded in Paraplast Plus (Sigma Chemical Co., St. Louis, MO, USA). Serial sections 5 or 10 µm thick of the POA were mounted on poly-L-Lysine (Sigma) coated slides. The sections were then de-paraffinized and rehydrated. The sections were incubated in citric acid pH 6 for 30 min at 90° C to antigen retrieval. To visualize cytoplasmic Sox2, antigen retrieval was not performed.

Immunocytochemistry in cryosections

Brains processed for cryostat sectioning were collected at 10 AM and fixed in 4% paraformaldehyde (PFA 4%) for 24 h at 4°C. The heads were decalcified in 0.2 Molar EDTA solution pH 7.6 for 48 h at 4°C and embedded in 1.5% agarose/5% sucrose blocks and submerged in 30% sucrose overnight at 4 °C. Blocks were frozen at -20°C with O.C.T. Compound (Tissue Tek®). Twenty µm sections were then cut using a cryostat.

Antibodies

The following primary antibodies were used: (see Table 1). The slices were incubated in primary antibody overnight at 4°C. They were then visualized using VECTASTAIN® ABC Kit (Vector Laboratories Inc, Burlingame, CA, USA) and ImmPACT® DAB Peroxidase (HRP) Substrate (VECTOR; SK-4105) or Alexa-labeled

secondary antibodies (1:500; Invitrogen). The nuclei were stained with DAPI (1:1000; Invitrogen) or ferric hematoxylin. For the LRH13 antibody, we have recently shown that the zebrafish genome lacks the gene encoding the hypothalamic form of GnRH (GnRH1) and that hypothalamic extracts do not contain any form of GnRH protein (Whitlock et al., 2019). Thus, we refer to the GnRH immunoreactivity in the hypothalamus as GnRH-like immune reactivity (GnRH-LIR). Sections stained for BrdU were pretreated with 2 M HCl for 15 min at 37°C and washed with 1M PO4 and incubated in BrdU (see Table 1). The labeling was visualized using Alexa-labeled secondary antibodies (1:250, Invitrogen). The nuclei were stained with DAPI (1:1000; Invitrogen).

Antigen	Host	Dilution	Manufacturer	Cat. No	Immunogen organism	Reference of ab used in zebrafish
Acetylated lysine	Rabbit	1:500	Cell Signal	9441	synthetic acetylated lysine	Not identified
BrdU	Rabbit	1:500	Invitrogen	PA5-32256	BrdU conjugated to KLH	Not identified
BrdU	Rat	1:500	Abcam	Ab6326	Not available	Edelmann et al., 2013
Cytokeratin (clones AE1/AE3)	Mouse	1:500	Dako	M3515	Human	Paquette et al., 2015
GFAP	Rabbit	1:500	DAKO	Z0334	Cow	Lazzari et al., 2014
GFP	Mouse	1:500	Invitrogen	A-11120	*Aequorea victoria*	Xi et al., 2011
GnRH (LHR13)	Mouse	1:100	M.K. Park and K. Wakabayashi	Not identified	Ser^{4}-Tyr^{5} of the synthetic GnRH	Cortes-Campos et al., 2015
P-histone	Rabbit	1:300	Santa Cruz	sc8656-R	Human	Chen, 2013
PCNA	Mouse	1:100	Sigma-Aldrich	P8825	Rat	Montgomery et al., 2010
Sox2	Mouse	1:200	Abcam	ab137385	Human	Not identified
Sox2	Rabbit	1:500	Abcam	Ab97959	Human	Dirian et al., 2014
Vimentin	Chicken	1:500	Millipore	AB5733	Human	Cortes-Campos et al., 2015
Zrf1	Mouse	1:500	Abcam	ab154474	Zebrafish	Yang et al., 2017

Table 1: Primary antibody list.

In situ hybridization and immunocytochemistry

Adult male fish were decapitated, and their heads fixed in PFA 4% overnight at 4°C. The heads were decalcified in 0.2 Molar EDTA solution pH 7.6 for 48 h at 4°C, embedded in 1.5% agarose/5% sucrose blocks and submerged in 30% sucrose overnight at 4 °C. Blocks were frozen at -20°C with O.C.T. Compound (Tissue Tek®). Twenty µm sections were cut using a cryostat. *In situ* hybridization was performed as described in Thisse et al., (Thisse et al., 1993a), except that the proteinase-K step was not performed. *nestin* probes were generated using previously described sequences (Mahler and Driever, 2007):

Forward primer, 5'- GTACCAGATGCTAGAGCTGAACCACCGCCTTG-3'

Reverse primer, 5'-GCATCTGCCTCTTGATCCTCGTGCTCTCCAG-3'.

After the *in situ* hybridization, the slices were fixed in PFA for 30 min to room temperature. Mouse anti-PCNA (1:100; Sigma-Aldrich; P8825) was then applied and visualized using Tyramide signal Amplification Kit (Invitrogen; T20914).

Hormone injection and BrdU incubation

The intraperitoneal injection procedure used was modified from (Kinkel *et al*., 2010). The day before the experiment (day 0), male adult zebrafish (1-2 years old) were separated from the female. On days 1, 3 and 7 they were anesthetized with tricaine (0.168 mg/ml) (A5040 Sigma-Aldrich), immobilized using a sponge and injected intraperitoneally using a #70 Hamilton syringe 15 µL per gram of 1 µM GnRH (Sigma-Aldrich; L4897) diluted in saline solution, or 1mg/mL testosterone (Sigma-Aldrich;T1500), diluted in 30% methanol and 70% saline solutions. Controls were injected with solution used to dilute each hormone. On days 3 and 7, fish were placed in

water containing 10 mM BrdU (B5002 Sigma-Aldrich) for 15 hour at 28°C, as previously described (Mueller and Wullimann, 2002). On day 8 the fish were sacrificed for immunocytochemistry.

Microscopy

Photomicrographs with light field were taken using a Leitz-Leica DMRBE microscope equipped with a DFC290 digital camera. Fluorescent images were obtained using an Olympus BX-DSU Spinning Disc microscope (Olympus Corporation, Shinjuku-ku, Tokyo, Japan) equipped with ORCA IR2 Hamamatsu camera (Hamamatsu Photonics, Higashi-ku, Hamamatsu City, Japan) and Olympus Cell-R software (Olympus Soft Imaging Solutions, Munchen, Germany). Stack of 0.5 µm thick were collected. The images were processed using the deconvolution software AutoQuantX 2.2.2 (Media Cybernetics, Bethesda, MD, USA) and ImageJ® software (National Institute of Health, Bethesda, Maryland, USA).

Statistical analyses

Quantification of BrdU, GnRH-LIR and cytoplasmic Sox2 cells were analyzed using the Shapiro-wilk test. Normal distribution of the data was checked under every condition. Statistical significance was evaluated by paired t test. Statistical analyses and graphs were done using GraphPad Prism Version 4.0 software (GraphPad Software, San Diego, CA, USA).

RESULTS

Hypothalamic neural progenitor cells are located in the wall of third ventricle in the POA.

To characterize neural progenitor cells in the POA of the adult zebrafish, we first describe the anatomy of the POA, which in fish is defined as the region located between the medial region of the ventral telencephalon and the optic chiasm (Fig. 2.1 A, rectangle). Forty-six paraffin transverse sections of 5 um were obtained from the POA of three 3 fish, and representative sections were categorized (PPa0, PPa1, PPa2, PPa3, PPa4 and PPp5), and analyzed (Fig. 2.1, B-I). The anterior parvocellular preoptic nucleus (PPa) begins at the anterior commissure, the last one is divided into the *pars dorsalis* (Cantd) and the *pars ventralis* (Cantv) (Fig. 2.1, B-C). These nuclei are localized adjacent to the diencephalic ventricle (DiV) (Fig. 2.1, C-G). In the ventral region of the PPa4 sections, cells with fusiform nuclei were found in along the wall of the DiV (Fig. 2.1, G, boxed, arrow). Fusiform nuclei cells disappeared in the posterior parvocellular preoptic nucleus (PPp) /suprachiasmatic (SC) (Fig. 2.1, H-I) in agreement with Wulliman *et al.,* (Wullimann et al., 1996).

In order to characterize progenitor cells in the POA, we selected 5 representative transverse sections and examined the label of Vimentin (Vim), Zrf1 (homologous to GFAP) and Sox2. These markers are found in tanycytes in the hypothalamus of mammals (Robins et al., 2013). In PPa1-PPa2 section sampled from 4 fish, cells with morphology of radial glia positive for Vim/Zrf1 were found more dorsal region of the wall of the DiV (Fig. 2.2, A, B). These cells extend their processes in to the PPa (Fig. 2.2, A', B'. arrow). Additionally, we identified anti-Vim^{+}/$Zrf1^{+}$ cells in the

ventro-lateral region of the POA with long processes that extend towards the DiV (Fig. 2.2, A, B, arrowheads). Similar cells were found in PP3 section (Fig. 2.2, C, arrowhead; Fig. S. 2.2, arrow). In PPa3 sections, we found a transition zone, where the anti-Vim^{+}/$Zrf1^{+}$ cells began to disappear from the wall of the DiV (Fig. 2.2, C, C'). Moreover, a group of anti-Vim^{+}/$Zrf1^{-}$ cells found in the posterior region of the POA, also contacted the floor of the DiV, by short process (Fig 2.2 C. arrow). Although, these cells were negative for Zrf1 antibody, positive immunoreactivity to mammals GFAP antibody was observed (Fig. S.2.1, arrow). In posterior section of the POA (PPa4) the Vim/Zrf1 expression decrease in the wall of DiV (Fig. 2.2, D) and Vim^{-}/$Zrf1^{-}$ cells with fusiform nuclei located in the ventral region were observed (Fig. 2, D, D´, arrow). In PPp1, Vim^{+}/$Zrf1^{+}$ cells lining the DiV appeared in the PM and PPp except for the SC (Fig. 2.2, E, rectangle). Although these cells were similar to those described in PPa1 and PPa2 sections (Fig. 2.2, E´ arrow), in PPp1 the cells processes extended towards the lateral side of the POA (Fig. S.2.2, arrowhead).

In mammals, subsets of tanycytes also express Sox2 (Haan et al., 2013), a transcription factor essential for neural stem cells, which is consistent with the observations that tanycytes can also act as neural stem/progenitor cells, generating new neurons in the postnatal and adult hypothalamus. We observed anti-$Sox2^{+}$ cells throughout the section of the Ppa/PPp. This expression had a homogeneous distribution along the wall of the DiV (Fig. 2.2, F-J; n=3 fish). In the wall of the DiV, anti-Vim^{+} cells were positive for Sox2 (Fig. 2.2, F´, G´, H´ and J, arrow). However, the anti-Vim^{+} cells located in ventral-lateral region were negative for Sox2 (Fig. 2.2, F, G, H, arrowhead). Positive expression of Sox2 was observed in cells with fusiform nucleus (Fig. 2.2. I´, arrows). Thus, we conclude that the POA contain cells with morphology of

radial glia positive for anti-Vim, Zrf1, and Sox2 and cells with fusiform nucleus that are anti- Sox2+.

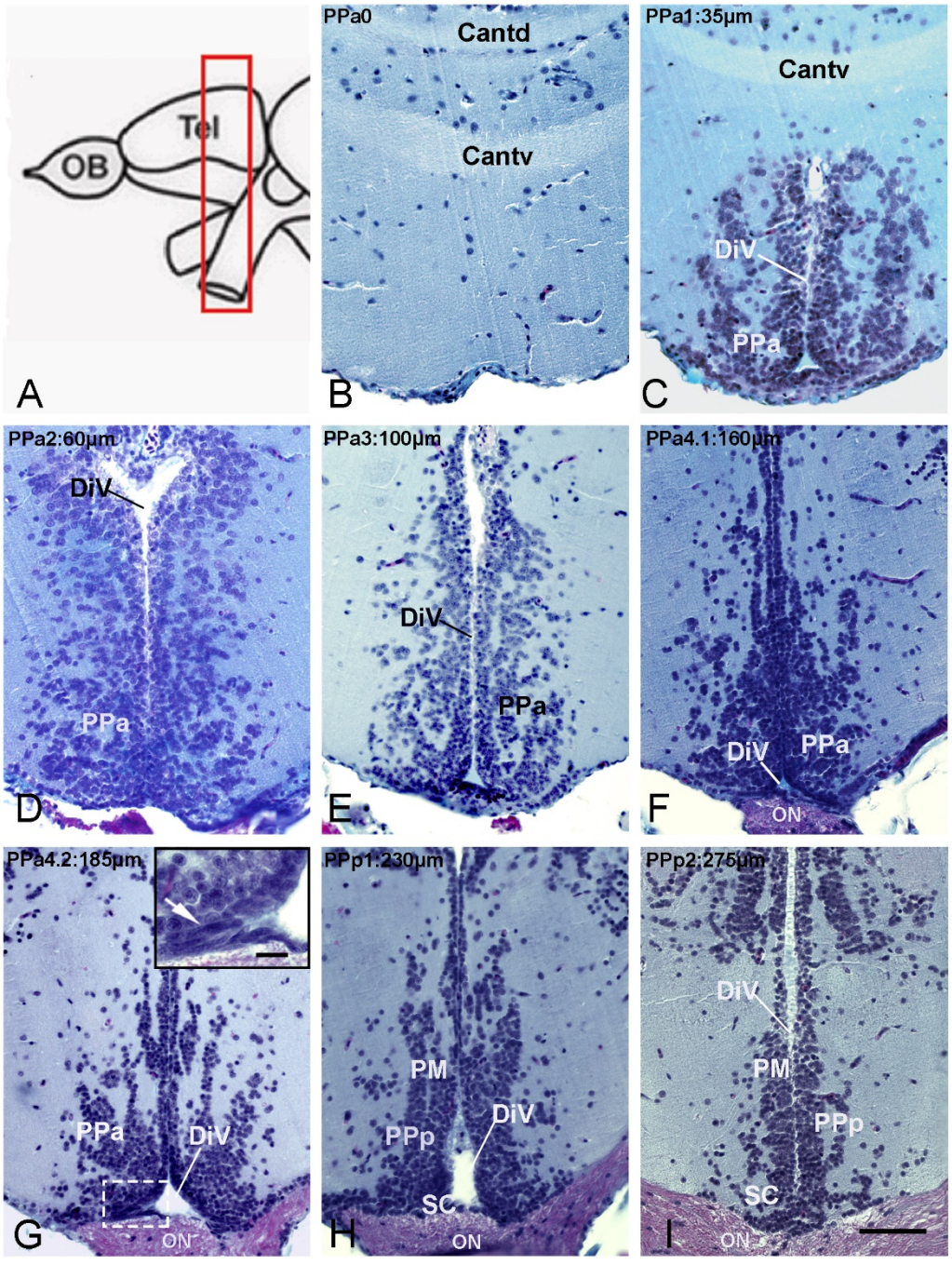
A
Tel
OB
PPa0
Cantd
Cantv
B
PPa1:35μm
Cantv
DiV
PPa
C
PPa2:60μm
DiV
PPa
D
PPa3:100μm
DiV
PPa
E
PPa4.1:160μm
DiV
PPa
ON
F
PPa4.2:185μm
PPa
DiV
ON
G
PPp1:230μm
PM
PPp
DiV
SC
ON
H
PPp2:275μm
DiV
PM
PPp
SC
ON
I

Figure 2.1. Anatomy of the preoptic area (POA) in adult zebrafish. (A) Schematic representation of zebrafish brain. Red, boxed area indicates the POA region. **(B-I)** Transverse paraffin sections of the POA stained using trichrome stain. POA region starts from the commissure anterior to the optic chiasm. Each slice corresponds to representative region of the POA, categorized with a code: PPa0, PPa1, PPa2, PPa3, PPa4, PPa5, PPp1, PPp2, where the numbers indicate the distance in μm from the beginning of the POA. **(G)** Cells with fusiform nucleus are observed in the ventral region of the PPa (arrow in boxed area). Commissure, pars dorsalis (Cantd); anterior commissure, pars ventralis (Cantv); diencephalic ventricle (DiV); anterior part of parvocellular preoptic nucleus (PPa); posterior part of parvocellular nucleus (PPp); optic nerve (ON); suprachiasmatic nucleus (SC); magnocellular nucleus (PM). Scale bar: **(F)** 50 μm, **(G)** in rectangle 10 μm.

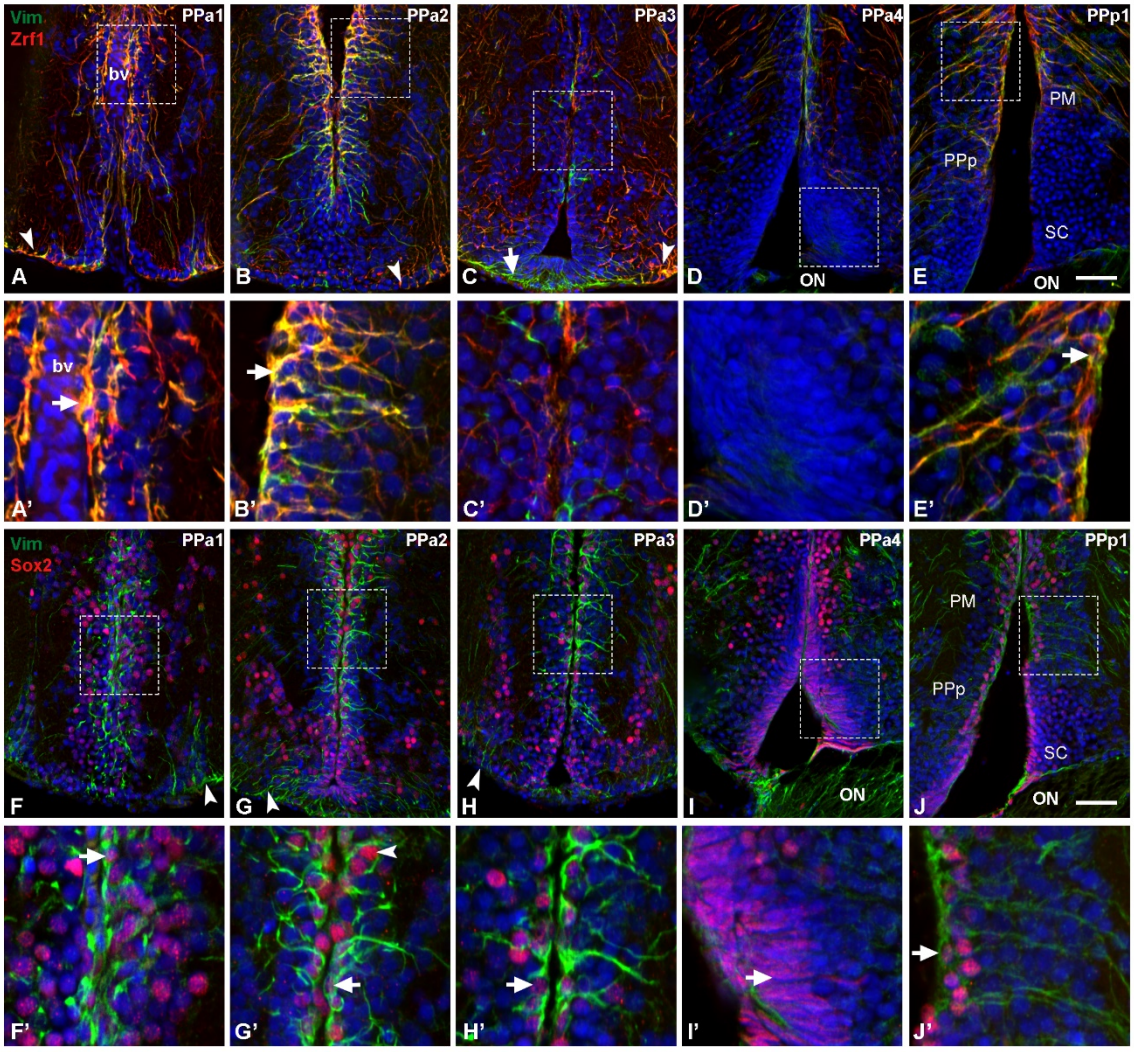
Vim
Zrf1
PPa1
bv
A
PPa2
B
PPa3
C
PPa4
D
ON
PPp1
PM
PPp
SC
E
ON
bv
A'
B'
C'
D'
E'
Vim
Sox2
PPa1
F
PPa2
G
PPa3
H
PPa4
I
ON
PPp1
PM
PPp
SC
J
ON
F'
G'
H'
I'
J'

Figure 2.2. Cells lining the diencephalic ventricle (DiV) express neural progenitor markers. **(A-J)** Expression of anti-Vim, Zrf1 and Sox2 in transverse paraffin-sections of 10 µm of the POA. **(A-E)** Cells are immuno-positive for Vim and Zrf1. **(A, B)** Anti-Vim/Zrf1 positive cells (green, red respectively) are distributed dorso-medially in the wall of the third ventricle (boxed area). However, cells distributed in the ventral region lining the DiV are negative for anti-Vim/Zrf1. **(A', B')** higher magnification views of boxed areas in A and, B, respectively, show co-localization of these signals (arrows). **(A, B, C)** Anti-Vim/Zrf1 cells located in the ventro-lateral region with long processes that extend towards the DiV (arrowheads). **(C)** Anti-Vim/Zrf1 cells beginning to disappear (box area. (**C**') Higher magnification views of boxed area of C. In **(C)** Anti-Vim/Zrf1-negative cells are distributed in the ventral region (arrow). **(D)** Cells with fusiform nucleus are negative for Vim/Zrf1 in the ventral region. **(F')** Higher magnification views of box area in D. **(E)** Anti-Vim/Zrf1 cells appear in the dorso-medial region (boxed area). **(E')** Higher magnification views of boxed area in E, shows the co-localization (arrow). **(F-J)** Cells are immune-positive for Vim and Sox2. **(F-H)** Anti-Vim positive cells also label with anti-Sox2 (red) (boxed area) and anti-Sox2 labeling extends along the dorsal ventral regions of the wall of the DiV. **(F'-H').** Higher magnification views of box areas in F-H show co-localization of Vim and Sox2 in the same cell (arrows). **(F-H)** Vim positive cells located in the ventro-lateral region are negative for Sox2 (arrowheads). **(I)** Cells with fusiform nuclei are positive for Sox2 (boxed area). **(I')** Higher magnification views of boxed area in I, shows nuclei positive for Sox2. **(J)** Anti-Vim positive cells label with anti-Sox2 (boxed area). **(J')** High magnification of boxed area I, show anti-Vim cells positive for anti-Sox2 (arrow). Blood vessels (bv); diencephalic ventricle (DiV); magnocellular nucleus (PM); optic nerve (ON); anterior part of parvocellular preoptic

nucleus (PPa); posterior part parvocellular nucleus (PPp); suprachiasmatic nucleus (SC). All sections were labeled with DAPI (blue). Scale bar: 30 μm.

Ependymal cells are located in the floor of the DiV.

To continue with the description of the progenitor cells, we wanted to study the expression of ependymal cells in the POA. These cells form an integral part of the stem cell niche (Mirzadeh et al., 2008). Although studies have shown expression of Cytokeratin in ependymal cells in the brain of adult mammals (Franko et al., 1987; Kasper et al., 1987), other studies have shown that ependymal cells express cytokeratin in embryonic stages and that this expression is reduced in the adult (Kasper et al., 1991). However, the cytokeratin labeling has been shown in the adult fish brain (Giordano et al., 1990). Therefore, cytokeratin could be a good candidate marker to identify ependymal cells in the POA of adult zebrafish. To determine the localization of ependymal cells, cytokeratin antibody was used as a potential ependymal cell marker in brain cross sections. We found immunoreactivity to cytokeratin in cells located in the saccus dorsalis (S. 2.4, arrow; 3 fish) a structure homologous to the mammalian choroid plexus of the DiV, and in cells lining the ventricle telencephalon (TelV) of the dorsal telencephalon (S.2.4, arrowhead). In both structures the anti-cytokeratin labeling of ependymal cells in adult zebrafish has been described (Lindsey et al., 2012; Henson et al., 2014). Moreover, we identified anti-cytokeratin positive cells in PPa3 sections, located adjacent to the floor of the DiV and in the ventral region of the POA (Fig. 2.3 A, arrow, arrowhead respectively; 3 fish). These cells had radial glia morphology with processes extending along the floor the ventricle (Fig. 2.3, A' arrows), being different from the typically ependymal cells shape observed in mammals. To examine whether the cytokeratin positive cells were positive for Vimentin, anti-Vim and anti-Cytokeratin antibody were used. A partial co-localization between anti-Vim and anti-Cytokeratin labeling was observed (Fig. 3. B, B´, B´´, arrow). This result indicates that the

ependymal cells have a different distribution in the DiV than what has been observed the mammals.

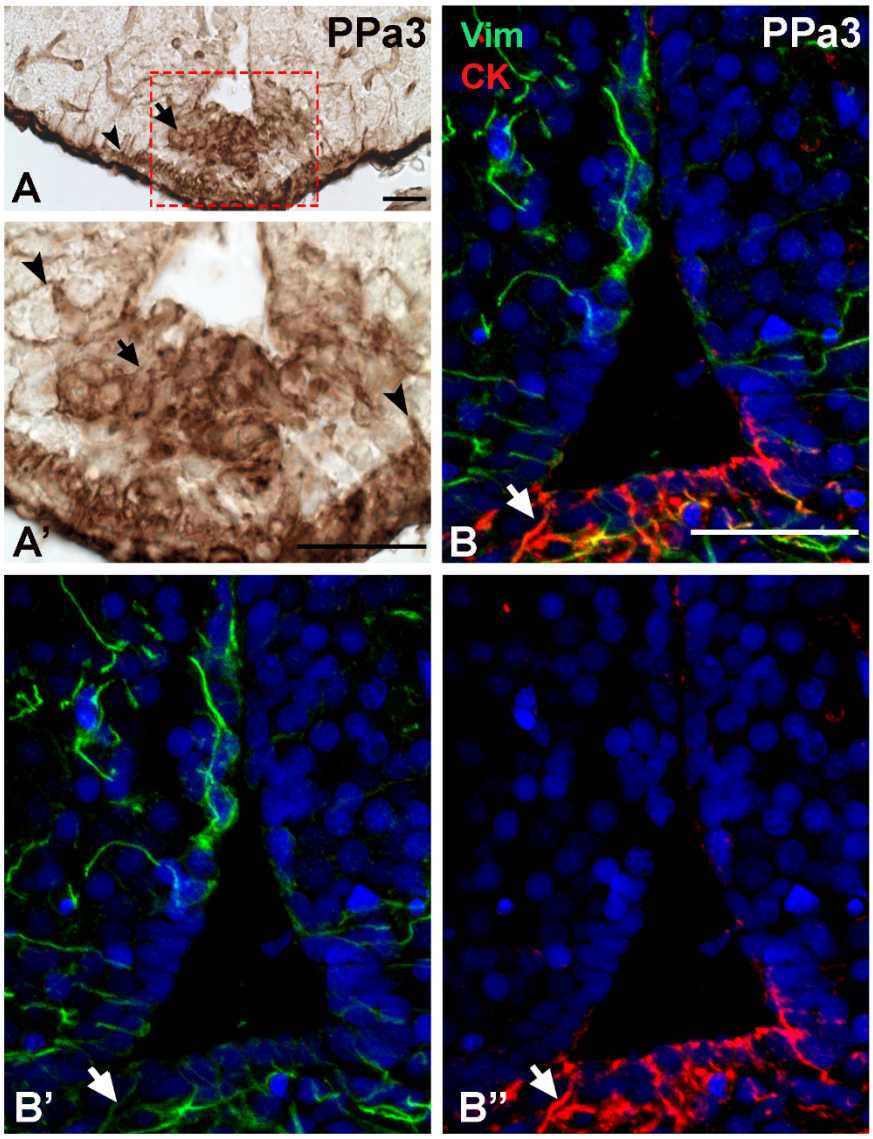

Figure 2.3. Cytokeratin positive cells are located in the ventral region lining the third ventricle. **(A-B)** Transverse paraffin-sections of 5 μm of POA **(A)** Anti-Cytokeratin (CK) labeling (brown) was observed in along the floor of the diencephalic ventricle (DiV) and in the ventral region of the POA (box area, arrow, arrowhead). **(A')** Higher magnification view of boxed area in A shows a group of anti-Cyto positive cells lining the floor of DiV (arrow) and processes extending along the DiV from cells located in the ventral region of the POA (arrowhead). **(B-B'')** Confocal image of processes of anti-Cyto-positive cells (red) and Vim (green) that showing partial co-localization (arrow). **(B´)**. Cytokeratin (red). **(B´´)** Vimentin (green). Diencephalic ventricle (DiV). Sections were also labeled with DAPI labeling (blue). Scale bar: 30μm.

Cytoplasmic Sox2 cells express *fezf2*:GFP in ventral region of the POA.

Previously, we described a group of HuC positive neurons with cytoplasmic Sox2 label in the parvocellular nuclei (Cortes-Campos et al., 2015). Using the Sox2 antibody we identified Sox2 positive cells with large nuclei and labeling in the cytoplasm (diameter: 6.41±1.2 μm) adjacent to the DiV located in PPp1 sections (Fig. 2.4, A) (6 fish). Because PPp1 correspond to the neurosecretory preoptic area (NPO), we believe that cytoplasmic Sox2 cells may have a neuroendocrine function. For this reason, we wanted to determine whether the cytoplasmic Sox2 positive cells expressed the transcription factor forebrain embryonic zinc finger (Fez) since it plays a role in neuroendocrine cells specification. In zebrafish, Fezf2 regulates the Orthopedia transcriptor factor (Otp) (Blechman et al., 2007), a transcription factor essential for neuroendocrine cells specification (Fernandes et al., 2013). To study whether cytoplasmic Sox2 cells co-localized with Fezf2:GFP, we used Sox2 antibody in the *fezf2:gfp* transgenic line (3 fish) (Berberoglu et al., 2009). In PPp1 sections, GFP antibody revealed with DAB, identified two types of cells positive to GFP: big cells with low expression and small cells with high expression of GFP (S. 2.5, arrows, arrowheads respectively). We determined that the cytoplasm of the large cells positive for Fezf2:GFP (Fig 2.4 B, arrowheads) also labeled with anti-Sox2 (Fig. 2.4, C, arrowhead). By contrast, the small cells with high expression of GFP were negative for cytoplasmic anti-Sox2 labeling (Fig. 2.4 A, B, C, arrow). Similar results were obtained using confocal microscopy (Fig. 2.4, D-F). These results suggest that cytoplasmic Sox2 is found in a group of endocrine cells location in the NPO.

While Sox2 is located in the nucleus, during the differentiation of embryonic stem cells, it later is acetylated in a lysine residue and becomes localized to the

cytoplasm, where it is degraded (Baltus et al., 2009). To study whether the cytoplasmic location of Sox2 is due to such acetylation process, we used an antibody against acetylated lysine (AcLysine) on PPp1 cryosections. We only we observed anti-AcLysine labeling in the nucleus (Fig. 2.4 G, arrow). Similar labeling with anti-AcLysine was observed in section treated with Sox2 antibody, yet, the anti-Sox2 signal did not co-localize with anti-AcLysine in the cytoplasm (Fig. 2.4 h, I, arrow). These results demonstrated that cytoplasmic labeling with Sox2 is independent of its acetylation status.

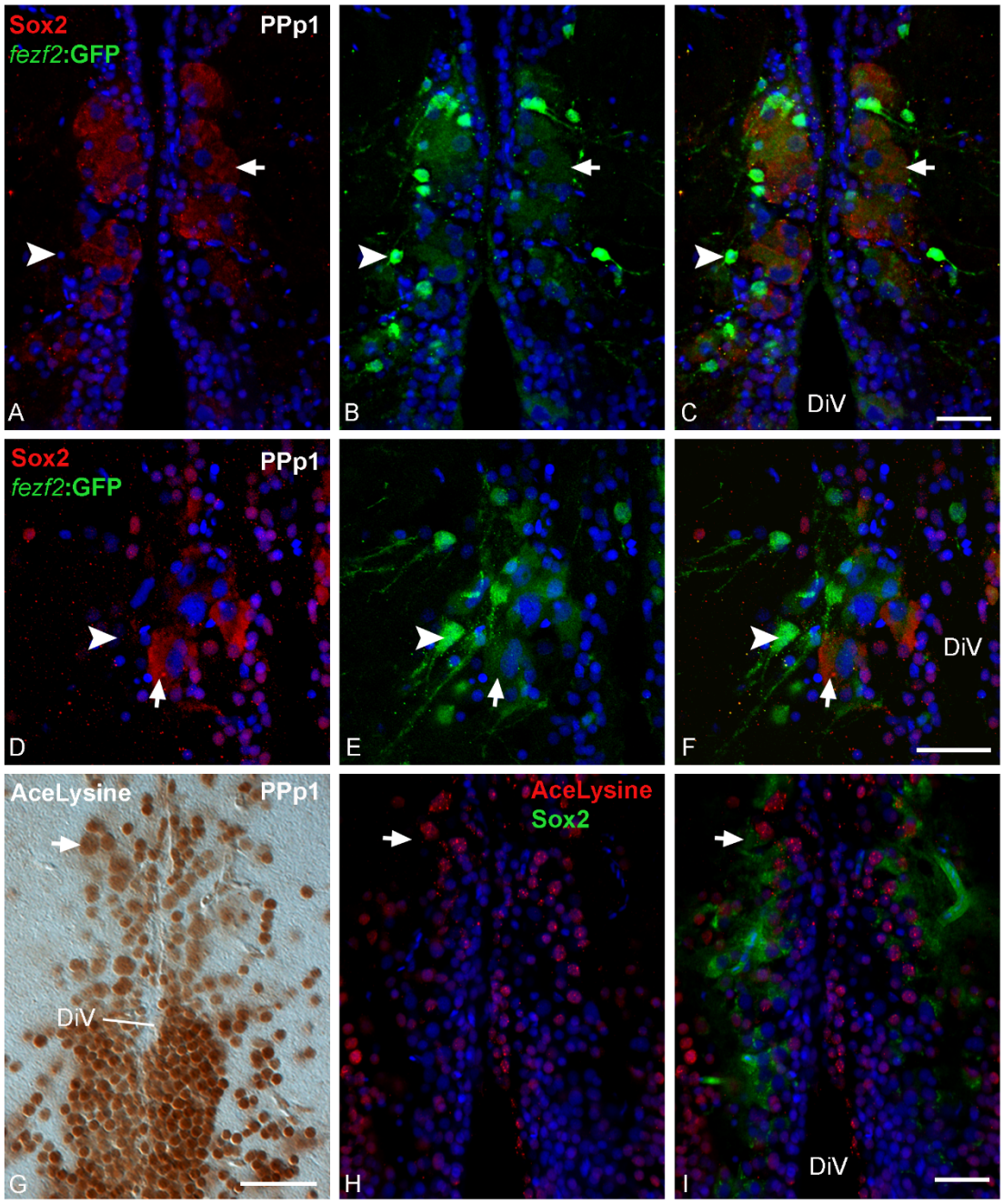
Sox2
fezf2:GFP
PPp1
A
B
C
DiV
Sox2
fezf2:GFP
PPp1
D
E
F
DiV
AceLysine
PPp1
DiV
G
AceLysine
Sox2
H
I
DiV

Figure 2.4. Cytoplasmic Sox2 cells co-localize with Fezf2:GFP. (A-I) Transverse cryosections of 20 µm of PPp1. **(A-C)** Larger cytoplasmic Sox2-positive cells express Fezf2:GFP (arrow), whereas, smaller ones are negative for Fezf2:GFP (arrowheads). **(A)** Anti-Sox2 labeling. **(B)** Fezf2:GFP expression. **(C)** Merge image. **(D-F)** Confocal images confirm that cytoplasmic cells express Fezf2:GFP (arrow), Fezf2:GFP cells negative for anti-sox2 (arrowheads). **(D)** Sox2. **(E)** Anti-GFP in Fezf2:GFP. **(C)** Merge showing nuclear labeling with anti-acetylated lysine (AcLysine) (brown, arrow). **(H, I)** AcLysine (red) do not co-localized with cytoplasmic anti-Sox2 labeling (green). **(H)** Anti-AcLysine labeling (red, arrow). **(I)** Anti-AcLysine labeling (red) and anti-Sox2 (green, arrow). **(A, B, C, D, F, H, I)**. Sections were labeled with DAPI (blue). Diencephalic ventricle (DiV). Scale bar: 30µm.

Description of proliferative cells in the POA.

It is well known that fish generate neurons throughout life (Kizil et al., 2012). However, the neurogenic potential of the hypothalamus is still not completely described in adult zebrafish. In order to describe the proliferative cells in the POA, we used the proliferating cell nuclear antigen PCNA (Fig. 2.5, A-E, I-J; 3 fish). Usually, we observed expression of PCNA in cells lining the DiV in almost all sections section; however, these cells were negative for anti-Vim labeling (Fig. 2.5, A-E, arrow). Nevertheless, about 62% of anti-PCNA^{+} cells were located in PPa4 sections (Fig. 2.5. D, rectangle) (Fig 2.6), including cells with fusiform nuclei (Fig. 2.5. F-H arrowhead). In addition, we used the Sox2 antibody to determine whether the anti-Sox2 positive cells had a proliferative capacity. We observed PCNA^{+}/Sox2^{+} cells in all section (Fig. 2.5, I-M, arrow). Similar to what was observed previously (see Fig. 2.5, A-E, arrow), PCNA expression was greatest in the ventral region of the PPa4 (Fig. 2.5, I-M, arrow), but, we found that all PCNA positive cells were anti-Sox2 positive, including the cells with fusiform nuclei (Fig. 2.5, rectangle, N-P, arrowhead). Therefore, these results indicate that the proliferative cells are located mainly in the PPa4 section and label with anti-Sox2.

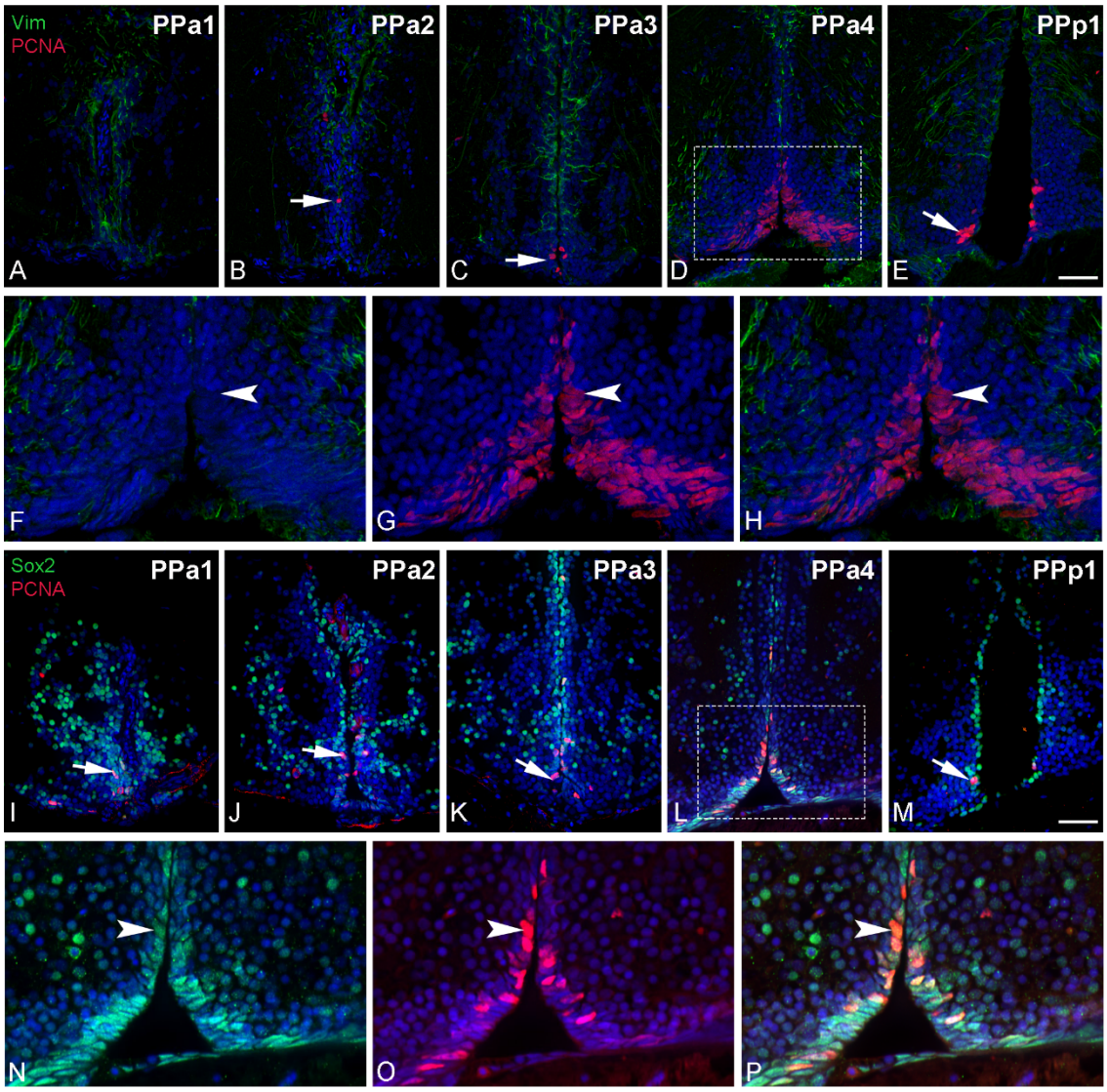
Vim
PCNA
PPa1
PPa2
PPa3
PPa4
PPp1
A
B
C
D
E
F
G
H
Sox2
PCNA
PPa1
PPa2
PPa3
PPa4
PPp1
I
J
K
L
M
N
O
P

Figure 2.5. Proliferating cell nuclear antigen (PCNA) is located primarily in the PPa4/PPp1 transition region. (A-P) Transverse paraffin-sections of 5 μm were obtain of the POA. **(A-E)** Anti-Vim labeling (green) in localized to the dorsal region of the POA in contrast anti-PCNA positive cells (red, arrow B, C, E) are found in the ventral of the POA. **(F-H)** Higher magnification view of boxed area in D. Anti-Vim labeling (F, H, green) does not co-localize with anti-PCNA labeling (G, H, red). **(H)** Merge. **(I-M)** Anti-Sox2 labeling (green) and anti-PCNA labeling colocalize in the ventral PPa4/PPp1 region of the POA (red). **(N-P)** Higher magnification view of boxed area in L. Anti-PCNA positive cells and anti-Sox2 positive cells (green, arrow) in the ventral PPa4. All sections were labeled with DAPI labeling (blue). Scale bar: 30μm.

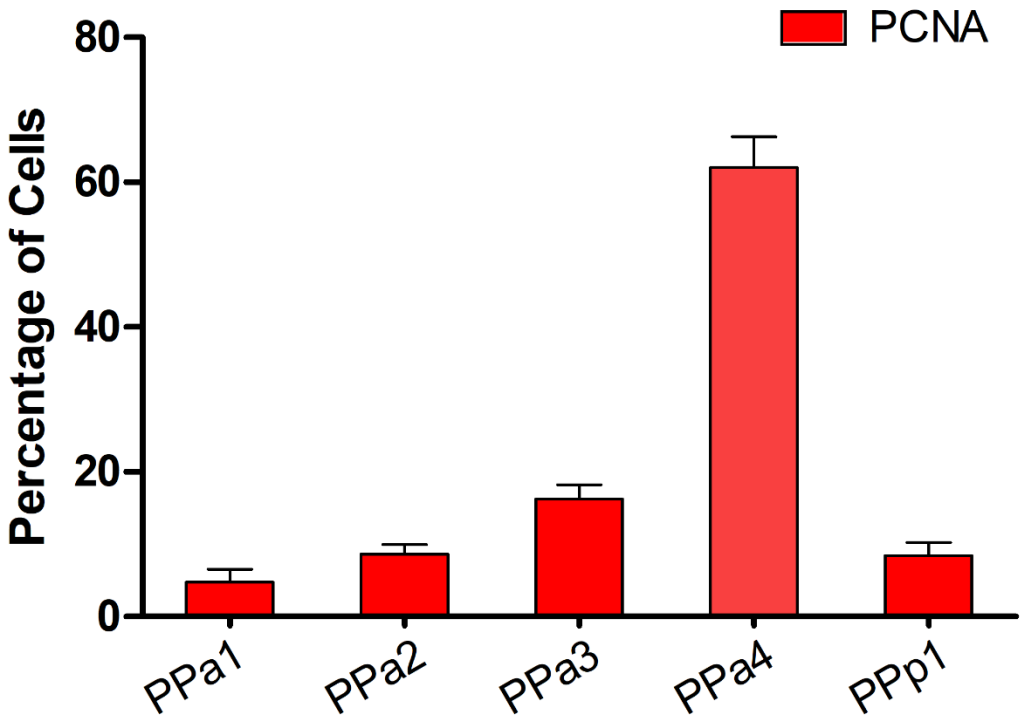

Figure 2.6. Quantification of the distribution of anti-PCNA positive cells in the POA. Percentage of anti-PCNA positive cells located in representative sections of the POA (PPa1, PPa2, PPa3, PPa4 and PPp1). For each representative section of the POA, a number of transverse paraffin sections (PPa1 = 4, PPa2 = 8, PPa3 = 10, PPa4 = 14 and PPp1 = 4) of 5 µm were obtained and the anti-PCNA positive cells were counted.

In the adult brain mammals neural progenitor cells have been described that the express GFAP (Garcia et al., 2004). To check whether the proliferative cells express GFAP in the POA of zebrafish, we performed an immunofluorescence using PCNA and GFAP antibodies and quantified the number of anti-PCNA^{+}/GFAP^{+} cells (3 fish). Of the total number of labeled cells, we determined that 40.8% of the cells were anti-PCNA^{+}/GFAP^{-} (Fig. 2.7, A-E. green. G) and 57.6% were anti-PCNA^{-}/GFAP^{+} (Fig. 2.7, A-E red, G). We observed a low proportion (1,6%) of the anti-PCNA^{+}/GFAP^{+} cells (Fig. 2.7, A, F, magnification image of boxed, arrow, G), which cells were distributed in PPa1, PPa2 and PPp1 (Fig. 2.7, H). This result was also observed in adult fish exposed to two pulses of BrdU on days 1 and 7 (3 fish per condition). About 74% of the total labeled cells were anti-BrdU^{+}/Zrf1^{-} (GFAP) (Fig. 2.8, A-E. green, G), 23% express anti-BrdU^{-}/Zrf1^{+} (Fig. 2.8, A-E, red, G) and only 3% were anti-BrdU^{+}/Zrf1^{+} (Fig. 2.8, A-E, magnification image of boxed, arrows, G), and were located in the PPa1, PPa2 and PPp1 (Fig. 2.8, H). These results suggest that the proliferative cells mostly do not express GFAP, a finding a different from what is observed in mammals.

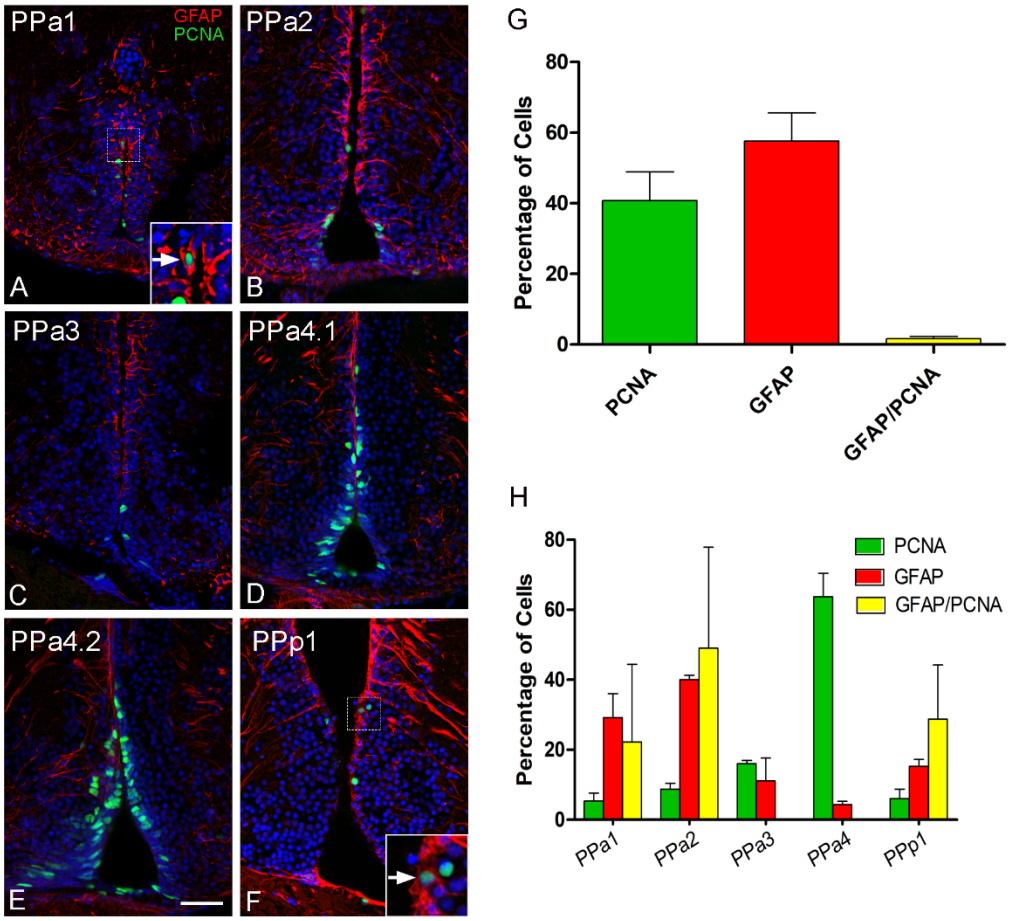
PPa1
GFAP
PCNA
A
PPa2
B
PPa3
C
PPa4.1
D
PPa4.2
E
PPp1
F
G
Percentage of Cells
80
60
40
20
0
PCNA
GFAP
GFAP/PCNA
H
Percentage of Cells
80
60
40
20
0
PCNA
GFAP
GFAP/PCNA
PPa1
PPa2
PPa3
PPa4
PPp1

Figure 2.7. The majority of anti-GFAP positive cells are non-proliferative. (A-F) PCNA/GFAP double immunofluorescence in transverse paraffin-section of 5 μm. Anti-GFAP positive tanycytes (red), generally do not co-localize with anti-PCNA (green), but a low number anti-GFAP positive cells are positive for PCNA (**A**, **F**, magnified image of boxed, arrow). All sections were labeled with DAPI labeling (blue). Scale bar: 30μm. **(G)** Percentage of anti-$PCNA^+$, anti-$GFAP^+$ and anti-$GFAP^+$/$PCNA^+$ cells distributed in the wall of the DiV of the POA. The cell count obtained of the total immunolabeling cells of the POA. Transverse paraffin-section of 5 μm were obtained from all POA. The graph shows the low percentage of anti-$GFAP^+$/$PCNA^+$ cells (yellow) compared to anti-$PCNA^+$ (green) and anti-$GFAP^+$ (red) cells. **(H)** Percentage of anti-$PCNA^+$, anti-$GFAP^+$ and anti-$GFAP^+$/$PCNA^+$ cells located in representative sections of the POA (PPa1, PPa2, PPa3, PPa4 and PPp1). The cells were counted from the total immunolabeling cells distributed along the wall of the DiV of the POA. For each representative section of the POA, a number of transverse paraffin section (PPa = 5, PPa2 = 6, PPa3 = 12, PPa4 = 14 and PPp1 = 4) of 5 μm were obtained and the anti-$PCNA^+$, anti-$GFAP^+$ and anti-$GFAP^+$/$PCNA^+$ cells were counted. Anti-$GFAP^+$/$PCNA^+$ cells (yellow) were distributed mainly in PPa1, PPa2 and PPp1 sections.

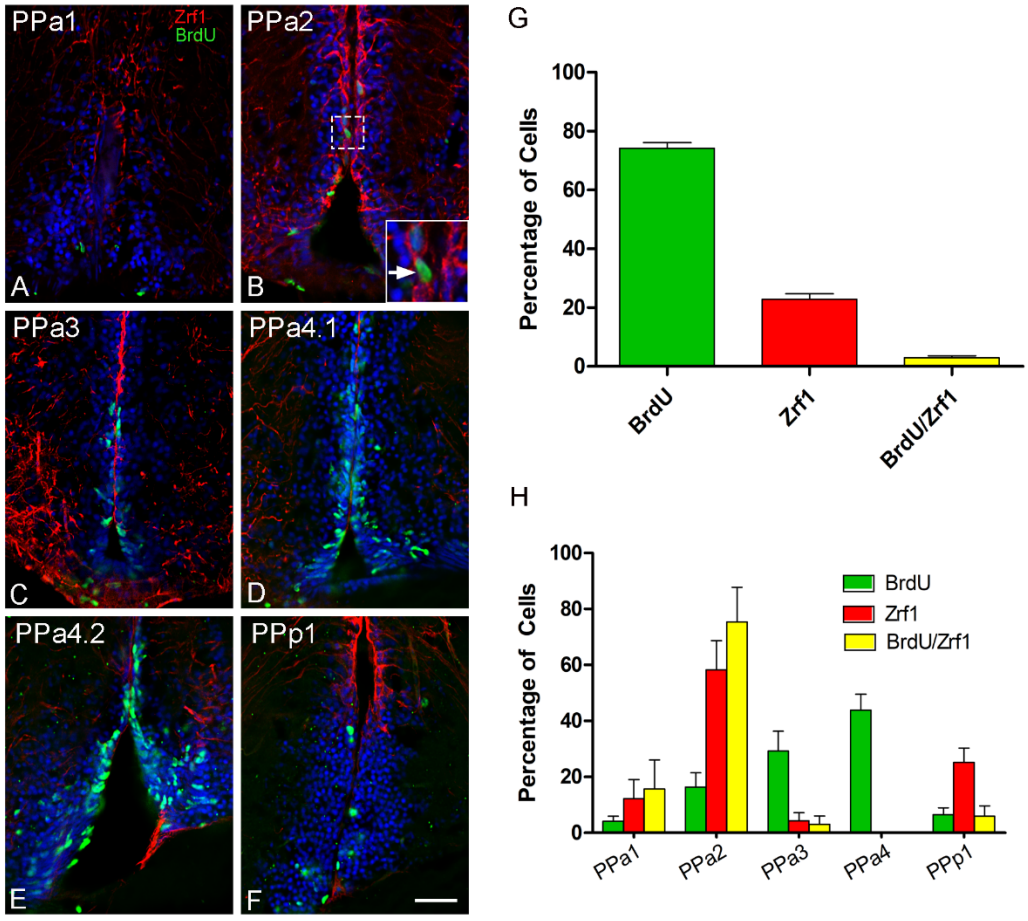
PPa1
Zrf1
BrdU
A
PPa2
B
PPa3
C
PPa4.1
D
PPa4.2
E
PPp1
F
G
Percentage of Cells
100
80
60
40
20
0
BrdU
Zrf1
BrdU/Zrf1
H
Percentage of Cells
BrdU
Zrf1
BrdU/Zrf1
PPa1
PPa2
PPa3
PPa4
PPp1

Figure 2.8. The majority of anti-Zrf1 positive cells are do not incorporate BrdU. (A-F) BrdU/Zrf1 double immunofluorescence in transverse cryosection of 20 µm. Treatment with two pulses of BrdU at 1 and 7 days, and the brains were fixed at 8 days. Anti-Zrf1 positive tanycytes (red), generally do not express BrdU (green), but a low number of anti-Zrf1 positive cells are positive for BrdU (**A**, **F**, magnified image of boxed, arrow). All sections were labeled with DAPI labeling (blue). Scale bar: 30µm. **(G)** Percentage of anti-$BrdU^+$, anti-$Zrf1^+$ and anti-$Zrf1^+$/$BrdU^+$ cells distributed in the wall of the DiV of the POA. The cell count was obtained of the total immunolabeling cells of the POA. Transverse cryosection of 20 µm were obtained from all POA. The graph shows the low percentage of anti-$Zrf1^+$/$BrdU^+$ cells (yellow) compared to anti-$BrdU^+$ (green) and anti-$Zrf1^+$ (red) cells. **(H)** Percentage of anti-$BrdU^+$, anti-$Zrf1^+$ and anti-$BrdU^+$/$zrf1^+$ cells located in representative sections of the POA (PPa1, PPa2, PPa3, PPa4 and PPp1). The cells were counted from the total immunolabeling cells distributed along the wall of the DiV of the POA. For each representative region of the POA, a number of transverse cryosections (PPa1 = 2, PPa2 = 2, PPa3 = 2, PPa4 = 3 and PPp1 = 2) of 20 µm were obtained and the anti-$BrdU^+$, anti-$Zrf1^+$ and anti-$Zrf1^+$/$BrdU^+$ cells were counted. Anti-$GFAP^+$/$PCNA^+$ cells (yellow) were distributed mainly in PPa2 section

Because GFAP are not neural progenitor marker in the POA of adult zebrafish, we studied the expression of *nestin* in proliferative regions of the POA, because, *nestin* has been identified in proliferative domain of the telencephalon (Ganz et al., 2010). By *in situ* hybridization, we identified the *nestin* transcript in cells located in the wall of the DiV in PPa4 sections (Fig. 2.9, D purple), *nestin* expression also was found in cells with fusiform nucleus (Fig. 2.9, D, purple). However, *nestin* transcripts were not observed in the other sections (Fig. 2.9, A, B, C, E). To determine whether the *nestin* positive cells are proliferative, we used PCNA antibody in combination with *nestin* labeling, and found PCNA^{+}/*nestin*$^{+}$ cells in the PPa4 section (Fig. 2.9, D). However, we identified PCNA^{+}/*nestin*$^{-}$ cells located in the PPa1, PPa2, PPa3 and PPp1 section (Fig. 2.9, A, B, C, E). Thus, our result suggests that in the POA there exist two proliferative cell populations the proliferative cells.

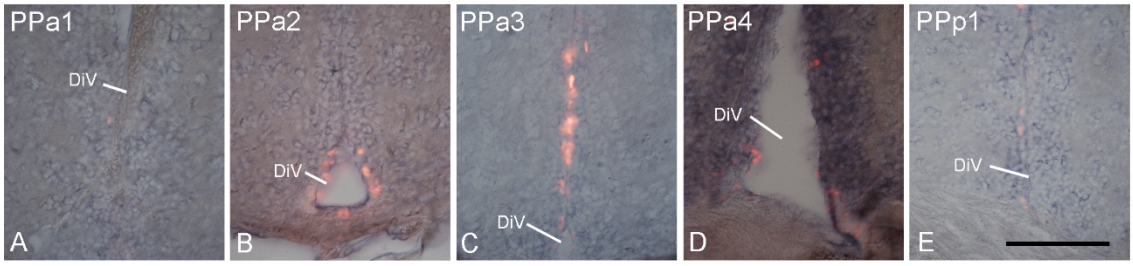

Figure 2.9. Proliferative cells located in the PPa4 region express *nestin*. (A-E) Double labeling with *nestin* probe and anti-PCNA antibody in transverse cryosection of 20 µm. **(A, B,C, E)** Anti-PCNA positive cells (red) are observed in the wall of the DiV and are negative for *nestin*. **(D)** *nestin* positive cells lie adjacent to the DiV (blue). A small population of PCNA positive cells (red) are *nestin* positive (arrowhead, arrow). Diencephalic ventricle (DiV). Scale bar: 30µm.

In addition, we determined whether neurogenesis occurs within 8 days in the POA. To test this, fish were treated with one pulse of BrdU and other group of fish was treated with two pulses of BrdU at days 1 and 7. The presence of proliferative cells was checked by BrdU/PCNA double immunofluorescence. In fish treated with one pulse (3 fish), about 41% of the cells labeled PCNA (Fig. 2.10, A-E, red, K), 58% were positive for anti-BrdU/PCNA (Fig. 2.10, A-E, yellow, K), but only 1% of cells only labeled BrdU (Fig. 2.10, A-E green, K). This labeling pattern was similar in all section (Fig. 2.10, L). When the fish were treated with two pulses of BrdU (3 fish), close to 31% of cells only were positive to anti-PCNA (Fig. 2.10, F-G, red, M), 44% positive to anti-BrdU/PCNA (Fig. 2.10, F-G, yellow. M) and 25% of cells were exclusively positive to anti-BrdU (Fig. 2.10, F-G, red, M). This increase in anti-BrdU positive cells was observed in all sections (Fig. 2.10, N). According to this result, we suggest that the POA generates new cells at 7 days.

Previously, we demonstrated proliferative cells in S, G1 and G2-phase lining the DiV in the POA using BrdU and PCNA antibodies. Thus, also we wanted to study the distribution of cells in mitotic-phase using the phospho-histone H3 antibody (pH3). The use of this mitotic-phase marker revealed that mitosis occurred in the nucleus adjacent to the DIV through the POA (Fig. 2.11, arrow). However, a reduced number of anti-pH3 positive cells that were negative for Zrf1 were localized along the lining of the ventricle in PPa3 and PPa4 (Fig. 2.11, arrowheads) in comparison with the PCNA and BrdU positive cells. Therefore, low proliferative cells in mitotic stages are in the wall of the DiV in the POA.

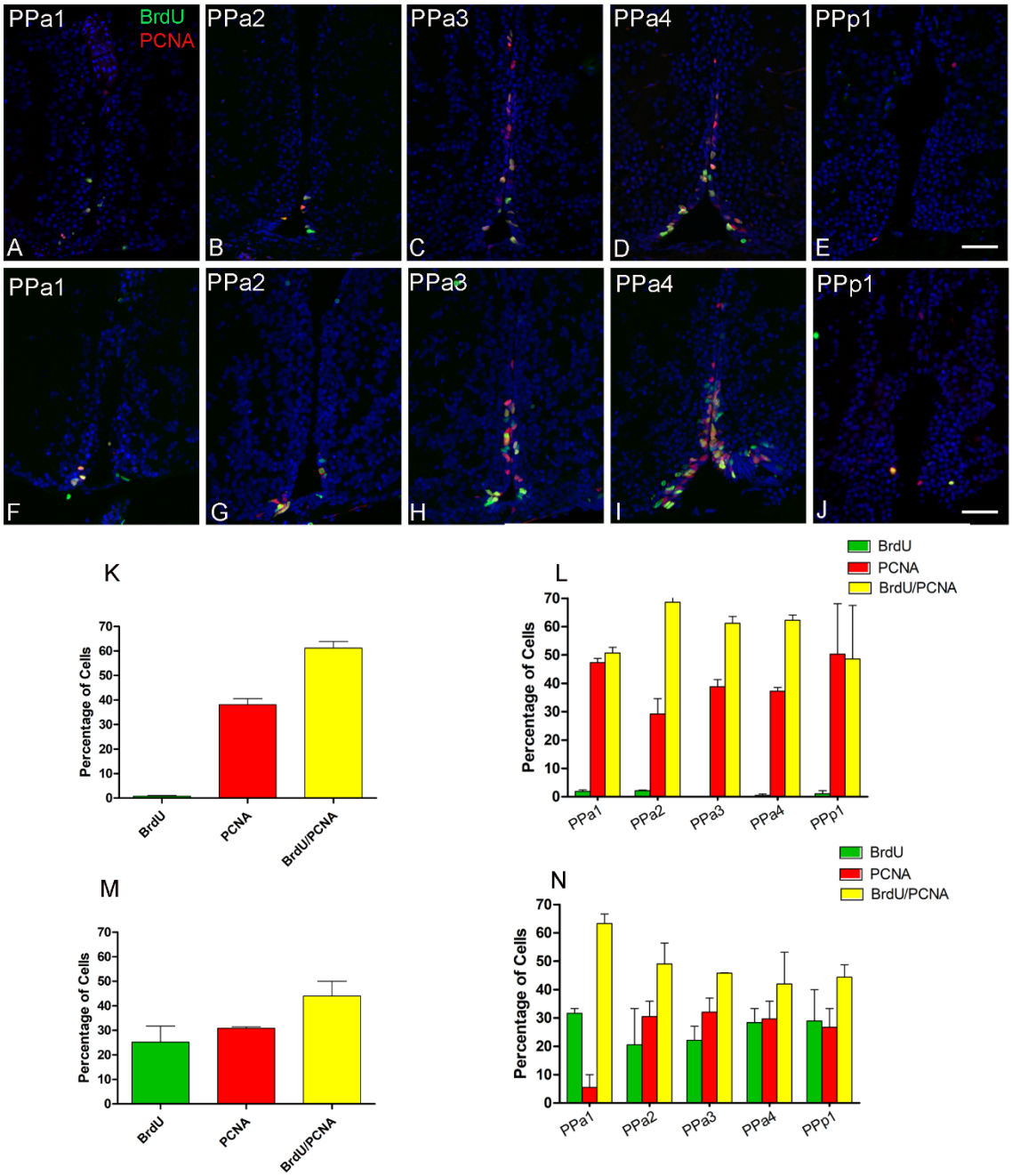
PPa1
BrdU
PCNA
A
PPa2
B
PPa3
C
PPa4
D
PPp1
E
PPa1
F
PPa2
G
PPa3
H
PPa4
I
PPp1
J
K
Percentage of Cells
BrdU
PCNA
BrdU/PCNA
L
Percentage of Cells
PPa1
PPa2
PPa3
PPa4
PPp1
M
Percentage of Cells
BrdU
PCNA
BrdU/PCNA
N
Percentage of Cells
PPa1
PPa2
PPa3
PPa4
PPp1

Figure 2.10. POA generates new cells at 8 days. (A-J) BrdU/PCNA double immunofluorescence in transverse paraffin sections of 5 μm. **(A-E)** Treatment with one pulse of BrdU on day 1 and the brains were fixed on the second day. **(F-J).** Treatment with two pulses of BrdU at 1 and 7 days, and the brains were fixed at 8 days. In both conditions three populations of cells were observed: anti-BrdU= green, anti-PCNA= red, anti-BrdU/PCNA= yellow. All sections were labeled with DAPI labeling (blue). Scale bar: 30μm. Percentage of cells double or single labeled for BrdU or PCNA located in the POA, with single-BrdU pulse on day 1 **(K)** and two BrdU pulses at 1 and 7 days **(M)**. By transverse paraffin section of 5 μm of the POA, the cells were counted from the total immunolabeled cells distributed along the wall of the DiV of the POA. Percentage of cells double or single labeled for BrdU or PCNA in representative sections of the POA (PPa1, PPa2, PPa3, PPa4 and PPp1), with single-BrdU pulse on day 1 **(L)** and two BrdU pulses at 1 and 7 days **(N)**. For each representative section of the POA, a number of transverse paraffin section **(L)** (PPa1= 5, PPa2 = 10, PPa3 = 13, PPa4 = 12, and PPp1= 4) and (**N**) (PPa1 = 5, PPa2 = 10, PPa3 = 13, PPa4 = 12, and PPp1 = 4) of 5 μm were obtained and the anti-BrdU^{+}, anti-PCNA^{+} and anti-BrdU^{+}/PCNA^{+} cells were counted.

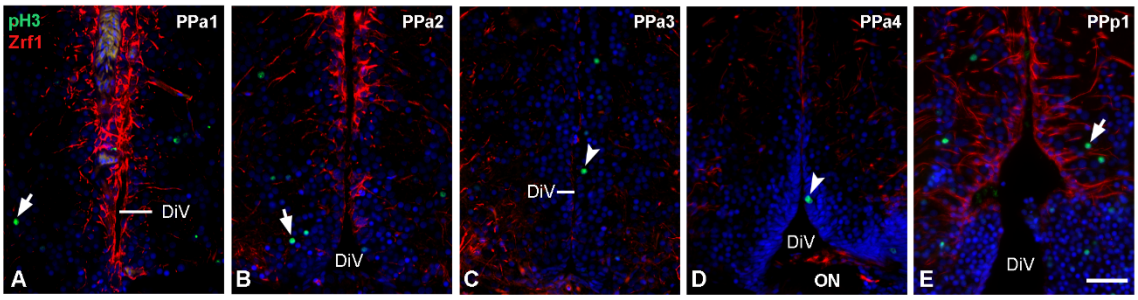

Figure 2.11. Distribution of Mitotic-phase cells in the POA. (A-E) Transverse 5 µm paraffin sections of the POA. **(A, B, E)** Anti-pH3 positive cells were found adjacent to the DiV (arrows). Anti-pH3 (green) labeling was not observed in Zrf1 positive cells (red). **(C, D)** Anti-pH3 positive cells found lining the ventricle were negative for Anti-Zrf1 (arrowheads). All sections were labeled with DAPI labeling (blue). Diencephalic ventricle (DiV). Scale bar: 30µm.

GnRH and testosterone treatments cause neurogenesis in the POA

Previously, we have shown that the exposure of GnRH or testosterone in neurospheres cultured from adult hypothalamus results in differentiation of neurons (Cortes-Campos et al., 2015). To test the effect of GnRH and testosterone on the neurogenesis of the POA *in vivo*, we performed intraperitoneal injection of GnRH and testosterone and quantified the changes in the number of positive cells for anti-GnRH, BrdU and cytoplasmic Sox2. Recently, it has been demonstrated that the zebrafish genome lacks the gene encoding the hypothalamic form of GnRH (GnRH1). Moreover, studies conducted by MALDI TOF in hypothalamic extracts did not identify any form of GnRH protein (Whitlock et al., 2019). Thus, we refer to the GnRH immuno-reactivity as GnRH-like immune reactivity (GnRH-LIR).

We performed a dose response curve to determine that 15 µL per gram of 1 µM GnRH and 1mg/mL testosterone were the optimal concentrations to use for this study (Fig. 2.12). In animals treated with GnRH, we observed a more than 2-fold increase in the number of anti-BrdU positive cells (GnRH treated: 409.7±60.6 cells, 9 fish; control: 173.8±38.1 cells, 9 fish) (Fig. 2.13, A). This significant increase in the anti-BrdU positive cells was observed in sections PPa1, PPa3 and PPa4 (Fig. 2.14, A). Whereas in PPa4, the control condition showed anti-BrdU positive cells mainly distributed along the lining of the DiV, in fish treated with GnRH, anti-BrdU positive cells were observed in nuclei adjacent to the DiV (Fig. 2.15, D', arrow). In contrast, fish treated with testosterone showed a slight increase of the number of anti-BrdU positive cells, but this increase was not significant with respect to the control (testosterone treated: 349±8 cells, 8 fish; control: 232.7±58 cells, 10 fish) (Fig. 2.13, D; Fig. 2.15, F-J'). Similar result was

observed when we analyzed the number of anti-BrdU positive cell of each section (Fig. 2.14, C).

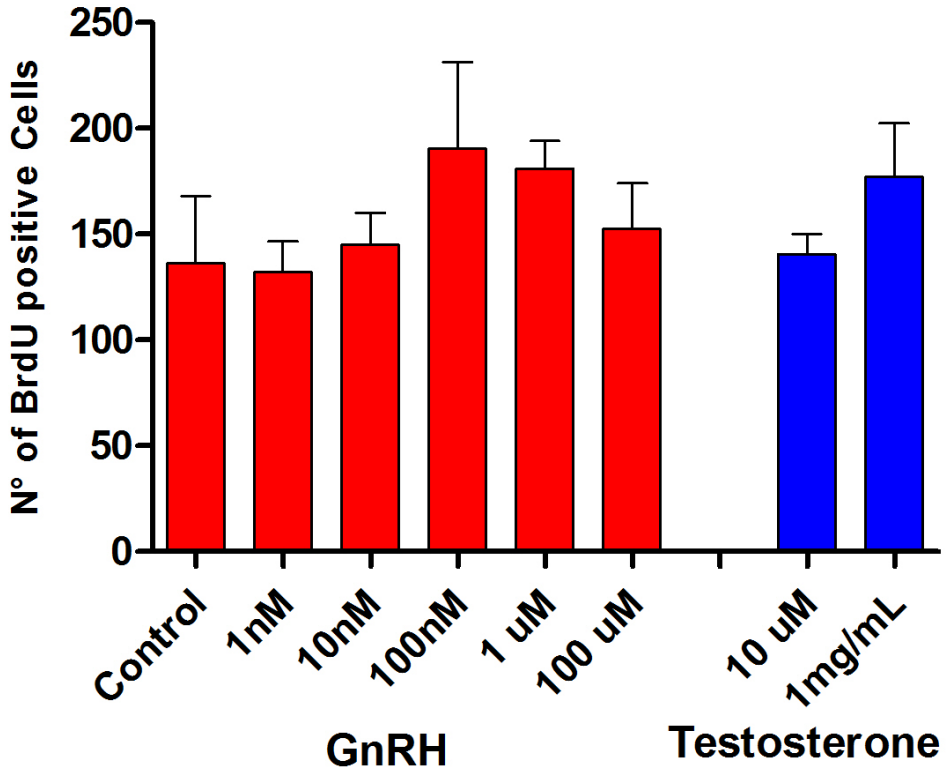

Figure 2.12. Determination of optimal GnRH and testosterone concentration. Optimal hormone concentration was determined according to the increase of number of anti-BrdU+ cells in treated versus control fish. Three fish were used for each treatment. The number of anti-BrdU+ cells were obtained through horizontal cryosections of 20 µm of the POA (10 sections).

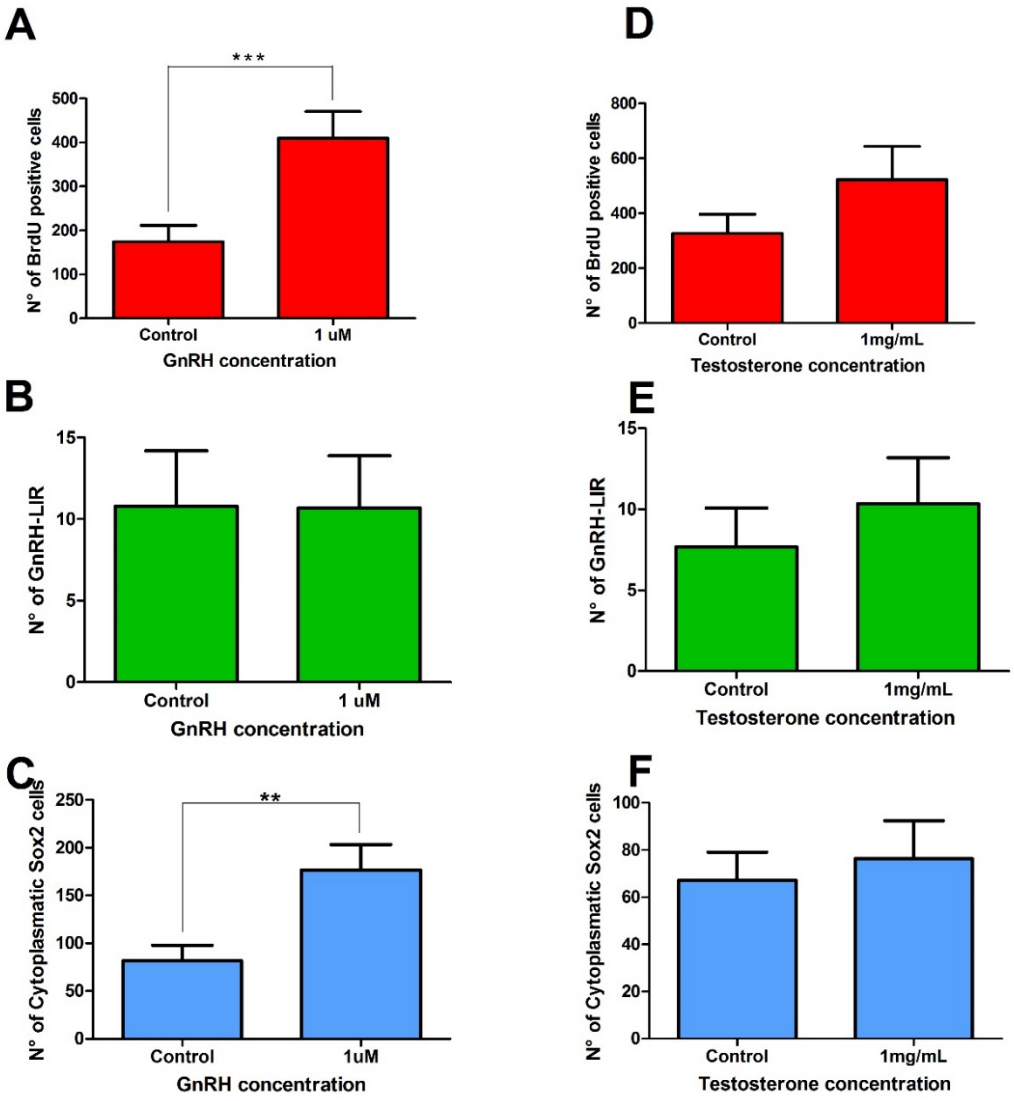
A
***
N° of BrdU positive cells
500
400
300
200
100
0
Control
1 uM
GnRH concentration
D
N° of BrdU positive cells
800
600
400
200
0
Control
1mg/mL
Testosterone concentration
B
N° of GnRH-LIR
15
10
5
0
Control
1 uM
GnRH concentration
E
N° of GnRH-LIR
15
10
5
0
Control
1mg/mL
Testosterone concentration
C
**
N° of Cytoplasmatic Sox2 cells
250
200
150
100
50
0
Control
1uM
GnRH concentration
F
N° of Cytoplasmatic Sox2 cells
100
80
60
40
20
0
Control
1mg/mL
Testosterone concentration

Figure 2.13. Only GnRH increases cell proliferation in the POA. (A-F) Quantification of the effects of GnRH and testosterone in POA of adult zebrafish. The number of cells were counted in transverse 20 µm cryosections of the POA (12 sections). **(A-C)** Animals were treated with 1 µM GnRH. **(A)** Number of anti-BrdU positive cells. **(B)** Number of anti-GnRH--LIR cells. **(C)** Number of cytoplasmic Sox2 cells. **(D-F)** Adult zebrafish treated with 1mg/mL testosterone. **(D)** Number of anti-BrdU positive cells. **(E)** Number of anti-GnRH-LIR cells. **(F)** Number of cytoplasmic Sox2. ***P<0.001; **P<0.01. Statistical significance was determined by Student's t-test.

Analysis of GnRH-LIR in lateral region of the PPa (Fig. 2.16 A. arrow) showed no significant differences in the number of GnRH-LIR positive cells in treated animals versus control for GnRH (GnRH treated: 10.7±3.2 cells, 6 fish; control: 4.7±1.8 cells, 6 fish) (Fig. 2.13, B) or testosterone (testosterone treated: 9.8±1.6 cells. 8 fish; control: 232.7±58. cells. 10 fish) (Fig. 2.13, E). Finally, we quantified the cytoplasmic anti-Sox2 positive cells. While we did not find significant differences when comparing testosterone treated with control (testosterone treated: 76.3±16.2 cells, 7 fish; control: 67.2±11.9 cells, 6 fish) (Fig. 2.13, F), the number of cytoplasmic Sox2 positive cells increased significantly in GnRH treated animals (GnRH treated: 176.6±26.7 cells. 8 fish; control: 81.7±16.1 cells, 9 fish) (Fig. 2.13, C). This increase in cytoplasmic Sox2 cells was found in PPp1 (Fig. 2.14, B). Also, in fish treated with GnRH, we observed a small number of cytoplasmic Sox2/BrdU positive cells in non proliferative zone located in the PPp1 (Fig. 2.16 B, C, arrow), these cells were not observed in fish with testosterone treatment. Thus, these results demonstrated that GnRH treatment promoted the neurogenesis in the POA.

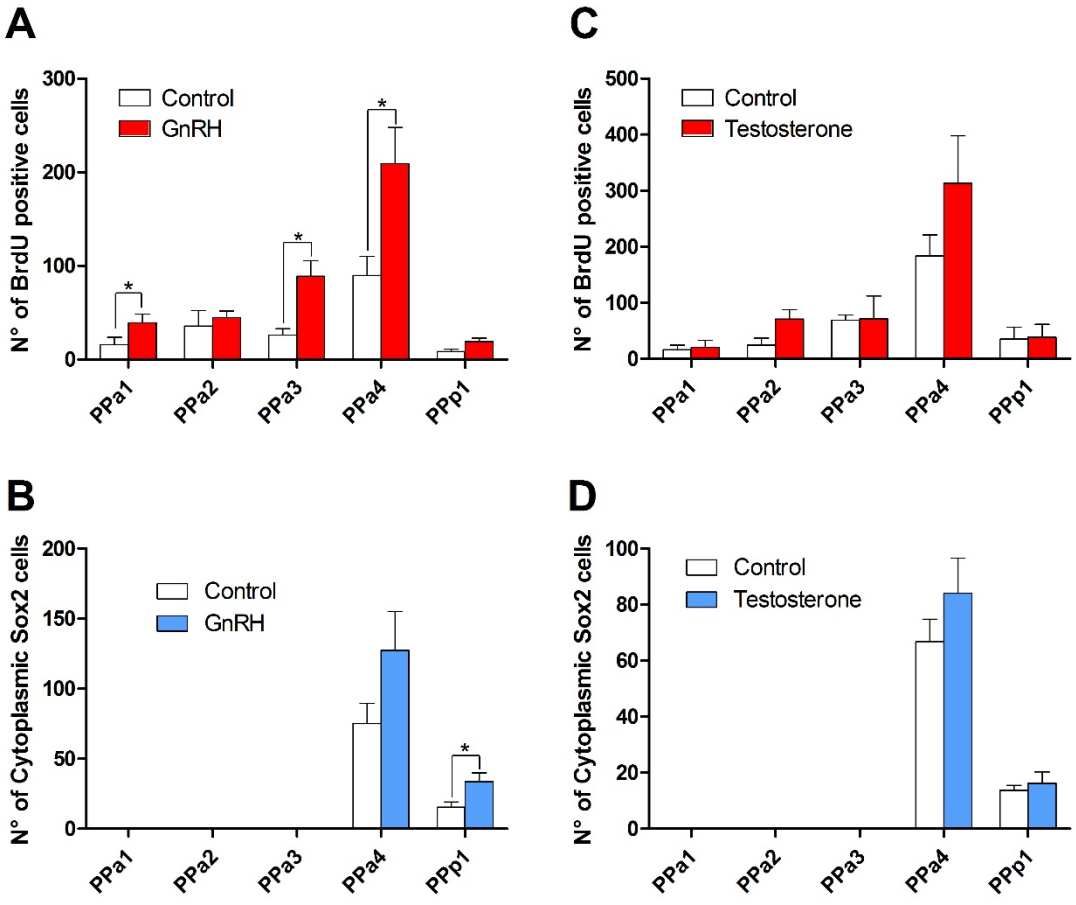

Figure 2.14. The PPa4 section of the POA showed hormone induced increases in cell proliferation. Number of cells located in representative regions of the POA (PPa1, PPa2, PPa3, PPa4 and PPp1). For each representative region of the POA, a number of transverse cryosection (PPa1 = 2, PPa2 = 2, PPa3 = 3, PPa4 = 4 and PPp1 = 2) of 20 µm were obtained. **(A)** Number of anti-BrdU+ cells and **(B)** number of cytoplasmic Sox2 cells in GnRH treated animals. **(C)** Number of BrdU+ cells and **(D)** number of cytoplasmic Sox2 cells in testosterone treated animals. *P<0.05. Statistical significance was determined by Student's t-test.

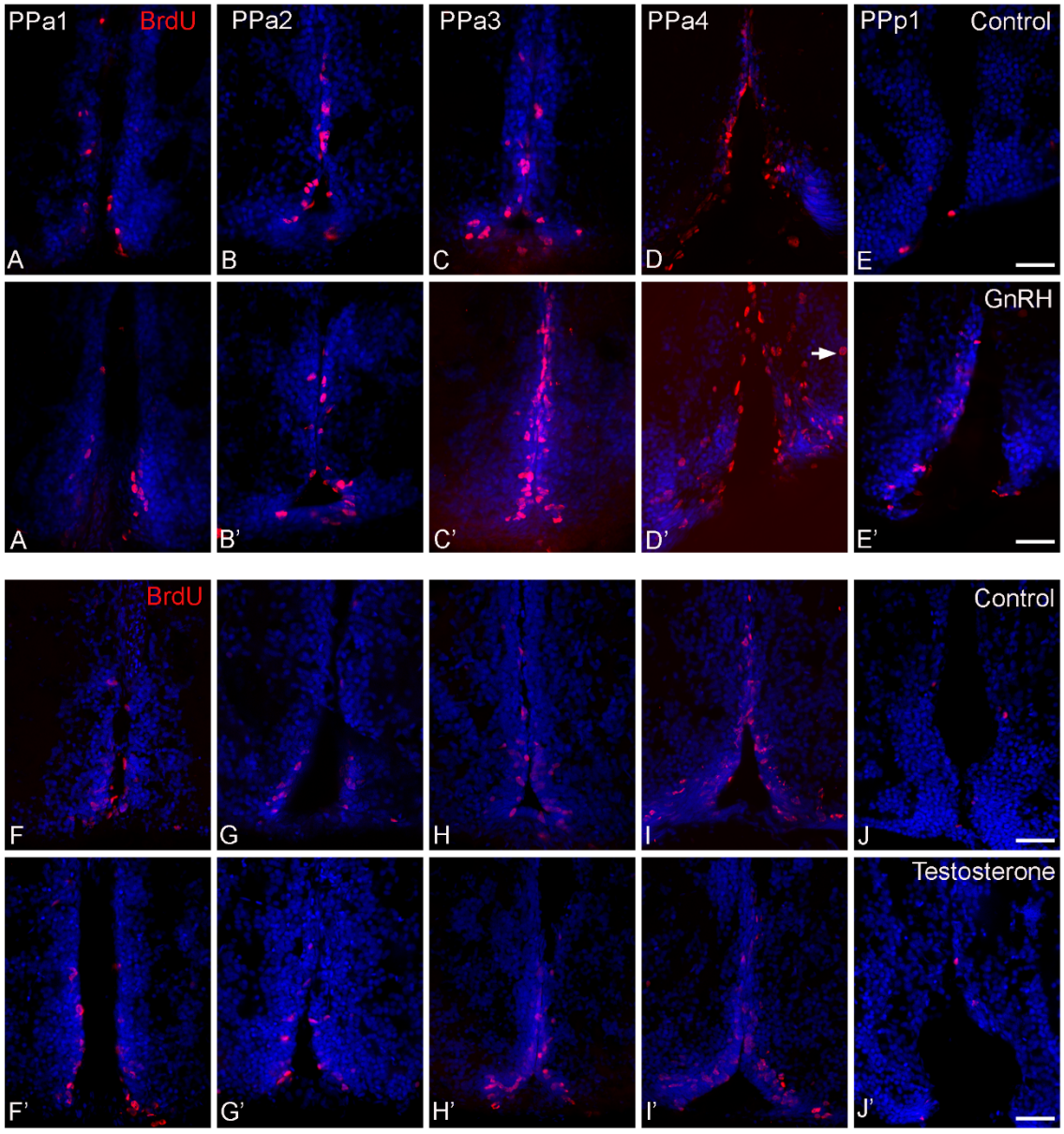

Figure 2.15. BrdU-Immunolabeling showed the GnRH-induced increase in the number of cells in the POA. **(A-J´)** Proliferative cells were detected by BrdU antibody in transverse cryosections of 20 µm of the POA. **(A-E)** GnRH control. **(A-E')** GnRH treatment. **(F- J)** Testosterone control. **(F'-J')** Testosterone treatment. All sections were labeled with DAPI labeling (blue). Scale bar: 30µm.

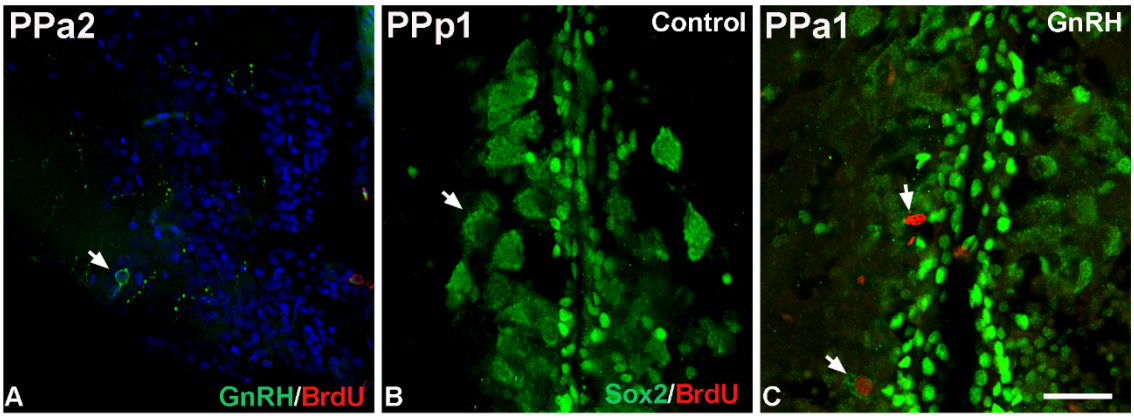

Figure 2.16. GnRH treatment increased the number of cytoplasmic Sox2 cells, but does not produce changes in the number of GnRH-LIR cells. (A-C) Transverse cryosections 20 µm of the PPa2 and PPp1. **(A)** Anti-GnRH-LIR positive cells localized laterally of the PPa (arrow). **(B-C)** Antibodies recognizing Sox2 (green) and BrdU (red) were used. **(B)** GnRH control, cytoplasmic Sox2 cells (green, arrow). **(C)** GnRH treatment cytoplasmic Sox2 cells (green) are positive to anti-BrdU labeling (red) (arrow). All sections were labeled with DAPI labeling (blue). Diencephalic ventricle (DiV). Scale bar: **(A-B)** 60µm. **(C-D)** 30µm.

DISCUSSION

Here, we characterized neural progenitors located in the anterior/posterior parvocelluar nucleus PPa/PPp of the POA. We found that this area was highly proliferative. Moreover, we described cells with cytoplasmic Sox2 expression, which co-localized with *fezf2*:GFP, are therefore like commitment to a neuroendocrine fate. We demonstrated in vivo that the GnRH, but not testosterone treatment increases the number of BrdU-labeling cells and of, cytoplasmic Sox2 positive cells. These results reveal for the first time the effect of treatment with GnRH and testosterone on neurogenesis in hypothalamus of adult zebrafish *in vivo*, being similar to what was observed in hypothalamic progenitor cells culture of adult zebrafish and the mammal model (Fowler et al., 2003; Zhang et al., 2013).

Neural progenitor cells in adult zebrafish.

In mammal hypothalamic tanycytes have neurogenic capacity (Kokoeva *et al.,* 2007; Pencea et al., 2001; Xu et al., 2005;). These cells are characterized by expressing neuro-progenitor cell markers including vimentin, nestin and Sox2 (Li et al., 2012; Robins et al., 2013; Rojczyk-Gołębiewska et al., 2014). In the case of GFAP, it is found in α2 subsets of tanycytes having neural progenitor capacity (Robins et al., 2013) (Fig 2.16, A). In the POA of adult rat, studies have been described neurogenesis (Matsuzaki et al., 2009; Matsuzaki et al., 2015; Matsuzaki et al., 2017), similar to observed in the POA of zebrafish (Grandel et al., 2006). We identified the same neuro-progenitor marker observed in the hypothalamus of mammals. Sox2 expression was homogeneously distributed thorough the DiV, as observed in the TelV of adult zebrafish

(März et al., 2010) and in the DiV of mammals (Batailler et al., 2014). We identified the expression of vimentin and GFAP, only in the more dorsal regions of the DiV in cells with radial glia morphology (Fig. 2.17, B). A similar pattern of expression was observed in the ventral telencephalon (TelV) (Ganz et al., 2010).

We identified proliferative zone located in the ventral walls of the DiV in the POA as it was described by (Grandel et al., 2006). Although studies have described the expression of GFAP in neuro-progenitor cells in the mammalian brain (Garcia et al., 2004), including the hypothalamus (Robins et al., 2013), we observed that the anti-GFAP positive cells have a reduced proliferative capacity. This result is in agreement with a study performed in the ventral telencephalon, where a progenitor population negative for this glial marker was described (Ganz et al., 2010), nevertheless the same authors also described proliferative cells that express glial marker like GFAP, S100β and Vimentin in the dorsal region of the telencephalon.

In the proliferative region of the POA, we identified a group of proliferative cells with fusiform nuclei that were positive for nestin. These cells were described previously by electron microscopy of ventral region of the PPa (Lindsey et al., 2012). Moreover, by using the *nestin*:GFP transgenic line, similar cells were identified in the ventral telencephalon, being negative for vimentin and GFAP (Ganz et al., 2010). These type of cells have been characterized as neuroepithelial (NE) progenitor cells, and express progenitor marker like Sox2 and Nestin (reviewed in Than-Trong and Bally-Cuif, 2015).

Cytokeratin cells in the floor of the third ventricle.

We found cytokeratin in the ventral region of the POA. We used anti-cytokeratin that includes the clone AE3, this has reactivity to cytokeratin 8 identified in teleost fish (Conrad et al., 1998). Similar to our result, in goldfish the cytokeratin expression do not

colocalized with GFAP, as was described in spinal cord and optic nerve (Giordano et al., 1990). Previously it has been shown that cytokeratin is found in ependymal cells in the human plexus choroideus (Kasper et al., 1986; Kasper et al., 1987). We showed that cytokeratin is found in ependymal cells located in the saccus dorsalis in the zebrafish brain, an analogue of the mammalian choroid plexus (Henson et al., 2014), and in the lining of the TelV in the dorsal telencephalon. As previously described, the ependymal cells are multiciliated cells that line the ventricle (Mathew, 2008). However, our results in adult zebrafish showed differences in the distribution and shape of ependymal cells. We observed expression of cytokeratin positive cells in the floor of the DiV. Due to its distribution and the presence of blood vessels in the parenchyma adjacent to the floor of DiV, these cells could play a role in the secretion of cerebrospinal fluid like saccus dorsalis. Another possibility is that the floor of the DiV is a neurogenic niche for ependymal cells. Similar results were observed in the telencephalon of zebrafish, where cells of ependymal appearance were found in the neurogenic niche in the dorsal part of the ventral TelV (Jacquet et al., 2009; Ogino et al., 2016).

Cytoplasmic Sox2 cells

We found cytoplasmic Sox2 cells in the neurosecretory preoptic are (NPO). In this region resident neurons release neuropeptides classified like vasotocin and isotocin (Eaton et al., 2008; Almeida and Oliveira, 2015). Moreover we identified cytoplasmic Sox2 cells were positive to Fezf2, transcriptional factor required for the development of neuroendocrine neurons (Guo et al., 1999; Levkowitz et al., 2003) through regulation of OTP (Blechman et al., 2007; Eaton et al., 2008) (Lohr et al., 2009; Fernandes et al., 2013). In the POA, Fezf2 labels is express in postmitotic neurons (Berberoglu et al.,

2009), therefore, we proposed that cytoplasmic Sox2 cells are neurosecretory neurons. It has been shown that cytoplasm Sox2 label is related with differentiation of cells. In the absence of FGF4, trophoblast stem cells differentiate into mature trophoblast cell types, and Sox2 becomes cytoplasmic (Avilion, 2003). Moreover, a study demonstrated that the cytoplasmic Sox2 label occur by the acetylation of a lysine residue in Sox2 protein that causes its transport to the cytoplasm in embryonic stem cells, during the differentiation (Baltus et al., 2009). However, we demonstrated that the cytoplasmic localization of the Sox2 is not due to acetylation of lysine residue in Sox2, suggesting that the cytoplasmic Sox2 label described in our results is due to another mechanism. A possible mechanism is through AKT, a serine/threonine-specific protein kinase. A study in breast carcinoma cells showed that inhibition of the AKT kinase (AKT essential for maintaining pluripotency: reviewed by Yu and Cui, 2016), results in cytoplasmic retention of SOX2, presumably via impaired nuclear import (Schaefer et al., 2015).

Hormone treatment and neurogenesis

Here, we observed that the GnRH and testosterone generated a differential effect in the neurogenesis of the POA (Fig. 2.18). Similar results was observed in hypothalamic progenitor cells culture of adult zebrafish treated with GnRH or testosterone (Cortes-Campos et al., 2015). In agreement with our results, GnRH can increase neurogenesis in both hypothalamus and hippocampus and also improve cognitive function in aged mice (Zhang et al., 2013). Although GnRH triggers neurogenesis, the expression of its receptor in neural progenitor cells is poorly studied. GnRH receptors (GnRH-Rs) belong to the G-protein-coupled receptor family (Chen and Fernald, 2008), expressing in several mammals brain regions including the hypothalamus (Jennes et al., 1988) (Badr and Pelletier, 1987) (Wen et al., 2011). These

receptors have also been identified in the hypothalamus of teleost fish as demonstrated in tilapia (Soga et al., 2005) (Kigerl et al., 2006). In zebrafish four GnRH-R isoforms have been described (Tello et al., 2008), although the GnRH-Rs have not been described in neural progenitor in the hypothalamus, three of four GnRH-R isoforms are located in cultured hypothalamic progenitor cells of adult zebrafish in zebrafish by RT-PCR (Cortes-Campos et al., 2015).

It has been described that ERK is activated by GNRH-R (rewieved in Caunt et al., 2006). ERK is a Mitogen-activated protein kinases (MAPK) cascades have pivotal roles in different process such a differentiation, proliferation and development (Naor, 2009), hence it is possible that GnRH generates neurogenesis by activating the extracellular signal-regulated kinase (ERK) pathway. Studies have shown that the use of U0126 (ERK inhibitor) decreased hippocampal cell proliferation and differentiation in rat P7 (Jiang et al., 2015). Also, a study performed in ERK1 and ERK2 knockout mice results in a smaller DG due to depletion of neurons, due to decreased proliferation and precocious maturation of radial glia (Vithayathil et al., 2015). In adult brain of zebrafish, while phosphorylated ERK (P-ERK) (active form) is found in telencephalic and hypothalamic proliferation zone, this expression is not directly related with proliferation status (Topp et al., 2008). However, P-ERK1/2- positive cells were significantly more abundant during the regenerative process, post-lesion telencephalic (Lim et al., 2016).

The androgen receptor (AR) is also expressed in the hypothalamus as was shown in the rat brain (Kerr et al., 1995). In zebrafish the AR has been identified (Hossain et al., 2008) and its expression has been localized in the brain including the wall of the DiV POA (Gorelick et al., 2008). This last result is in agreement with our previous study where the *ar* was found in zebrafish hypothalamic cells culture by RT-

PCR (Cortes-Campos et al., 2015), this indicates that *ar* is expressed in neural progenitor cells in the POA of zebrafish.

Although we found a slight increase in the proliferation with testosterone treatment, this result was not significant. This result was consistent with our previous study performed in hypothalamic neural progenitor cells *in vitro*, demonstrating that the testosterone treatment causes only a small but significant increase in neurons in culture of hypothalamic progenitor cells (Cortes-Campos et al., 2015). Thus limited effects of testosterone on neurogenesis have been observed in the hypothalamus of zebrafish. The administration of testosterone and its metabolites 5α-dihydrotestosterone (DHT) did not generate neurogenesis in the ventromedial nucleus of the hypothalamus (VMH) in meadow voles (Fowler et al., 2003), and in hypothalamus of hamster (Antzoulatos et al., 2008). Nevertheless, several studies have demonstrated that testosterone generate neurogenesis in the hippocampus of mammals (Farinetti et al., 2015; Pan and Zhang, 2013), this indicate that testosterone has a differential effect on neurogenesis, depending of the brain region.

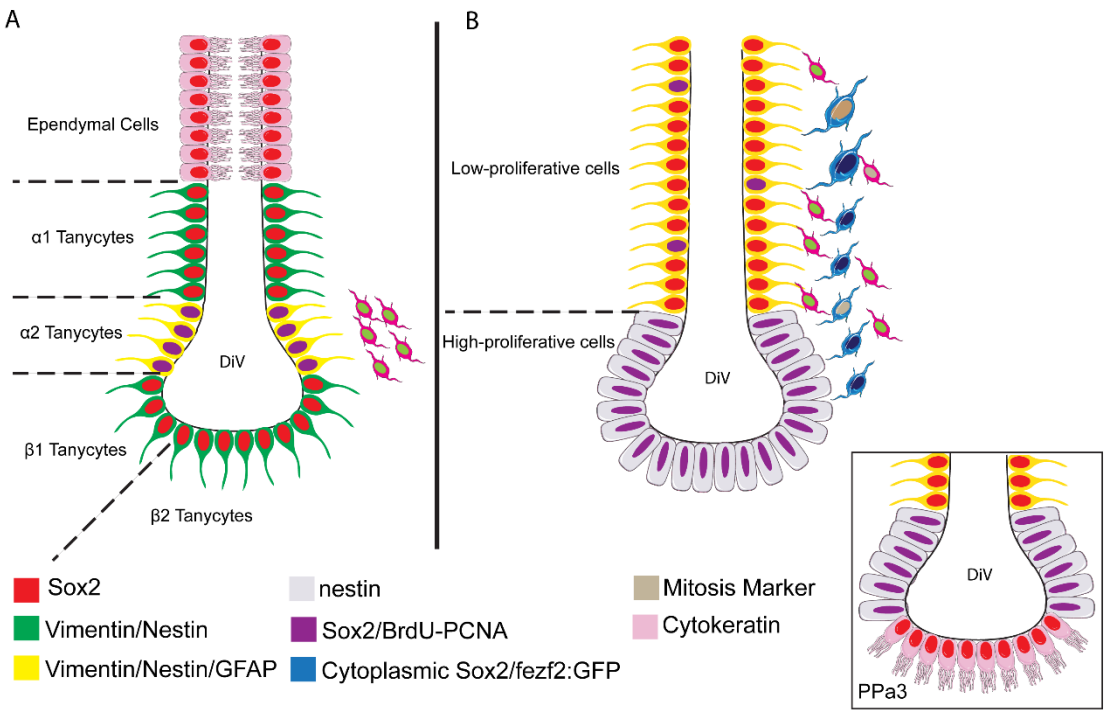

Figure 2.17. Summary of the distribution of neural progenitors in the POA of adult zebrafish. (A) Distribution of neural progenitors lining the DiV in the hypothalamus of mammals according to (Robins et al., 2013). α2 tanycytes have proliferative capacity (positive to BrdU-PCNA), express: Vim, Nestin, Sox2 and GFAP, while the no-proliferative tanycytes do not express GFAP. Ependymal cells are distributed in the dorsal region. However, **(B)** in zebrafish, we described a low-proliferative cell positive for Vimentin, Sox2 and GFAP, and high proliferative cells positive to Nestin and Sox2. We found a group of cytoplasmic Sox2/Fezf2:GFP cells adjacent to the DiV. Cytokeratin cells are express in the ventral region of the POA (rectangle).

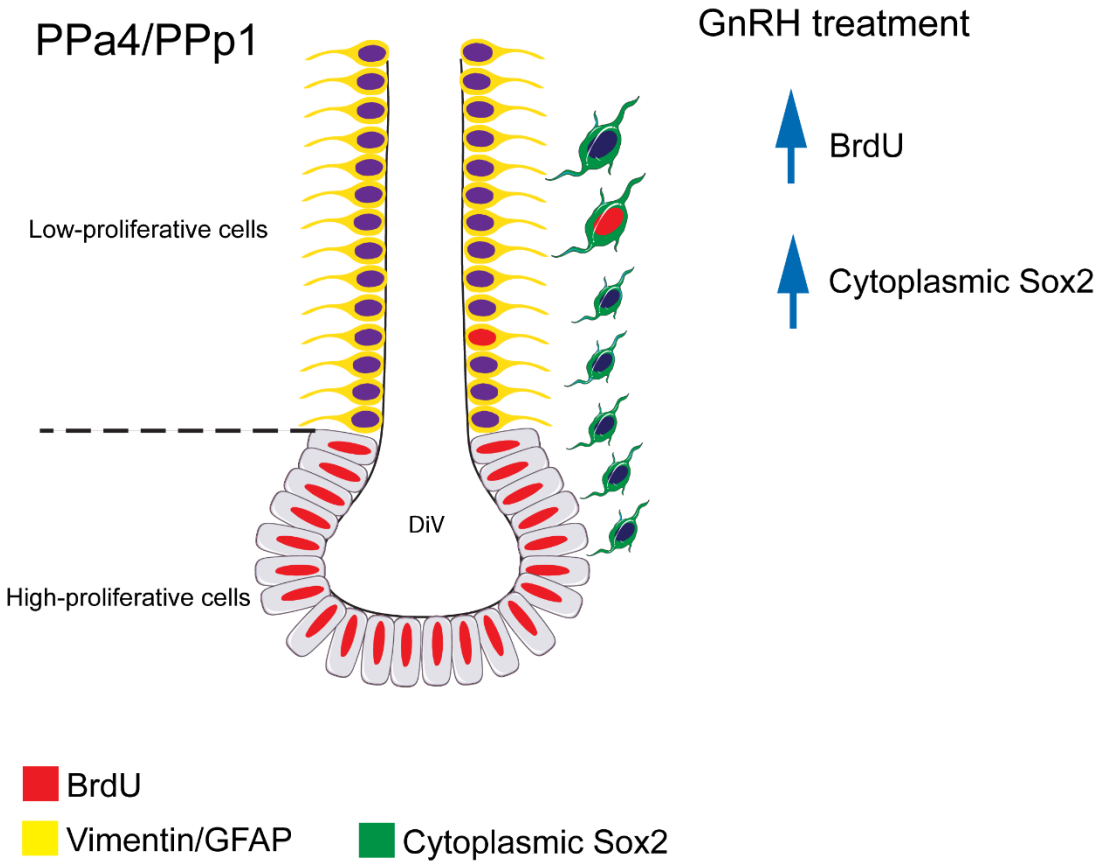

Figure 2.18. Effect of GnRH treatment in the POA in adult zebrafish. GnRH treatment in adult zebrafish increased the number of proliferative cells (BrdU positive) and the cytoplasmic Sox2 cells. In some cytoplasmic Sox2 positive cells, the expression of BrdU was also observed.

ACKNOWLEDGEMENTS

We would like to acknowledge Donald Brown for use of his histology facility and Andrea Moscoso and Maria Trinidad Ordenes for excellent management of the zebrafish facility.

REFERENCES

1. **Cameron HA, Mckay RDG.** Adult neurogenesis produces a large pool of new granule cells in the dentate gyrus. *J. Comp. Neurol.* 2001;435(4):406–417.
2. **Kempermann G, Jessberger S, Steiner B, Kronenberg G.** Milestones of neuronal development in the adult hippocampus. *Trends Neurosci.* 2004;27(8):447–452.
3. **Kaplan mMchael. S, Hinds J.** Neurogenesis in the adult rat: electron microscopic analysis of light radioautographs. *Science (80-.).* 1977;197(4308):1092–1094.
4. **Doetsch F, Alvarez-Buylla a.** Network of tangential pathways for neuronal migration in adult mammalian brain. *Proc. Natl. Acad. Sci. U. S. A.* 1996;93(25):14895–14900.
5. **Pencea V, Bingaman KD, Wiegand SJ, Luskin MB.** Infusion of brain-derived neurotrophic factor into the lateral ventricle of the adult rat leads to new neurons in the parenchyma of the striatum, septum, thalamus, and hypothalamus. *J. Neurosci.* 2001;21(17):6706–6717.
6. **Klein C, Butt SJB, Machold RP, Johnson JE, Fishell G.** Cerebellum- and forebrain-derived stem cells possess intrinsic regionalcharacter. *Development* 2005;132(20):4497–4508.
7. **Gould E, reeves AJ, Graziano MSA, Gross CG.** Neurogenesis in the neocortex of adults primates. *Science (80-.).* 1999;286(October):548–552.
8. **Xu Y, Tamamaki N, Noda T, Kimura K, Itokazu Y, Matsumoto N, Dezawa M, Ide C.** Neurogenesis in the ependymal layer of the adult rat 3rd ventricle. *Exp. Neurol.* 2005;192(2):251–64.
9. **Kokoeva M V, Yin H, Flier JS.** Evidence for Constitutive Neural Cell Proliferation in the Adult Murine. 2007;220(September 2006):209–220.
10. **Rodríguez EM, Blázquez JL, Pastor FE, Peláez B, Peña P, Peruzzo B, Amat P.** Hypothalamic tanycytes: a key component of brain-endocrine interaction. *Int. Rev. Cytol.* 2005;247(05):89–164.
11. **Yoo S, Blackshaw S.** Regulation and function of neurogenesis in the adult mammalian hypothalamus. *Prog. Neurobiol.* 2018;(April):0–1.
12. **Robins SC, Stewart I, McNay DE, Taylor V, Giachino C, Goetz M, Ninkovic J, Briancon N, Maratos-Flier E, Flier JS, Kokoeva M V, Placzek M.** α-Tanycytes of the adult hypothalamic third ventricle include distinct populations of FGF-responsive neural

progenitors. *Nat. Commun.* 2013;4(May):2049.

13. **Lévy F, Batailler M, Meurisse M, Migaud M.** Adult neurogenesis in sheep: Characterization and contribution to reproduction and behavior. *Front. Neurosci.* 2017;11(OCT):1–15.
14. **Lindvall O, Kokaia Z.** Stem cells for the treatment of neurological disorders. *Nature* 2006;441(7097):1094–1096.
15. **S. Wray GH.** A developmental study of the quantitative distribution of LHRH neurons within the central nervous system of postnatal male and female rats. *J. Comp. Neurol.* 1986;531:522–531.
16. **Terasawa E, Fernandez DL.** Neurobiological mechanisms of the onset of puberty in primates. *Endocr. Rev.* 2001;22(1):111–51.
17. **Dodé C, Hardelin J-P.** Kallmann syndrome. *Eur. J. Hum. Genet.* 2009;17(2):139–46.
18. **Raivio T, Falardeau J, Dwyer A, Quinton R, Hayes FJ, Hughes V a, Cole LW, Pearce SH, Lee H, Boepple P, Crowley WF, Pitteloud N.** Reversal of idiopathic hypogonadotropic hypogonadism. *N. Engl. J. Med.* 2007;357(9):863–73.
19. **Sidhoum VF, Chan YM, Lippincott MF, Balasubramanian R, Quinton R, Plummer L, Dwyer A, Pitteloud N, Hayes FJ, Hall JE, Martin K a., Boepple P a., Seminara SB.** Reversal and relapse of hypogonadotropic hypogonadism: Resilience and fragility of the reproductive neuroendocrine system. *J. Clin. Endocrinol. Metab.* 2014;99(3):861–870.
20. **Ransome MI, Turnley AM.** Growth hormone signaling and hippocampal neurogenesis: Insights from genetic models. *Hippocampus* 2008;18(10):1034–1050.
21. **López-Juárez A, Remaud S, Hassani Z, Jolivet P, Pierre Simons J, Sontag T, Yoshikawa K, Price J, Morvan-Dubois G, Demeneix BA.** Thyroid hormone signaling acts as a neurogenic switch by repressing Sox2 in the adult neural stem cell niche. *Cell Stem Cell* 2012;10(5):531–543.
22. **Zhang G, Li J, Purkayastha S, Tang Y, Zhang H, Yin Y, Li B, Liu G, Cai D.** Hypothalamic programming of systemic ageing involving IKK-β, NF-κB and GnRH. *Nature* 2013;497(7448):211–6.
23. **Galea L a M, Wainwright SR, Roes MM, Duarte-Guterman P, Chow C, Hamson DK.** Sex, hormones and neurogenesis in the hippocampus: Hormonal modulation of neurogenesis and potential functional implications. *J. Neuroendocrinol.* 2013;25(11):1039–1061.

24. **Farinetti a., Tomasi S, Foglio B, Ferraris a., Ponti G, Gotti S, Peretto P, Panzica GC.** Testosterone and estradiol differentially affect cell proliferation in the subventricular zone of young adult gonadectomized male and female rats. *Neuroscience* 2015;286:162–170.
25. **Cortes-Campos C, Letelier J, Ceriani R, Whitlock KE.** Zebrafish adult-derived hypothalamic neurospheres generate gonadotropin-releasing hormone (GnRH) neurons. *Biol. Open* 2015:1–10.
26. **Kizil C, Kaslin J, Kroehne V, Brand M.** Adult neurogenesis and brain regeneration in zebrafish. *Dev. Neurobiol.* 2012;72(3):429–61.
27. **Grandel H, Kaslin J, Ganz J, Wenzel I, Brand M.** Neural stem cells and neurogenesis in the adult zebrafish brain: origin, proliferation dynamics, migration and cell fate. *Dev. Biol.* 2006;295(1):263–77.
28. **Whitlock K., Wolf C., Boyce M.** Gonadotropin-releasing hormone (gnrh) cells arise from cranial neural crest and adenohypophyseal regions of the neural plate in the zebrafish, danio rerio. *Dev. Biol.* 2003;257(1):140–152.
29. **Whitlock KE, Smith KM, Kim H, Harden M V.** A role for foxd3 and sox10 in the differentiation of gonadotropin-releasing hormone (GnRH) cells in the zebrafish Danio rerio. *Development* 2005;132(24):5491–502.
30. **Berberoglu MA, Dong Z, Mueller T, Guo S.** fezf2 expression delineates cells with proliferative potential and expressing markers of neural stem cells in the adult zebrafish brain. *Gene Expr Patterns* 2009;9(6):411–422.
31. **Edelmann K, Glashauser L, Sprungala S, Hesl B, Fritschle M, Ninkovic J, Godinho L, Chapouton P.** Increased radial glia quiescence, decreased reactivation upon injury and unaltered neuroblast behavior underlie decreased neurogenesis in the aging zebrafish telencephalon. *J. Comp. Neurol.* 2013;521(13):3099–3115.
32. **Paquette CE, Kent ML, Peterson TS, Wang R, Dashwood RH, Löhr C V.** Immunohistochemical characterization of intestinal neoplasia in zebrafish Danio rerio indicates epithelial origin. *Dis. Aquat. Organ.* 2015;116(3):191–197.
33. **Lazzari M, Bettini S, Franceschini V.** Immunocytochemical characterisation of olfactory ensheathing cells of zebrafish. *J. Anat.* 2014;224(2):192–206.
34. **Xi Y, Yu M, Godoy R, Hatch G, Poitras L, Ekker M.** Transgenic zebrafish expressing

green fluorescent protein in dopaminergic neurons of the ventral diencephalon. *Dev. Dyn.* 2011;240(11):2539–2547.

35. **Chen J.** Impaired Cardiovascular Function Caused by Different Stressors Elicits a Common Pathological and Transcriptional Response in Zebrafish Embryos. *Zebrafish* 2013;10(3):389–400.
36. **Montgomery JE, Parsons MJ, Hyde DR.** A novel model of retinal ablation demonstrates that the extent of rod cell death regulates the origin of the regenerated zebrafish rod photoreceptors. *J. Comp. Neurol.* 2010;518(6):800–814.
37. **Dirian L, Galant S, Coolen M, Chen W, Bedu S, Houart C, Bally-Cuif L, Foucher I.** Spatial Regionalization and Heterochrony in the Formation of Adult Pallial Neural Stem Cells. *Dev. Cell* 2014;30(2):123–136.
38. **Yang Q, Yan C, Yin C, Gong Z.** Serotonin Activated Hepatic Stellate Cells Contribute to Sex Disparity in Hepatocellular Carcinoma. *Cmgh* 2017;3(3):484–499.
39. **Thisse C, Thisse B, Schilling TF, Postlethwait JH.** Structure of the zebrafish snail1 gene and its expression in wild-type, spadetail and no tail mutant embryos. *Development* 1993;119(4):1203–15.
40. **Mahler J, Driever W.** Expression of the zebrafish intermediate neurofilament Nestin in the developing nervous system and in neural proliferation zones at postembryonic stages. *BMC Dev. Biol.* 2007;7:1–11.
41. **Kinkel MD, Eames SC, Philipson LH, Prince VE.** Intraperitoneal injection into adult zebrafish. *J. Vis. Exp.* 2010;4(42):3–6.
42. **Mueller T, Wullimann MF.** BrdU-, neuroD (nrd)- and Hu-studies reveal unusual non-ventricular neurogenesis in the postembryonic zebrafish forebrain. *Mech. Dev.* 2002;117(1–2):123–135.
43. **Wullimann MF, Rupp B, Reichert H.** *Neuroanatomy of the Zebrafish Brain. A topological Atlas*.; 1996. doi:10.1007/978-3-0348-8979-7.
44. **Haan N, Goodman T, Najdi-Samiei A, Stratford CM, Rice R, El Agha E, Bellusci S, Hajihosseini MK.** Fgf10-Expressing Tanycytes Add New Neurons to the Appetite/Energy-Balance Regulating Centers of the Postnatal and Adult Hypothalamus. *J. Neurosci.* 2013;33(14):6170–6180.
45. **Mirzadeh Z, Merkle FT, Soriano-Navarro M, Garcia-Verdugo JM, Alvarez-Buylla A.** Neural Stem Cells Confer Unique Pinwheel Architecture to the Ventricular Surface in Neurogenic Regions of the Adult Brain. *Cell Stem Cell* 2008;3(3):265–278.

46. **Kasper M, Goertchen R, Stosiek P, Perry G, Karsten U.** Coexistence of cytokeratin, vimentin and neurofilament protein in human choroid plexus - An immunohistochemical study of intermediate filaments in neuroepithelial tissues. *Virchows Arch. A Pathol. Anat. Histopathol.* 1987;410(3):173–177.
47. **Franko MC, Gibbs Jr. CJ, Rhoades DA, Gajdusek DC.** Monoclonal antibody analysis of keratin expression in the central nervous system. *Proc. Natl. Acad. Sci. U. S. A.* 1987;84(10):3482–3485.
48. **Kasper M, Perry G, Stosiek P.** Cytokeratin expression in human spinal meninges and ependymal cells. *J. Hirnforsch.* 1991;32(1):19–25.
49. **Giordano S, Hall C, Quitschke W, Glasgow E, Schechter N.** Keratin 8 of simple epithelia is expressed in glia of the goldfish nervous system. *Differentiation* 1990;44(3):163–172.
50. **Lindsey BW, Darabie A, Tropepe V.** The cellular composition of neurogenic periventricular zones in the adult zebrafish forebrain. *J. Comp. Neurol.* 2012;520(10):2275–2316.
51. **Henson HE, Parupalli C, Ju B, Taylor MR.** Functional and genetic analysis of choroid plexus development in zebrafish. *Front. Neurosci.* 2014;8(OCT):1–19.
52. **Blechman J, Borodovsky N, Eisenberg M, Nabel-Rosen H, Grimm J, Levkowitz G.** Specification of hypothalamic neurons by dual regulation of the homeodomain protein Orthopedia. *Development* 2007;134(24):4417–4426.
53. **Fernandes AM, Beddows E, Filippi A, Driever W.** Orthopedia Transcription Factor otpa and otpb Paralogous Genes Function during Dopaminergic and Neuroendocrine Cell Specification in Larval Zebrafish. *PLoS One* 2013;8(9). doi:10.1371/journal.pone.0075002.
54. **Baltus GA, Kowalski MP, Zhai H, Tutter AV, Quinn D WD and KS.** Acetylation of Sox2 Induces Its Nuclear Export in Embryonic Stem Cells. *Stem Cells* 2009;27(9):213–220.
55. **Garcia a DR, Doan NB, Imura T, Bush TG, Sofroniew M V.** GFAP-expressing progenitors are the principal source of constitutive neurogenesis in adult mouse forebrain. *Nat. Neurosci.* 2004;7(11):1233–41.
56. **Ganz J, Kaslin J, Hochmann S, Freudenreich D, Brand M.** Heterogeneity and Fgf

dependence of adult neural progenitors in the zebrafish telencephalon. *Glia* 2010;58(11):1345–63.

57. **Whitlock KE, Postlethwait J, Ewer J.** Neuroendocrinology of reproduction: Is gonadotropin-releasing hormone (GnRH) dispensable? *Front. Neuroendocrinol.* 2019;(November 2018):0–1.
58. **Fowler CD, Freeman ME, Wang Z.** Newly Proliferated Cells in the Adult Male Amygdala Are Affected by Gonadal Steroid Hormones. *J. Neurobiol.* 2003;57(3):257–269.
59. **Li J, Tang Y, Cai D.** IKKβ/NF-κB disrupts adult hypothalamic neural stem cells to mediate a neurodegenerative mechanism of dietary obesity and pre-diabetes. *Nat. Cell Biol.* 2012;14(10):999–1012.
60. **Rojczyk-Gołębiewska E, Pałasz A, Wiaderkiewicz R.** Hypothalamic subependymal niche: a novel site of the adult neurogenesis. *Cell. Mol. Neurobiol.* 2014;34(5):631–42.
61. **Matsuzaki K, Katakura M, Hara T, Li G, Hashimoto M, Shido O.** Proliferation of neuronal progenitor cells and neuronal differentiation in the hypothalamus are enhanced in heat-acclimated rats. *Pflugers Arch. Eur. J. Physiol.* 2009;458(4):661–673.
62. **Matsuzaki K, Katakura M, Sugimoto N, Hara T, Hashimoto M, Shido O.** Neural progenitor cell proliferation in the hypothalamus is involved in acquired heat tolerance in long-term heat-acclimated rats. *PLoS One* 2017;12(6):1–16.
63. **Matsuzaki K, Katakura M, Inoue T, Hara T, Hashimoto M, Shido O.** Aging attenuates acquired heat tolerance and hypothalamic neurogenesis in rats. *J. Comp. Neurol.* 2015;523(8):1190–1201.
64. **März M, Chapouton P, Diotel N, Vaillant C, Hesl B, Takamiya M, Lam CS, Kah O, Bally-Cuif L, Strähle U.** Heterogeneity in progenitor cell subtypes in the ventricular zone of the zebrafish adult telencephalon. *Glia* 2010;58(7):870–888.
65. **Batailler M, Droguerre M, Baroncini M, Fontaine C, Prevot V, Migaud M.** DCX-expressing cells in the vicinity of the hypothalamic neurogenic niche: a comparative study between mouse, sheep, and human tissues. *J. Comp. Neurol.* 2014;522(8):1966–85.
66. **Than-Trong E, Bally-Cuif L.** Radial glia and neural progenitors in the adult zebrafish central nervous system. *Glia* 2015;63(8):1406–1428.
67. **Conrad M, Lemb K, Schubert T, Markl J.** Biochemical identification and tissue-

specific expression patterns of keratins in the zebrafish Danio rerio. *Cell Tissue Res.* 1998;293(2):195–205.

68. **Kasper M, Karsten U, Stosiek P.** Detection of cytokeratin (s) in epithelium of human Plexus choroideus by monoclonal antibodies. *Acta Histochem* 1986;78(19):101–103.

69. **Mathew TC.** Regional analysis of the ependyma of the third ventricle of rat by light and electron microscopy. *J. Vet. Med. Ser. C Anat. Histol. Embryol.* 2008;37(1):9–18.

70. **Jacquet B V., Salinas-Mondragon R, Liang H, Therit B, Buie JD, Dykstra M, Campbell K, Ostrowski LE, Brody SL, Ghashghaei HT.** FoxJ1-dependent gene expression is required for differentiation of radial glia into ependymal cells and a subset of astrocytes in the postnatal brain. *Development* 2009;136(23):4021–4031.

71. **Ogino T, Sawada M, Takase H, Nakai C, Herranz-Pérez V, Cebrián-Silla A, Kaneko N, García-Verdugo JM, Sawamoto K.** Characterization of multiciliated ependymal cells that emerge in the neurogenic niche of the aged zebrafish brain. *J. Comp. Neurol.* 2016;524(15):2982–2992.

72. **Eaton JL, Holmqvist B, Glasgow E.** Ontogeny of vasotocin-expressing cells in zebrafish: Selective requirement for the transcriptional regulators orthopedia and single-minded 1 in the preoptic area. *Dev. Dyn.* 2008;237(4):995–1005.

73. **Almeida O, Oliveira RF.** Social status and arginine vasotocin neuronal phenotypes in a cichlid fish. *Brain. Behav. Evol.* 2015;85(3):203–213.

74. **Guo S, Wilson SW, Cooke S, Chitnis AB, Driever W, Rosenthal A.** Mutations in the Zebra sh Unmask Shared Regulatory Pathways Controlling the Development of Catecholaminergic Neurons. *Dev. Biol.* 1999;487:473–487.

75. **Levkowitz G, Zeller J, Sirotkin HI, French D, Schilbach S, Hashimoto H, Hibi M, Talbot WS, Rosenthal A.** Zinc finger protein too few controls the development of monoaminergic neurons. *Nat. Neurosci.* 2003;6(1):28–33.

76. **Lohr H, Ryu S, Driever W.** Zebrafish diencephalic A11-related dopaminergic neurons share a conserved transcriptional network with neuroendocrine cell lineages. *Development* 2009;136(6):1007–1017.

77. **Avilion AA.** Multipotent cell lineages in early mouse development depend on SOX2 function. *Genes Dev.* 2003;17(1):126–140.

78. **Yu JSL, Cui W.** Proliferation, survival and metabolism: the role of PI3K/AKT/mTOR signalling in pluripotency and cell fate determination. *Development* 2016;143(17):3050–

3060.

79. **Schaefer T, Wang H, Mir P, Konantz M, Pereboom TC, Paczulla AM, Merz B, Fehm T, Perner S, Rothfuss OC, Kanz L, Schulze-Osthoff K, Lengerke C.** Molecular and functional interactions between AKT and SOX2 in breast carcinoma. *Oncotarget* 2015;6(41). doi:10.18632/oncotarget.6183.
80. **Chen CC, Fernald RD.** GnRH and GnRH receptors: Distribution, function and evolution. *J. Fish Biol.* 2008;73(5):1099–1120.
81. **Jennes L, Dalati B, Michael Conn P.** Distribution of gonadrotropin releasing hormone agonist binding sites in the rat central nervous system. *Brain Res.* 1988;452(1–2):156–164.
82. **Badr M, Pelletier G.** Characterization and autoradiographic localization of LHRH receptors in the rat brain. *Synapse* 1987;1(6):567–571.
83. **Wen S, Götze IN, Mai O, Schauer C, Leinders-Zufall T, Boehm U.** Genetic identification of GnRH receptor neurons: A new model for studying neural circuits underlying reproductive physiology in the mouse brain. *Endocrinology* 2011;152(4):1515–1526.
84. **Soga T, Ogawa S, Millar RP, Sakuma Y, Parhar IS.** Localization of the three GnRH types and GnRH receptors in the brain of a cichlid fish: Insights into their neuroendocrine and neuromodulator functions. *J. Comp. Neurol.* 2005;487(1):28–41.
85. **Kigerl KA, McGaughy VM, Popovich PG.** Comparative analysis of lesion development and intraspinal inflammation in four strains of mice following spinal contusion injury. *J. Comp. Neurol.* 2006;494(4):578–594.
86. **Caunt CJ, Finch AR, Sedgley KR, McArdle CA.** GnRH receptor signalling to ERK: kinetics and compartmentalization. *Trends Endocrinol. Metab.* 2006;17(8):308–313.
87. **Naor Z.** Signaling by G-protein-coupled receptor (GPCR): Studies on the GnRH receptor. *Front. Neuroendocrinol.* 2009;30(1):10–29.
88. **Jiang P, Zhu T, Xia Z, Gao F, Gu W, Chen X, Yuan T, Yu H.** Inhibition of MAPK/ERK signaling blocks hippocampal neurogenesis and impairs cognitive performance in prenatally infected neonatal rats. *Eur. Arch. Psychiatry Clin. Neurosci.* 2015;265(6):497–509.
89. **Vithayathil J, Pucilowska J, Goodnough LH, Atit RP, Landreth GE.** Dentate Gyrus Development Requires ERK Activity to Maintain Progenitor Population and MAPK Pathway Feedback Regulation. *J. Neurosci.* 2015;35(17):6836–6848.

90. **Topp S, Stigloher C, Komisarczuk AZ, Adolf B, Becker TS, Bally-Cuif L.** Fgf signaling in the zebrafish adult brain: Association of Fgf activity with ventricular zones but not cell proliferation. *J. Comp. Neurol.* 2008;510(4):422–439.
91. **Lim FT, Ogawa S, Parhar IS.** Spred-2 expression is associated with neural repair of injured adult zebrafish brain. *J. Chem. Neuroanat.* 2016;77:176–186.
92. **Kerr JE, Allore RJ, Beck SG, Handa RJ.** Distribution and hormonal regulation of androgen receptor (AR) and AR messenger ribonucleic acid in the rat hippocampus. *Endocrinology* 1995;136(8):3213–3221.
93. **Hossain MS, Larsson A, Scherbak N, Olsson P-E, Orban L.** Zebrafish Androgen Receptor: Isolation, Molecular, and Biochemical Characterization1. *Biol. Reprod.* 2008;78(2):361–369.
94. **Gorelick D a., Watson W, Halpern ME.** Androgen receptor gene expression in the developing and adult zebrafish brain. *Dev. Dyn.* 2008;237(10):2987–2995.
95. **Antzoulatos E, Magorien JE, Wood RI.** Cell proliferation and survival in the mating circuit of adult male hamsters: Effects of testosterone and sexual behavior. *Horm. Behav.* 2008;54(5):735–740.
96. **Pan M, Zhang C.** Stimulatory effect of gonadal hormones on fetal rat hippocampal neural proliferation requires neurotrophin receptor activation in vitro. *Neurosci. Lett.* 2013;546:1–

SUPPLEMENTAL FIGURES

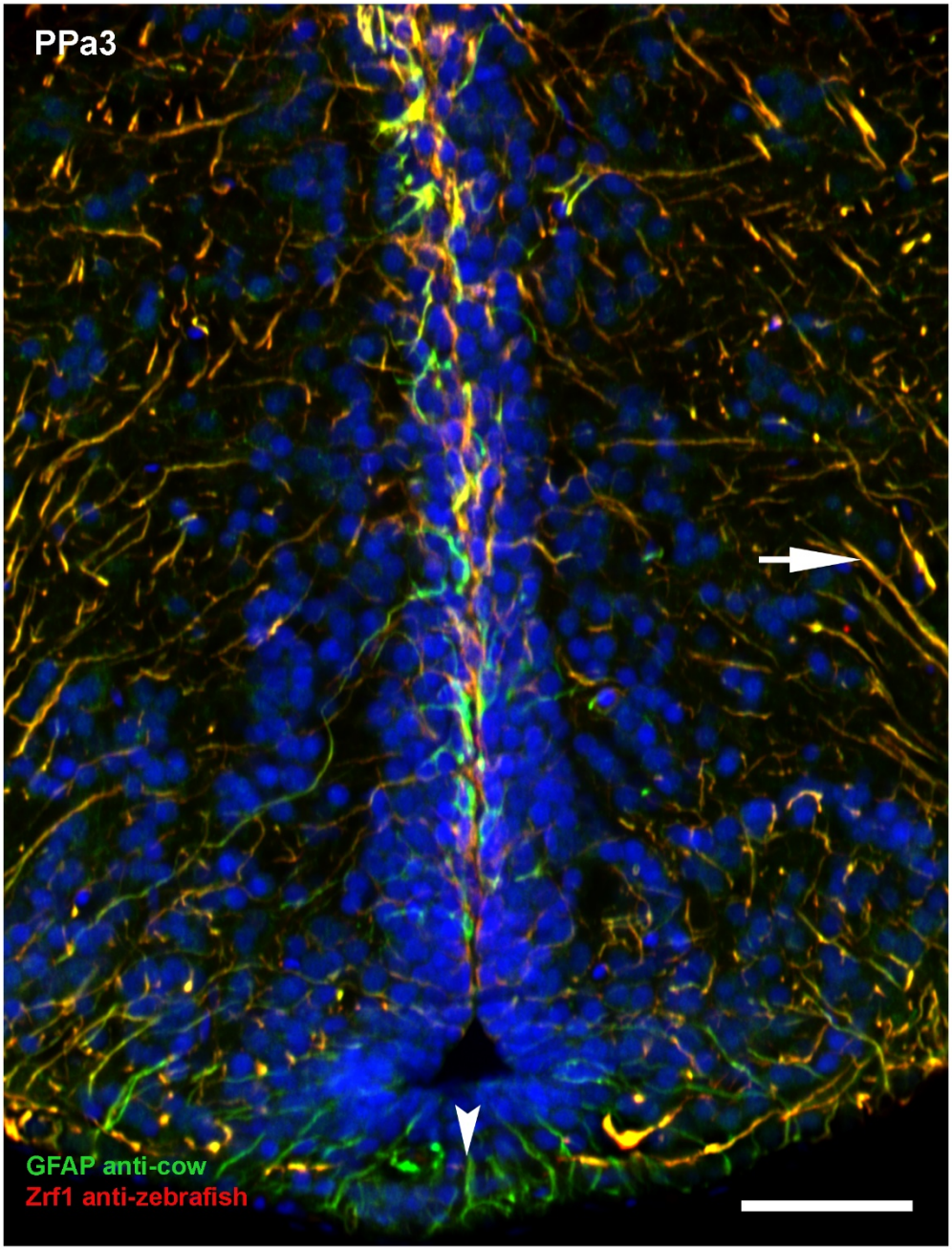

Supplemental Figure 2.1. Comparison between anti-cow GFAP and anti-zebrafish Zrf1 antibody expression. Double labeling with anti-cow GFAP and anti-zebrafish Zrf1 antibodies shows a high degree of co-localization in PPa3 transverse paraffin section of 5 µm. High co-localization was found (yellow, arrow), however, a group of cells located in the ventral region with processes that extend in to the DiV did not label with the anti-zebrafish Zrf1 antibody. All sections were labeled with DAPI labeling (blue). Diencephalic ventricle (DiV). Scale bar: 30µm.

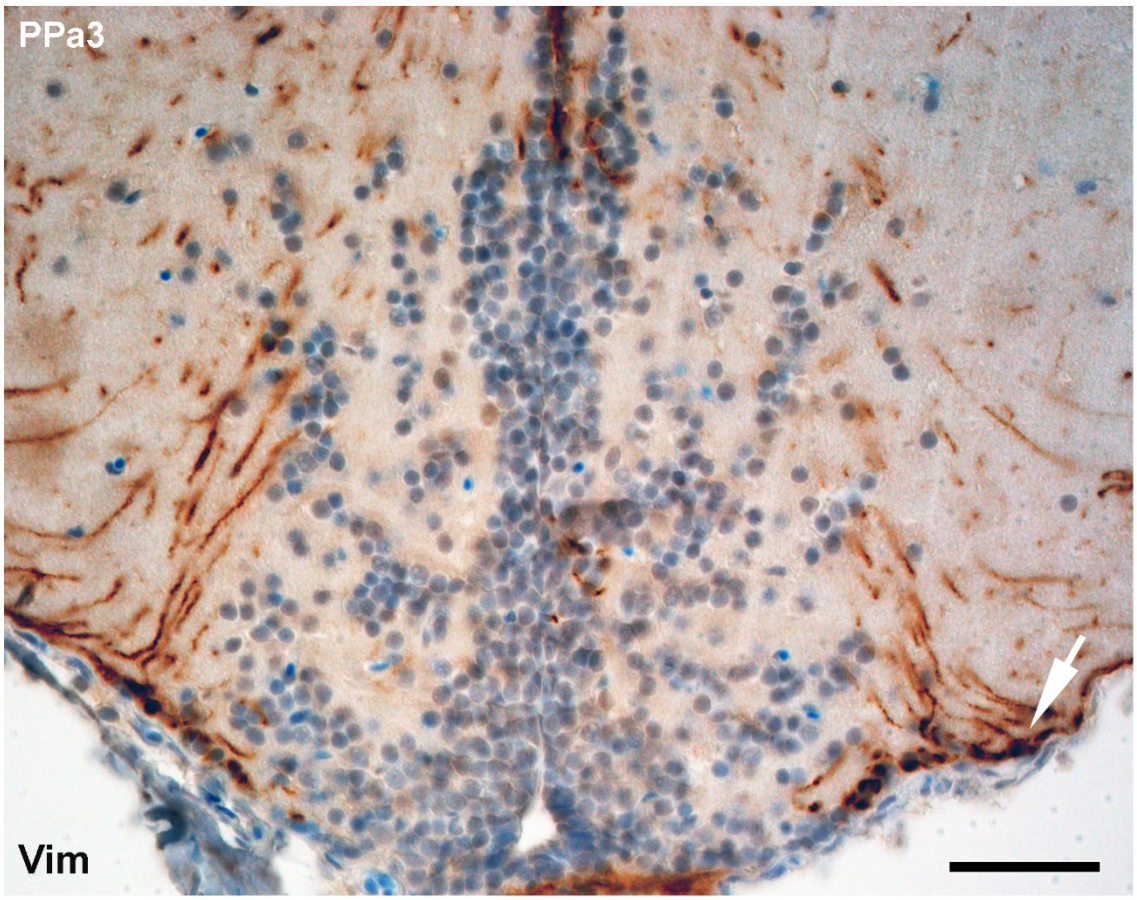

Supplemental Figure 2.2. Ventro-lateral cells positive for anti-vimentin labeling project processes towards the ventricle. Transverse paraffin section of 5 µm was immunolabeled with anti-vimentin antibodies and visualized with DAB. Arrow indicates the anti-Vim positive cells located in the ventro-lateral region of the POA. To visualize nuclei, the sections were labeled with hematoxilin (blue). Scale bar: 30µm.

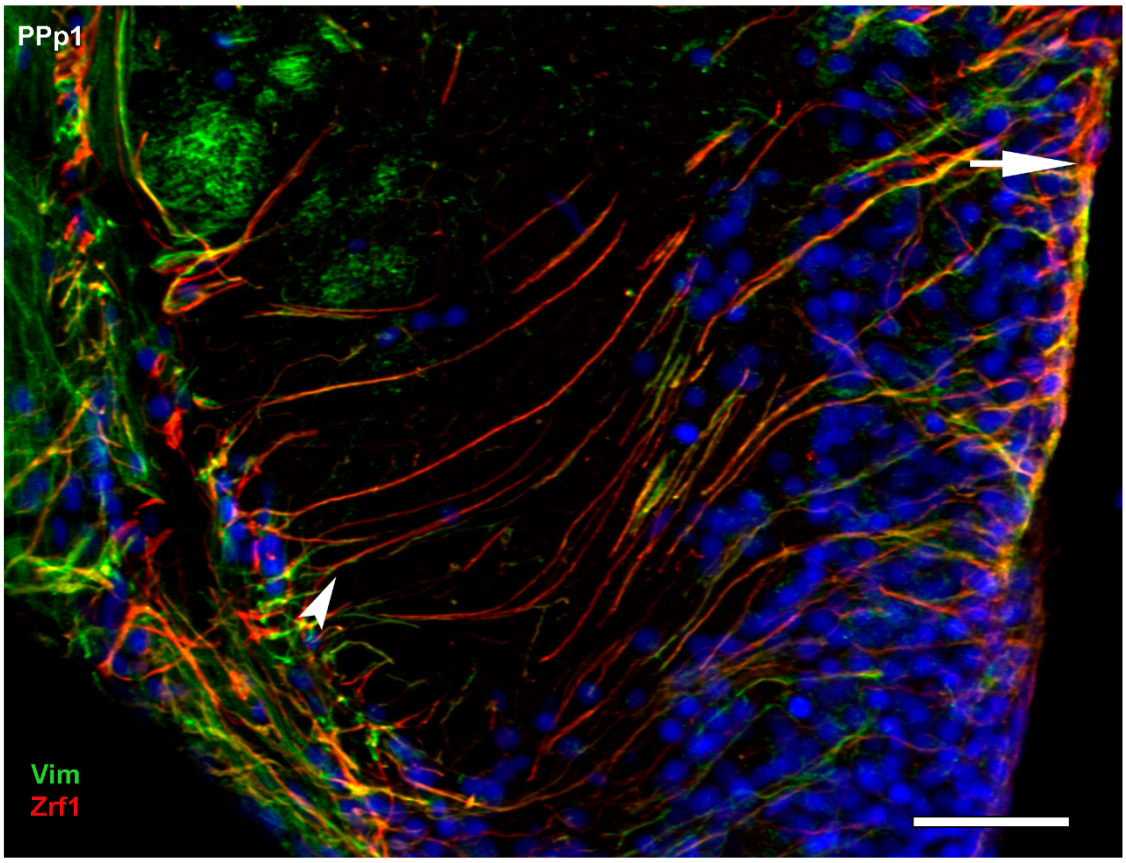

Supplemental Figure 2.3. Anti-Vim/Zrf1 positive cells in the wall of the DiV projects processes towards the lateral region of the POA in PPp1. Transverse paraffin section of 5 µm was treated with anti-Vim (green) and anti-Zrf1 (red) antibodies. Cells bodies are located in the wall of the DiV (arrow), and their processes extending along the lateral region in PPp1 (arrowheads). All sections were labeled with DAPI labeling (blue). Diencephalic ventricle (DiV). Scale bar: 30µm.

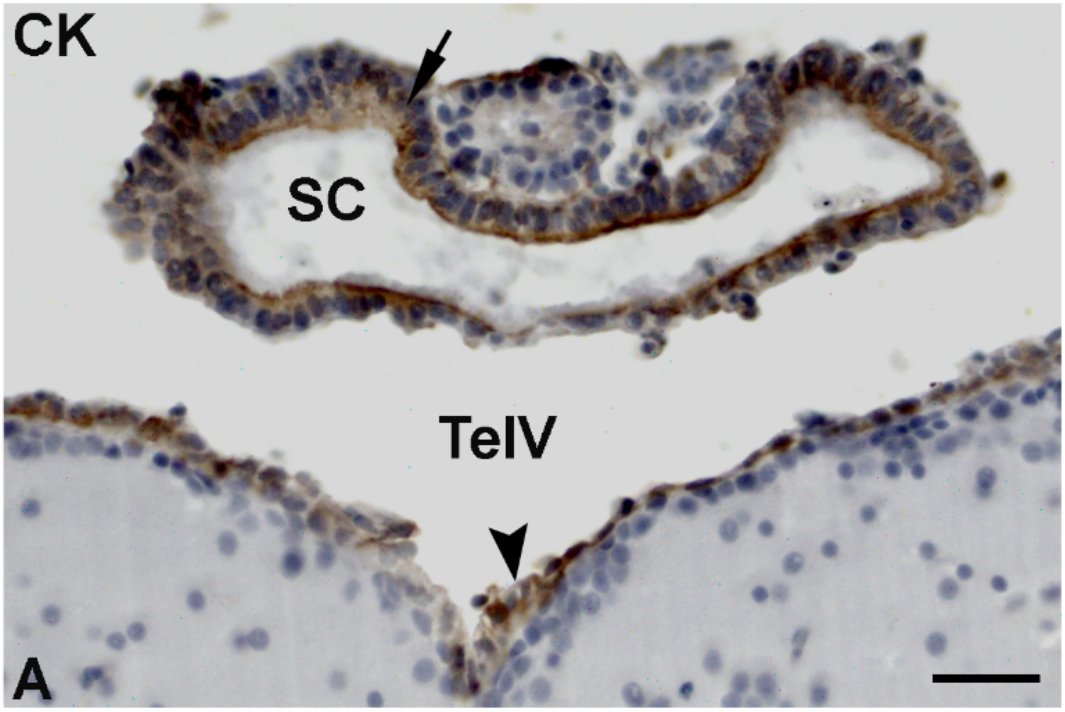

Supplemental Figure 2.4. Cytokeratin positive cells are located in the saccus dorsalis and lining the TelV. Transverse paraffin section of 5 μm was immunolabeled with anti-cytokeratin antibody and visualized with DAB. Cytokeratin (CK) positive cells (brown) in the epithelial cells in the saccus dorsalis (SC) (arrow) and wall of the telencephalic ventricle (TelV) (arrowhead). The sections were labeled with hematoxilin labeling (blue). Scale bar: 30μm.

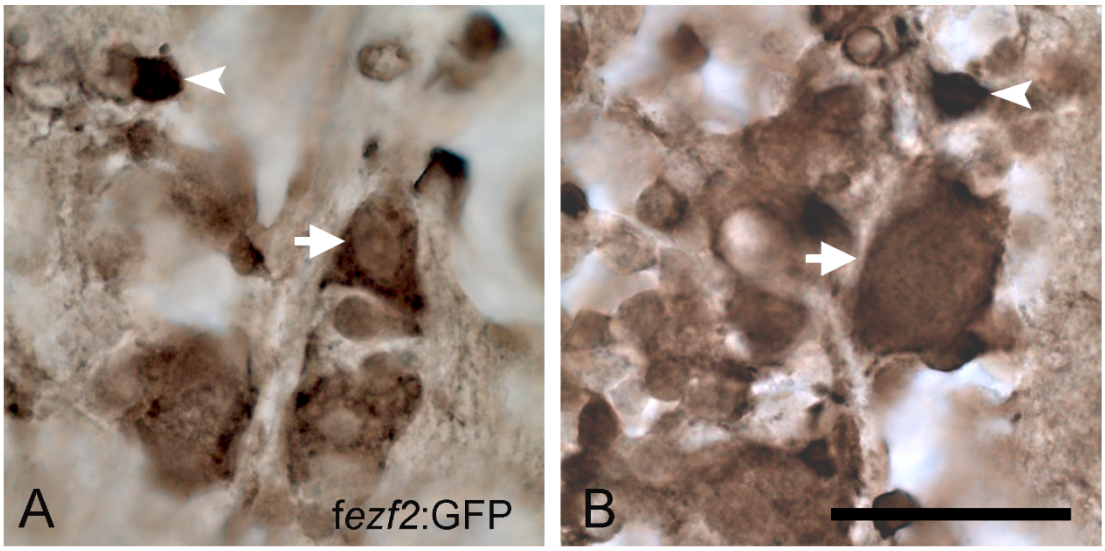

Supplemental Figure 2.5. Two populations of Fezf2:GFP are found in the POA. (A-B) Anti-GFP labeled cells in transverse cryosection of 20 µm of the PPp1 from *fezf2:gfp* adult animal. Large diameter Fezf2:GFP+ cells (20±6.4 µm) are found (arrows) and small diameter cells (6.2±1.6 µm) (arrowheads) positive for GFP (brown) was identified. Scale bar: 30µm

CHAPTER 3: IDENTIFY GNRH3 ISOFORM IN THE HYPOTHALAMUS

INTRODUCTION

The neuropeptide gonadotropin-releasing hormone (GnRH) is widely known for its role in the control of reproductive functions (reviewed in Okubo and Nagahama, 2008). Multiple GnRH isoforms have been identified in vertebrates that are classified into three main groups according to their location and sequence, namely GnRH1, GnRH2 and GnRH3 (Guilgur et al., 2007; reviewed in Lethimonier et al., 2004). The GnRH1 group contains the hypophysiotropic GnRH forms that are located in the preoptic area. It regulates gonadal maturation through stimulation of gonadotropins cells in the pituitary. The GnRH2 group, contains GnRH form located in the midbrain, its functions are related with modulated sexual and feeding behavior. Finally, the GnRH3 group, which is found only in teleost fish, localized in the ventral forebrain, it exert neuromodulatory functions (reviewed Tostivint, 2011).

All GnRH isoforms are encoded by a large precursor, consisting of four exons: exon 1 encodes the 5'-UTR; exon 2 encodes the signal peptide, GnRH decapeptide, a proteolytic cleavage site and the N-terminus of the GnRH-associated peptide (GAP); exon 3 encodes the central portion of GAP and exon 4 encodes the C- terminus of GAP along with the 3´-UTR (reviewed White and Fernald, 1998). Like the three isoforms, high level of the conservation is observed in the GnRH precursor, except for the GAP that has high divergence (White et al., 1995).

Most brain of teleosts express GnRH2 and GnRH3, but there are species that express the three isoforms of GnRH (Amano et al., 2004; Okubo et al., 2000). Analysis of RNA-seq data from our lab suggested that the gnrh1 expression is absent in zebrafish (Whitlock et al., 2019). Recently, analysis of the zebrafish genome using the

last version (Z11), confirmed that the gnrh1 is not express, and that the kctd9 gene that flanked gnrh1 on the left in other teleost species, is in opposite orientation in zebrafish indicating an inversion of the gnrh1 syntenic region (Whitlock et al., 2019). Thus, these dates conclude that the gnrh1 is absent in zebrafish.

While, it was showed that *gnrh1* is not expressed in zebrafish. It has described that GnRH3 replaced GnRH1 both in distribution and reproductive function in the hypothalamus of zebrafish (Abraham et al., 2008; Zhao et al., 2013). But, contradictory results obtained by *in situ* hybridization showed that *gnrh3* is not expressed in the hypothalamus at 56 hpf (Whitlock et al., 2003; Whitlock et al., 2005). However, we identified GnRH cells in the parvocellular preoptic nucleus of the hypothalamus, using four GnRH antibodies in fertile male zebrafish (Cortes-Campos et al., 2015). This GnRH immunoreactivity observed in the hypothalamus of zebrafish, would indicate us that there is a possibility that *gnrh3* is expressed in the hypothalamus. Thus, it was necessary to study *gnrh3* expression in the hypothalamus of zebrafish.

The objective of this work is determining whether *gnrh3* isoform is located in the hypothalamus. We used three different *gnrh3* probes previously published to detect the expression pattern of *gnrh3* by in situ hybridization in embryos of 3dpf and fertile male adult fish. In addition, we used MALDI-TOFF analysis in hypothalamus of fertile adult male zebrafish to also determine whether the *gnrh3* isoforms exist in the hypothalamus.

MATERIALS AND METHODS

Animals

The Valparaiso wild-type and Cornell wild-types strains, derived from the AB genetic background, were used for all experiments. The fish were maintained at 28 °C on a light–dark cycle of 14 and 10 h, respectively. The Institutional Animal Use and Care Committee of the Universidad de Valparaíso approved all animal procedures (#BA084-2016).

In situ hybridization

Whole mount in situ hybridization

Zebrafish embryos 3dpf were fixed in phosphate-buffered (100 mM) 4% paraformaldehyde (PFA 4%). Whole mount in situ hybridization was performed as described in Thisse et al.,(Thisse et al., 1993a) using single-stranded RNA probes labeled with digoxigenin-UTP (Roche, Mannheim, Germany). Three *gnrh3* probes were generated using previously described sequences**:** (Gopinath et al., 2004; Whitlock et al., 2005; Wu et al., 2006; Onuma et al., 2011) (Table 1). In addition, three *gnrh3* probes that exclude the GAP were designed using the primers (shown in Table 2).

Adult brain in situ hybridization

Brain from adult male zebrafish aged 1 years that underwent a “mating-training” were used. This training consists in crossing the animals two times a week for two weeks. Fertile males were selected and sacrificed at 10 AM, decapitated and their heads were fixed in PFA 4% overnight at 4°C (Cortes-Campos et al., 2015). The heads were decalcified in 0.2 Molar EDTA solution pH 7.6 for 48 h at 4°C, embedded in 1.5%

agarose/5% sucrose blocks and submerged in 30% sucrose overnight at 4 °C. Blocks were frozen at -20°C with O.C.T. Compound (Tissue Tek®). Twenty µm sections were cut using a cryostat. In situ hybridization was performed as described in Thisse et al., (Thisse et al., 1993a), except that, the proteinase-K step was not performed. *gnrh3* probes used are shown Table 1.

Immunohistochemistry

Whole mount immunohistochemistry

The embryos 3dpf were fixed in 4% paraformaldehyde with 7% saturated picric acid for two hours at room temperature. Immunocytochemistry procedures were carried out as previously described (Whitlock et al., 2003). To detect GnRH neurons, Mouse anti-GnRH LHR13 antibody (Park and Wakabayashi, 1986) was used at (1:100). Antibody labeling was visualized with goat anti-mouse secondary (1:200) followed by mouse peroxidase anti-peroxidase (1:500; Sternberger monoclonals) and ImmPACT® DAB Peroxidase (HRP) Substrate (VECTOR; SK-4105).

Adult brain immunohistochemistry

Male adult brain 1 years old were used. Prior to the immunohistochemistry, the male adult zebrafish were subjected to a “mating-training” (Cortes-Campos et al., 2015). Then, brains were fixed in PFA 4% with 7% saturated Picric Acid for 4 h at room temperature and heads were decalcified in 0.2 Molar EDTA solution pH 7.6 for 48 h at 4°C. Next, the heads were embedded in 1.5% agarose/5% sucrose blocks and submerged in 30% sucrose overnight at 4 °C. Blocks were mounted using O.C.T. Compound (Tissue Tek®) and frozen at -20°C. Twenty µm sections were cut using a cryostat. Mouse anti-GnRH LHR13 (1:100) (Park and Wakabayashi, 1986) was used. The labeling was visualized using VECTASTAIN elite ABC HRP kit (Rabbit IgG.

VECTOR; PK-6101) and ImmPACT® DAB Peroxidase (HRP) Substrate (VECTOR; SK-4105).

MALDI-TOF mass spectrometry

To prepare the samples, 12 males zebrafish aged 1 years that underwent a mating-training (Cortes-Campos et al., 2015) were used. The hypothalamus were dissected in dissectiong saline: 128 mM NaCl, 2 mM KCl, 1.8 mM CaCl2, 4 mM MgCl2, 36 mM sucrose, 5 mM HEPES, pH 7.1. Each hypothalamus was carefully cut into small pieces using fine scissors and transferred to the MALDI target and left to dry. The samples were analyzed by MALDI-TOF mass spectrometry as described in (Wegener et al., 2010).

Microscopy and images processing

Bright field images were obtained using a Leica DMR microscope (Leica Microsystems CMS GmbH, Wetzlar, Germany) and a Leica DFC 480 camera (Leica Microsystems Ltd, Heerbrugg, Switzerland) and processed with the Leica Application Suite 2.3.3 software (Leica Microsystems Ltd). All images were edit using ImageJ® software (National Institute of Health, Bethesda, Maryland, USA).

RESULTS

To determine whether *gnrh3* is expressed in the hypothalamus, we generated three probes recognizing *gnrh3* based on previously published studies (Gopinath et al., 2004; Whitlock et al., 2005; Wu et al., 2006; Onuma et al., 2011). All probes included the GnRH-associated protein (GAP) which is highly divergent between the different forms of GnRH, although each probe was a slightly different size: probe 1 (213 nucleotides), probe 2 (255 nucleotides) and probe 3 (354 nucleotides) (Fig. 3.1).

In agreement with our previously published work (Gopinath et al., 2004) Whitlock et al., 2005), all probes recognized the *gnrh3* cells of the terminal nerve at 3dpf (Fig. 3.2, A-C, arrowhead). Consistent with our previous findings, none of the probes labeled cells in the developing hypothalamus (Gopinath et al., 2004). The LRH13 antibody recognizes both the GnRH cells of the terminal nerve (Fig. 3.2, D, arrowhead) and cells in the developing hypothalamus (Fig. 3.2, D, arrow). To expand our previous analysis we used the same *gnrh3* probes in cryosections of adult tissue following the protocol of selecting reproductive males zebrafish (Cortes-Campos et al., 2015). In agreement with not only our previous publications but those of others the *gnrh3* probes (Whitlock et al., 2005; Wu et al., 2006) did not recognize cells in the parvocellular region of the adult brain (Fig. 3.3, A-B, probe 1; Fig. 3.3, C-D, probe 2). Surprisingly, different results were obtained using the sequence published by (Onuma et al., 2011) (Fig 3.1, probe 3), where a small population of *gnrh3* positive cells were found in the lateral region near the dorsomedial optic tract (DOT) (Fig. 3.3, E-H), this result was consistent with the immunohistochemistry using LRH13 antibody in adult brain (Fig. 3.4, A, B). We performed an alignment of the three sequence of the gnrh3 probes generated (Fig 3.1, A, B). The alignment showed that the probe generated by

Onuma et al., 2011) had 73 nucleotides more than the probes generated by (Whitlock et al., 2005; Wu et al., 2006), located in the 3´UTR (Fig 3.5, arrow). Thus, this increase in the number of nucleotides in the 3´UTR of the gnrh3 probes published by (Onuma et al., 2011) could recognize cells in the lateral region near the DOT.

Primer	Sequence (5´-3´)	Direction	
1F-GnRH3	CAGCACTGGTCATATGGTTGGCTTCCCGG	F	Whitlock *et al.*, 2005
1R-GnRH3	CACTCTTCCCCGTCTGTCGG	R	
2F-GnRH3	TTAGCATGGAGTGGAAAGGAAGGTTG	F	Wu*et al.*, 2006
2R-GnRH3	CTTTCAGAGGCAAACCTTCAGCAT	R	
3F-GnRH3	GCATGGAGTGGAAAGGAAGG	F	Onuma *et al.*, 2011
3R-GnRH3	GGAGTCCAAAAACATGGTCT	R	

A

ATCTTGAACAAACACAGCAGTTTTAGCATGGAGTGGAAAGGAAGGTTGTTGG
TCCAGTTGTTGCTGTTAGTTTGTGTGTTGGAGGTCAGTCTTTGCCAGCACTG
GTCATATGGTTGGCTTCCCGGTGGAAAAAGAAGCGTTGGTGAAATGGAGGCA
ACATTCAGGATGTTGGATCCAGGTGACACAGTGCTGTCTATTCCTGCTGATT
CTCCAATGGAGCAGCTTTCACCAATACACATAGTGAATGAGGTGGATGCTGA
AGGTTTGCCTCTGAAAGGACAAAGATATTCCGACAGACGGGGAAGAGTGTAA
AAATATAAATGATGAAGCTGATATGAGTATGAATTTTGTTCCATAGGAGACC
ATGTTTTTGGACTCCTAATGAAATATCCTCCAAATTATGGATTTAATAAATA
CACTTCACTGAAGGAAC

Signal peptide: GnRH3-coding region: Cut site: GnRH asociated peptide:

B

Figure 3.1. Analysis of the *gnrh3* probes. **(A)** Primer list used to generate *gnrh3* probes. **(B)** Sequence of the cDNA encoding *gnrh3* precursor. All probes include *gnrh3*-coding region and GnRH associated peptide.

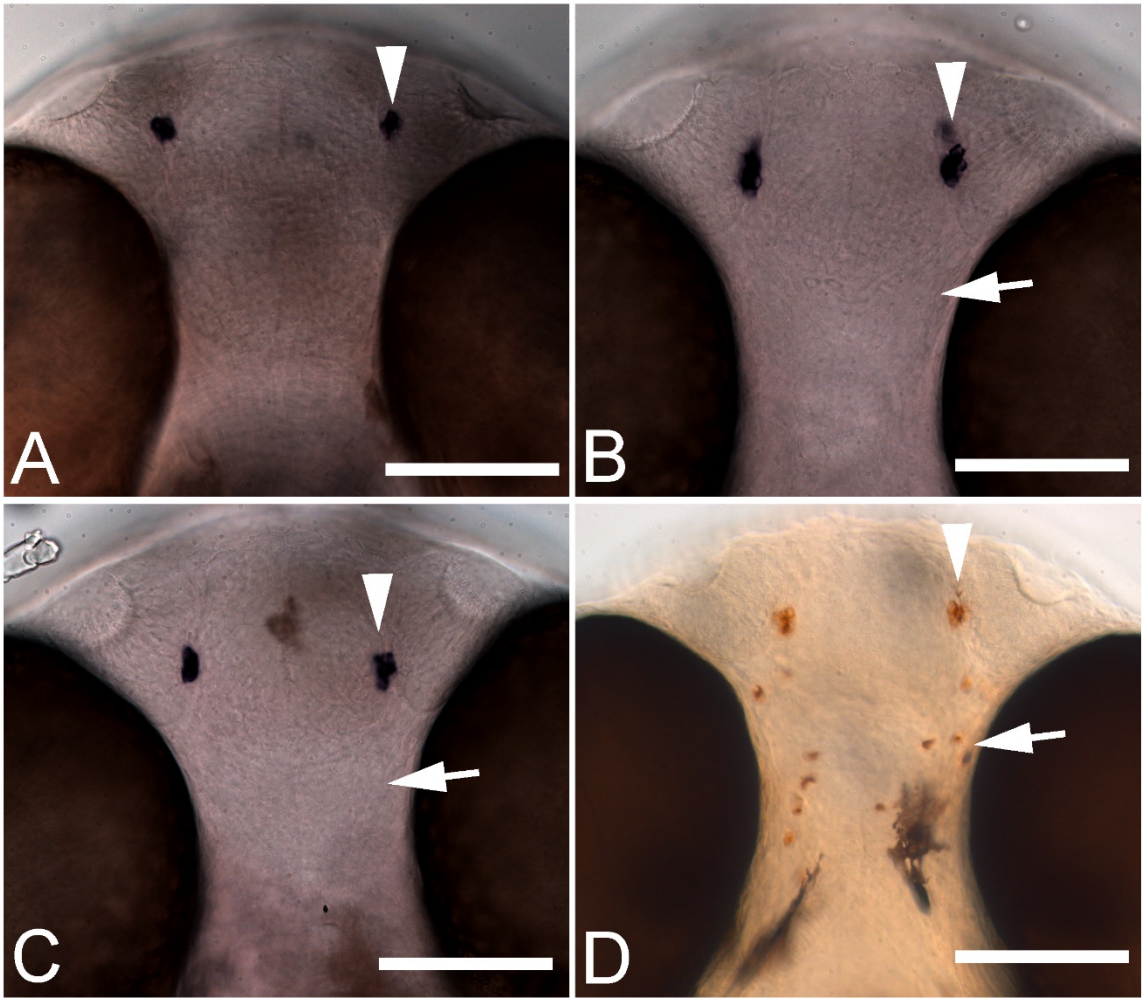

Figure 3.2. *gnrh3* is not expressed in the hypothalamus of embryos 3 dpf. (A-C) *In situs* hybridization in embryos using three different *gnrh3* probes. **(A)** Whitlock et al., 2005. **(B)** Wu et al., 2004. **(C)** Onuma et al., 2011. **(D)** Immunohistochemical to GnRH using the LRH13 antibody. (arrowhead) indicate *gnrh3* neurons in the terminal nerve (arrow) and indicates hypothalamic GnRH neurons. Scale bar: 100µm.

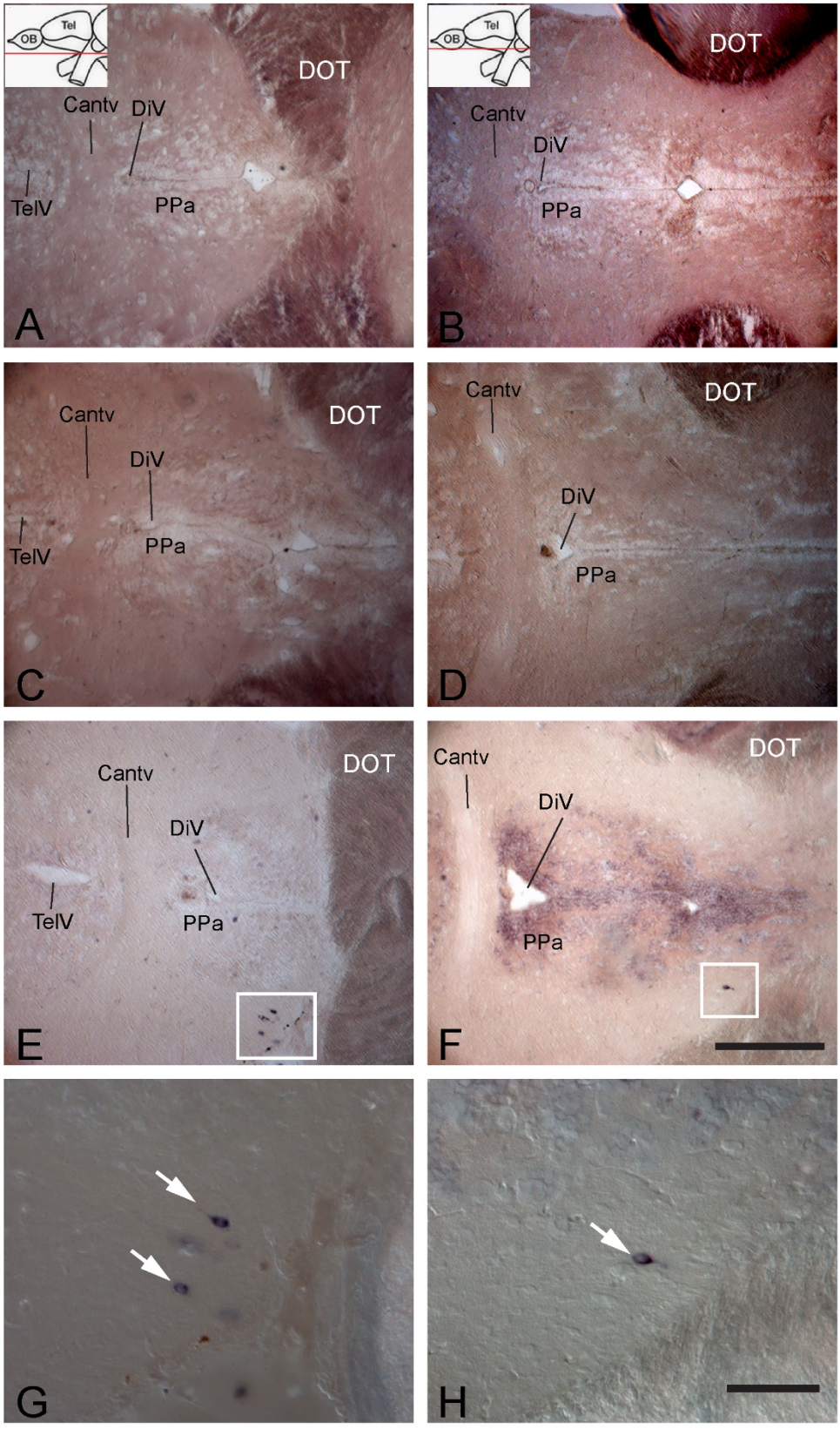
OB
Tel
DOT
Cantv
DiV
TelV
PPa
A
B
C
D
E
F
G
H

Figure 3.3. *gnrh3* (Onuma et al., 2011) probe recognize cells located in the ventral-lateral region of the POA of adult zebrafish. (A-H) *In situ* hybridization of *gnrh3* in horizontal cryosections of the PPa with three different probes. **(A-B)** Whitlock et al., 2005. **(C-D)** Wu et al., 2006. **(E-F)** Onuma et al., 2011. **(A, C, E)**. Sections corresponding to ventral region (**A**, schematic figure, up, left) and **(B, D, F)** dorsal region (**B**, schematic figure, up, left) to the PPa. **(E-F)** *gnrh3* positive cells are found in the lateral region of the PPa. **(G-H)**. High magnification of *gnrh3* positive cells (arrow) of square of G and H respectively. Commissura anterior, pars ventralis (Cantv). Diencephalic ventricle (DiV). dorsomedial optic tract (DOT). Parvocelullar preoptic nucleus, anterior part (PPa). Telencephalic ventricle (TelV). Scale bar **(F)** 150 μm and **(H)** 50μm.

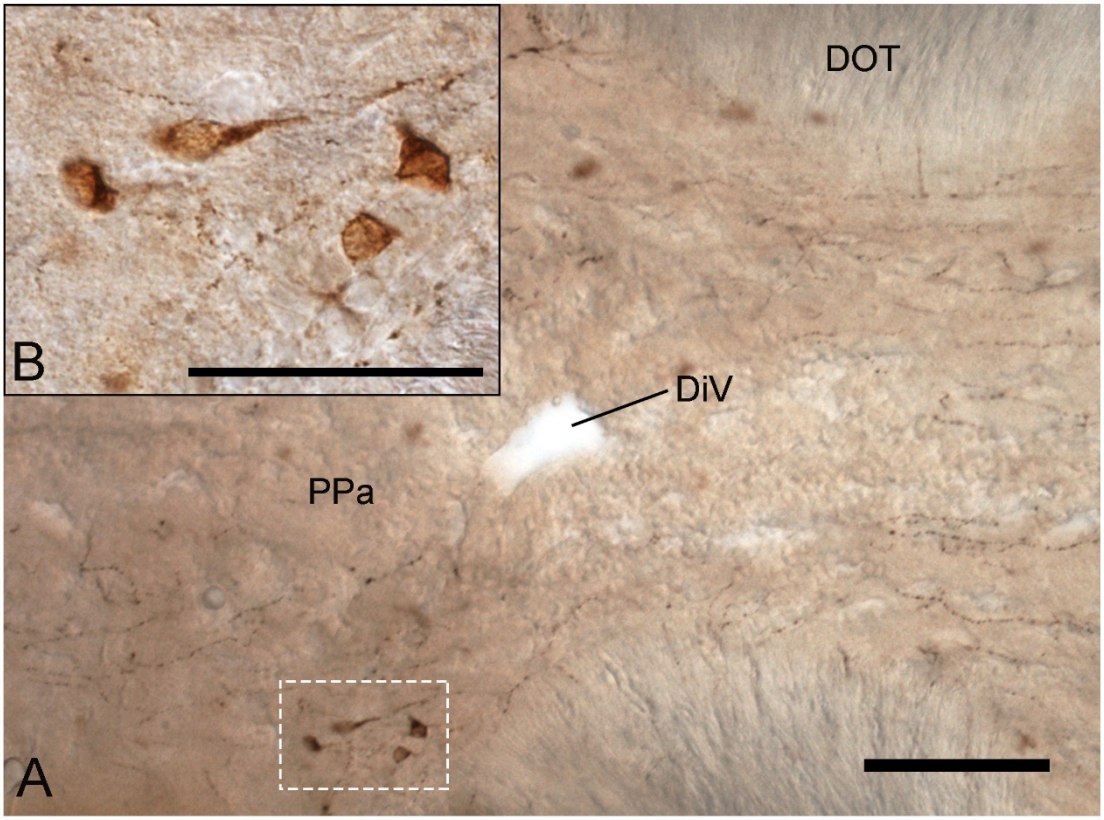

Figure 3.4. LRH13 antibody labels cells similar to those observed with *gnrh3* probe (Onuma). (A-B) immunocytochemistry in horizontal cryosections of PPa. **(A)** Cells positive for anti-LRH13 antibody are located near the dorsomedial optic tract (DOT) (box). **(B)** Magnification of box of (A). Diencephalic ventricle (DiV). Parvocelullar preoptic nucleus, anterior part (PPa). Scale bar 60 μm.

Figure 3.5. Alignment of the *gnrh3* probes. *gnrh3* probes designed by Wu (Wu et al., 2006), Whitlock by (Whitlock et al., 2005) and Onuma (Onuma et al., 2011) were aligned with Crustal Omega. The probe generated by Onuma et al., 2011 has 73 nucleotides more in the 3´UTR (arrow).

While in GnRH preprohormone is quite conserved, the GAP coding sequences are highly divergent between GnRH isoforms (White et al., 1995). Because of this, we generated three probes to *gnrh3* with different size that exclude the GAP (Table 3.1) and thus generate non-specific *gnrh3* probes that could recognize *gnrh* in the hypothalamus. However, *in situs hybridization* in 3dpf embryos showed expression of *gnrh3* only in the terminal nerve (Fig. 3.6, A-C, arrowhead) contrary to the result obtained with the LRH13 antibody also has immunoreactivity in the hypothalamus (Fig 3.6, D, arrow), in agreement with the work of our lab and other lab (Torgersen et al., 2002; Whitlock et al., 2005). It is surprising that the expression of *gnrh3* was not observe in the hypothalamus because previously we have shown anti-GnRH positive cells, in the hypothalamus using a variety of antibodies recognizing GnRH: LHR13 (Park and Wakabayashi, 1986), HU11B (Millipore), BB8 (Kah et al., 1986), anti-mGnRH (Sigma-Aldrich) (Cortes-Campos et al., 2015).

Primer	Sequence (5´-3´)	Direction	Size of probe (nt)
1NGAP-GnRH3	GCATGGAGTGGAAAGGAAGGTTGT	F	88
1NGAP-GnRH3	CCATATGACCAGTGCTGGCAAAGA	R	
2NGAP-GnRH3	AGCATGGAGTGGAAAGGAAGGTTG	F	89
2NGAP-GnRH3	CCATATGACCAGTGCTGGCAAAGA	R	
3NGAP-GnRH3	GCATGGAGTGGAAAGGAAGGTTGT	F	107
3NGAP-GnRH3	TTTTCCACCGGGAAGCCAACCATA	R	

Table 3.1. Primer to design *gnrh3* probes that exclude the GAP.

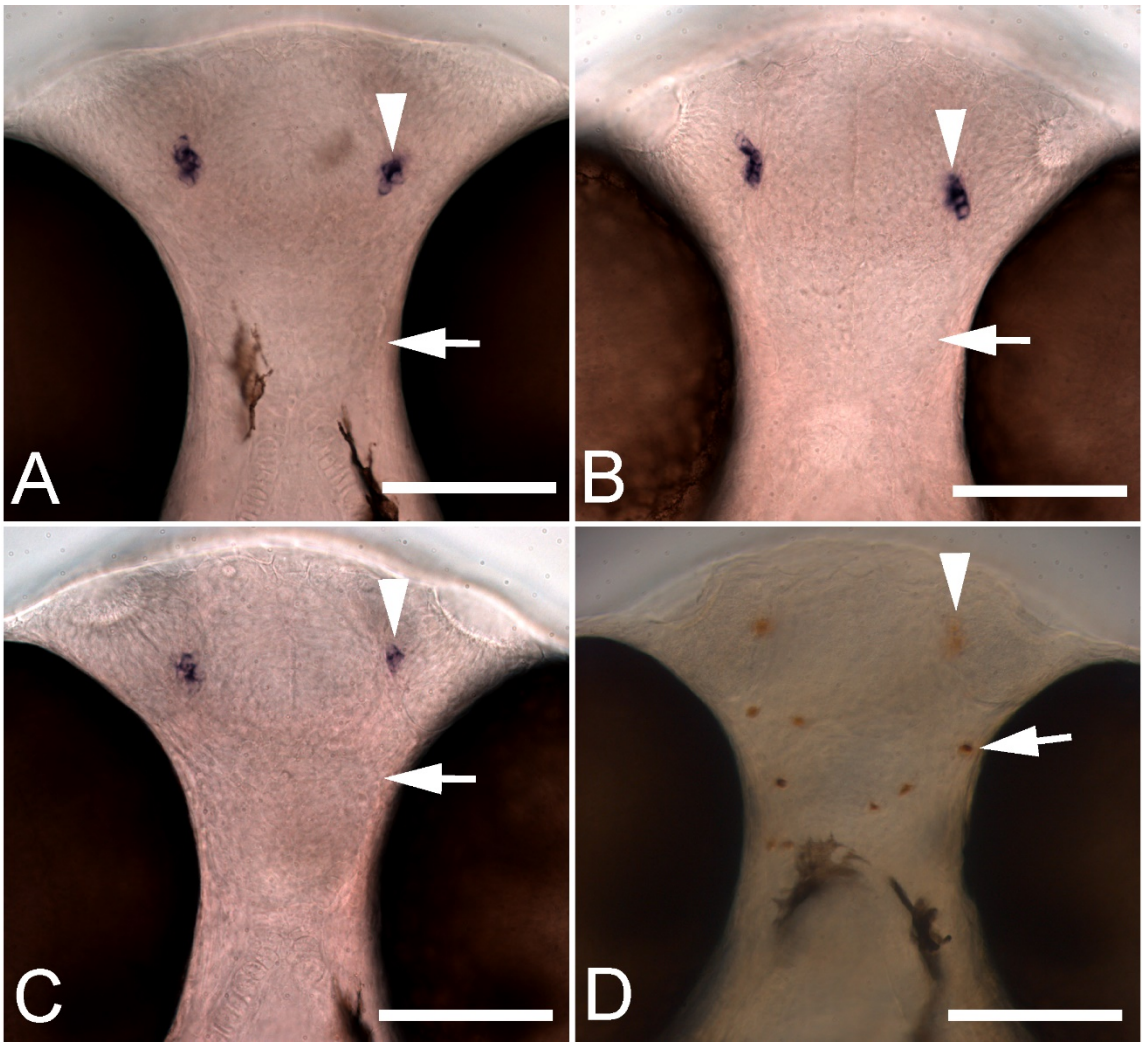

Figure 3.6. *gnrh3* probes excluding the GAP do not recognize GnRH transcript in the hypothalamus in embryos of 3dpf. (A-C) *In situs* in 3dpf embryos using three different *gnrh3* probes. **(D)** Immunohistochemical to GnRH using the LRH13 antibody. (arrowhead) indicate *gnrh3* neurons located in the terminal nerve and (arrow) show hypothalamic GnRH neurons. Scale bar: 100μm.

In order to determine whether any GnRH isoforms were detectable in the adult hypothalamus, we collaborated with Dr Chistian Wegener (University of Würzburg, Germany) to perform protein analysis on tissue dissected from the hypothalamus of the adult zebrafish. Despite of the detection a variety of hypothalamic peptides, we did not detect GnRH1, GnRH2 or GnRH3 isoforms in the hypothalamus by MALDI-TOF or ORBITRAP methods (Fig. 3.7; Table 3.2). Surprisingly, these results suggest that the GnRH peptide is not found in the hypothalamus of zebrafish.

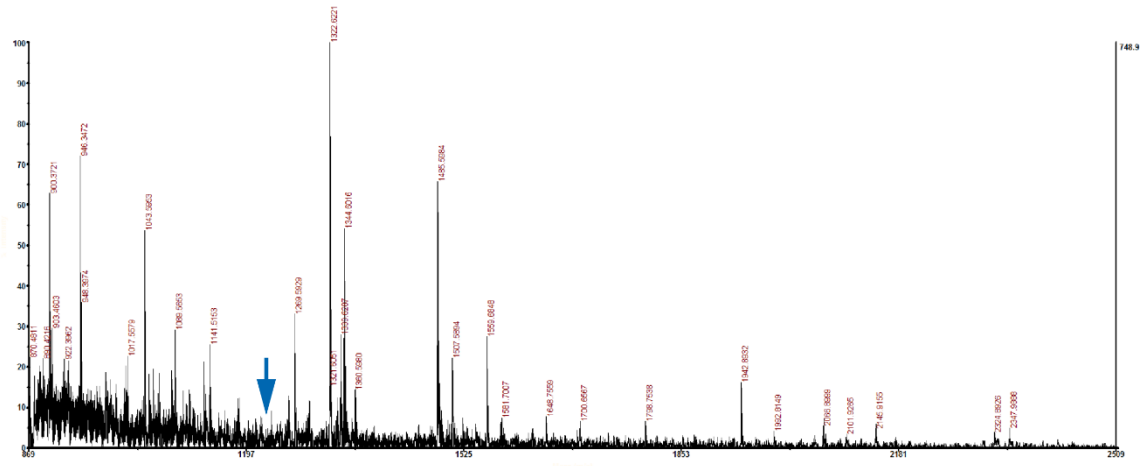

Figure 3.7. GnRH1, GnRH2 and GnRH3 peptides are not located in the hypothalamus. Mass spectrometry analysis of the hypothalamus of adult male zebrafish. Arrow indicate the peak of GnRH1 (1212,336), GnRH2 (1254,32), GnRH3 (MW: 1212,31) if they were located in the hypothalamus. All fish were selected for mating training (Cortes-Campos et al., 2015).

Peptides identified in the zebrafish brain by nanoLC-MS/MS.
proSAAS
neuroendocrine protein 7B2
secretogranin-2[a]
secretogranin-2b
chromogranin-A
Somatostatin
somatostatin-2
somatostatin-3/cortistatin
Dynorphin
enkephalin-A
enkephalin-B
enkephalin (partial)
neuropeptide FF
neuropeptide VF
neuropeptide Y
Galanin
galanin isoform X1
corticotropin releasing factor
thyrotropin-releasing hormone, thyroliberin
tachykinin 3[a]
vasoactive intestinal polypeptide type I
pituitary adenylate cyclase-activating polypeptide isoform 1
growth hormone-releasing hormone
cocaine- and amphetamine-regulated transcript precursor
calcitonin gene-related peptide 2
neuromedin-B
Nociceptin
melanin-concentrating hormone
neuroendocrine convertase 1 / proprotein convertase 1/3
peptidyl-glycine alpha-amidating monooxygenase A
ephrin A1a
fibrinogeen alpha chain
Apolipoprotein
relaxin 3[a]
KiSS-1 metastasis-suppressor precursor
kisspeptin 2 precursor

Table 3.2. Peptides identified in the zebrafish brain by nanoLC-MS/MS.

DISCUSSION

Here, by using two *gnrh3* probes published by (Onuma et al., 2011; Whitlock et al., 2005; Wu et al., 2006), we confirmed, in agreement with previous work, *gnrh3* is not expressed in the magnocellular and/or parvocellular nuclei of the POA of developing 3dpf and fertile adult zebrafish. The probe generated from sequence in Onuma et al labeled *gnrh3* positive cells in the lateral region of the POA in fertile adult fish. The anti-GnRH antibody that detects GnRH cells in the parvocellular nucleus of the POA (Cortes-Campos et al., 2015) also detects cells similar to the expressing *gnrh3* in the lateral POA. However, MALDI-TOF analysis did not show any GnRH isoforms in the hypothalamus. Therefore, these results are in agreement with recent publications showing that knock-out of the three *gnrh* genes does not affect the control of reproduction in zebrafish (Spicer et al., 2016; Liu et al., 2017; Marvel et al., 2018).

The expression of *gnrh3* in the hypothalamus of zebrafish is still a controversy, because non-convincing studies performed by *in situ* hybridization to *gnrh3* (Palevitch et al., 2007) and *gnrh3*:GFP reporting line (Abraham et al., 2008) (Abraham et al., 2009), support the expression of *gnrh3* in the hypothalamus. Contradictory evidence was obtained by (Gopinath et al., 2004; Whitlock et al., 2005), that demonstrated the *gnrh3* transcript is not express in the hypothalamus of zebrafish. Thus, the results in this thesis confirm the results obtained by Gopinath et al (2006) and Whitlock et al. (2005).

While, our results obtained by MALDI-TOF, *in situ* hybridization, and zebrafish genome analysis (Whitlock et al., 2018), did not show any GnRH isoforms in the hypothalamus of zebrafish, our previous study using 4 different antibodies that recognizes GnRH1 and GnRH3 showed GnRH immunoreactivity cells located in

parvocellular nucleus (Cortes-Campos et al., 2015). These data are consistent with observations of GnRH cells in the parvocellular nucleus performed in dwarf gourami and tilapia using GnRH antibody (Yamamoto et al., 1998), but these fishes have three genes coding for *gnrh*, unlike zebrafish (Whitlock et al., 2019). Moreover, here, we detected cells positive to GnRH3 and *gnrh3* transcript using GnRH antibody and *gnrh3* probes published by Onuma et al respectively, located in the lateral region of the POA, a region that is not involved in the release of reproductive hormones. Furthermore, the morphology of the *gnrh3* positive cells that we describe here, are not consistent with them being peptidergic calling into question their identity and role in reproduction. Finally, these data are most likely erroneous because our protein analysis showed that there is no GnRH protein in the hypothalamus of the adult zebrafish. Thus, the GnRH immunoreactivity, we reported previously (Cortes-Campos et al., 2015) and the *gnrh3* gene expression reported here, remains unresolved.

Recently, two studies generated *gnrh3*-null zebrafish, found that gnrh3 mutation does not produce change in the gametogenesis and reproductive capacity (Spicer et al., 2016; Liu et al., 2017). These studies are contradictory to a study that reported the laser ablation of GnRH3:GFP neurons generate infertility in zebrafish, suggesting that GnRH3 might play a role in reproduction (Abraham et al., 2010). However, the GnRH3:GFP cells may contain other important peptides and neuron ablation damage surrounding neurons that contain other peptides important for the reproductive process. Here, we showed that GnRH isoforms are not located in the hypothalamus of zebrafish, supporting the lack of effect on the reproduction observed in *gnrh3*-knock-out zebrafish.

Studies showing that *gnrh3* did not play role in the reproduction led to possibility that the *gnrh2* gene is important for reproduction in zebrafish. A study carried out using a *gnrh2:egfp* reporter line, showed *gnrh2*:*egfp* positive neurons located in the midbrain,

project their axons towards the pituitary (Xia et al., 2015). The function of GnRH2 in vertebrates is unclear but it is known that GnRH2 can activate all four GnRH receptors in zebrafish (Tello et al., 2008). However, knockout of *gnrh2* alone or with *gnrh3* in zebrafish did not cause reproductive defects (Marvel et al., 2018).These results combined with our data indicate that none of the GnRH isoforms in zebrafish control reproduction, thus suggesting the presence of another peptide replacing the role of GnRH in reproduction.

The hypothalamic pathway controlling reproduction in mammals and teleosts differs in structure: unlike mammals, teleosts do not have a median eminence where GnRH is released into the vascular system. In teleosts the neurosecretory fibers of the hypothalamus directly innervate the pituitary, triggering release from the endocrine cells (Peter et al., 1990). This direct neuroendocrine regulation could increase the possibilities for reproductive control. In fact, gonadotroph containing cells can respond not only to neuropeptides, but also aminergic and amino acid neurotransmitters (rewieved in Chang et al., 2009; Trudeau, 2018). Due to this direct endocrine regulation, in zebrafish has been suggested a compensatory mechanism to stimulate the reproductive axis in absence of GnRH. This possible compensatory mechanism may involve genes whose increased their expression in the *gnrh3* knockout animals: follicle-stimulating hormone beta (*fshb*), luteinizing hormone beta (lhb), and chorionic gonadotropin subunit alpha (*cga*) (Spicer et al., 2016). Changes in gene expression were also observed in double knockouts of *gnrh2/gnrh3* where increases in gonadotropin inhibitory hormone (*gnih*), secretogranin (scg2), tachykinin 3a (*tac3a*), and pituitary adenylate cyclase-activating peptide 1 (*pacap1*) were observed and agouti-related peptide 1 (*agrp1*) decreased in expression (Marvel et al., 2018).

Because of its role in reproduction in some vertebrate Kisspeptin (Kiss) a regulation in the secretion of GnRH in mammals (reviewed in Dungan et al., 2006), In zebrafish, two *kiss* genes called *kiss1* and *kiss2* have been identified, but according to their expression in the hypothalamus, *kiss2* is associated with a reproductive functions (Servili et al., 2011). Because of this *Kiss2* is a potential candidate for reproductive control in zebrafish in the absence of GnRH. Yet, there were no reproductive defects in the triple knockout of *gnrh3*, *kiss1* and *kiss2*, genes in adult zebrafish, but the triple knockout animals had an increase in gene expression of neuropeptide Y (*npy*), tachykinin 3 (*tac3*) and secretogranin 2 (*scg2*) (Liu et al., 2017).

In conclusion, we did not identify any GnRH isoforms in the hypothalamus of zebrafish. Several studies including our result indicate that exist another mechanism independent of GnRH and Kiss in the reproductive control in zebrafish. In order to identify an alternative mechanism for the reproductive control, our analysis of unidentified peaks in the MALDI-TOF data led to a protein recently identified called Phoenixin (PNX). It is widely found in the hypothalamus, promoting the release of LH from the pituitary (Yosten et al., 2013), by increasing the expression of GnRH-Receptor (GnRH-R) (Yosten et al., 2013), GnRH and Kiss (Treen et al., 2016).

REFERENCES

1. **Okubo K, Nagahama Y.** Structural and functional evolution of gonadotropin-releasing hormone in vertebrates. *Acta Physiol. (Oxf).* 2008;193(1):3–15.
2. **Guilgur LG, Ortí G, Strobl-Mazzulla PH, Fernandino JI, Miranda LA, Somoza GM.** Characterization of the cDNAs encoding three GnRH forms in the pejerrey fish Odontesthes bonariensis (Atheriniformes) and the evolution of GnRH precursors. *J. Mol. Evol.* 2007;64(6):614–627.
3. **Lethimonier C, Madigou T, Muñoz-Cueto J-A, Lareyre J-J, Kah O.** Evolutionary aspects of GnRHs, GnRH neuronal systems and GnRH receptors in teleost fish. *Gen. Comp. Endocrinol.* 2004;135(1):1–16.
4. **Tostivint H.** Evolution of the gonadotropin-releasing hormone (GnRH) gene family in relation to vertebrate tetraploidizations. *Gen. Comp. Endocrinol.* 2011;170(3):575–581.
5. **White RB, Fernald RD.** Genomic structure and expression sites of three gonadotropin-releasing hormone genes in one species. *Gen. Comp. Endocrinol.* 1998;112(1):17–25.
6. **White SA, Kasten TL, Bond CT, Adelman JP, Fernald RD.** Three gonadotropin-releasing hormone genes in one organism suggest novel roles for an ancient peptide. *Proc. Natl. Acad. Sci.* 1995;92(18):8363–8367.
7. **Amano M, Okubo K, Yamanome T, Oka Y, Kawaguchi N, Aida K, Yamamori K.** Ontogenic Development of Three GnRH Systems in the Brain of a Pleuronectiform Fish, Barfin Flounder(Endocrinology). *Zoolog. Sci.* 2004;21(3):311–317.
8. **Okubo K, Amano M, Yoshiura Y, Suetake H, Aida K.** A novel form of gonadotropin-releasing hormone in the medaka, Oryzias latipes. *Biochem. Biophys. Res. Commun.* 2000;276(1):298–303.
9. **Whitlock KE, Postlethwait J, Ewer J.** Neuroendocrinology of reproduction: Is gonadotropin-releasing hormone (GnRH) dispensable? *Front. Neuroendocrinol.* 2019;(November 2018):0–1.
10. **Abraham E, Palevitch O, Ijiri S, Du SJ, Gothilf Y, Zohar Y.** Early development of forebrain gonadotrophin-releasing hormone (GnRH) neurones and the role of GnRH as an autocrine migration factor. *J. Neuroendocrinol.* 2008;20(3):394–405.
11. **Zhao Y, Lin M-C a, Farajzadeh M, Wayne NL.** Early development of the gonadotropin-releasing hormone neuronal network in transgenic zebrafish. *Front. Endocrinol.*

(Lausanne). 2013;4(August):107.

12. **Whitlock K., Wolf C., Boyce M.** Gonadotropin-releasing hormone (gnrh) cells arise from cranial neural crest and adenohypophyseal regions of the neural plate in the zebrafish, danio rerio. *Dev. Biol.* 2003;257(1):140–152.
13. **Whitlock KE, Smith KM, Kim H, Harden M V.** A role for foxd3 and sox10 in the differentiation of gonadotropin-releasing hormone (GnRH) cells in the zebrafish Danio rerio. *Development* 2005;132(24):5491–502.
14. **Cortes-Campos C, Letelier J, Ceriani R, Whitlock KE.** Zebrafish adult-derived hypothalamic neurospheres generate gonadotropin-releasing hormone (GnRH) neurons. *Biol. Open* 2015:1–10.
15. **Thisse C, Thisse B, Schilling TF, Postlethwait JH.** Structure of the zebrafish snail1 gene and its expression in wild-type, spadetail and no tail mutant embryos. *Development* 1993;119(4):1203–15.
16. **Gopinath A, Andrew Tseng L, Whitlock KE.** Temporal and spatial expression of gonadotropin releasing hormone (GnRH) in the brain of developing zebrafish (Danio rerio). *Gene Expr. Patterns* 2004;4(1):65–70.
17. **Wu S, Page L, Sherwood NM.** A role for GnRH in early brain regionalization and eye development in zebrafish. *Mol. Cell. Endocrinol.* 2006;257–258:47–64.
18. **Onuma TA, Ding Y, Abraham E, Zohar Y, Ando H, Duan C.** Regulation of Temporal and Spatial Organization of Newborn GnRH Neurons by IGF Signaling in Zebrafish. *J. Neurosci.* 2011;31(33):11814–11824.
19. **Park MK, Wakabayashi K.** Preparation of a monoclonal antibody to common amino acid sequence of LHRH and its application. *Endocrinol. Jpn.* 1986;33(2):257–272.
20. **Wegener C, Neupert S, Predel R.** Direct MALDI-TOF Mass Spectrometric Peptide Profiling of Neuroendocrine Tissue of Drosophila. In: *Recenti Progressi in Medicina*.Vol 102.; 2010:117–127.
21. **Torgersen J, Nourizadeh-Lillabadi R, Husebye H, Aleström P.** In silico and in situ characterization of the zebrafish (Danio rerio) gnrh3 (sGnRH) gene. *BMC Genomics* 2002;3(1):25.
22. **Spicer OS, Wong TT, Zmora N, Zohar Y.** Targeted mutagenesis of the hypophysiotropic Gnrh3 in zebrafish (Danio rerio) reveals no effects on reproductive performance. *PLoS One* 2016;11(6):1–22.

23. **Liu Y, Tang H, Xie R, Li S, Liu X, Lin H, Zhang Y, Cheng CHK.** Genetic evidence for multifactorial control of the reproductive axis in zebrafish. *Endocrinology* 2017;158(3):604–611.
24. **Marvel M, Spicer OS, Wong T-T, Zmora N, Zohar Y.** Knockout of the Gnrh genes in zebrafish: effects on reproduction and potential compensation by reproductive and feeding-related neuropeptides†. *Biol. Reprod.* 2018;99(3):565–577.
25. **Palevitch O, Kight K, Abraham E, Wray S, Zohar Y, Gothilf Y.** Ontogeny of the GnRH systems in zebrafish brain: In situ hybridization and promoter-reporter expression analyses in intact animals. *Cell Tissue Res.* 2007;327(2):313–322.
26. **Abraham E, Palevitch O, Gothilf Y, Zohar Y.** The zebrafish as a model system for forebrain GnRH neuronal development. *Gen. Comp. Endocrinol.* 2009;164(2–3):151–160.
27. **Yamamoto N, Parhar IS, Sawai N, Oka Y, Ito H.** Preoptic gonadotropin-releasing hormone (GnRH) neurons innervate the pituitary in teleosts. *Neurosci. Res.* 1998;31(1):31–8.
28. **Abraham E, Palevitch O, Gothilf Y, Zohar Y.** Targeted gonadotropin-releasing hormone-3 neuron ablation in zebrafish: effects on neurogenesis, neuronal migration, and reproduction. *Endocrinology* 2010;151(1):332–40.
29. **Xia W, Smith O, Zmora N, Xu S, Zohar Y.** Comprehensive Analysis of GnRH2 Neuronal Projections in Zebrafish. *Sci. Rep.* 2015;4:1–11.
30. **Tello JA, Wu S, Rivier JE, Sherwood NM.** Four functional GnRH receptors in zebrafish: Analysis of structure, signaling, synteny and phylogeny. *Integr. Comp. Biol.* 2008;48(5):570–587.
31. **Peter RE, Yu K -L, Marchant TA, Rosenblum PM.** Direct neural regulation of the teleost adenohypophysis. *J. Exp. Zool.* 1990;256(4 S):84–89.
32. **Trudeau VL.** Facing the challenges of neuropeptide gene knockouts: Why do they not inhibit reproduction in adult teleost fish? *Front. Neurosci.* 2018;12(MAY):1–8.
33. **Chang JP, Johnson JD, Sawisky GR, Grey CL, Mitchell G, Booth M, Volk MM, Parks SK, Thompson E, Goss GG, Klausen C, Habibi HR.** Signal transduction in multifactorial neuroendocrine control of gonadotropin secretion and synthesis in teleosts-studies on the goldfish model. *Gen. Comp. Endocrinol.* 2009;161(1):42–52.

34. **Dungan HM, Clifton DK, Steiner RA.** Minireview: Kisspeptin neurons as central processors in the regulation of gonadotropin-releasing hormone secretion. *Endocrinology* 2006;147(3):1154–1158.

35. **Servili A, Le Page Y, Leprince J, Caraty A, Escobar S, Parhar IS, Seong JY, Vaudry H, Kah O.** Organization of two independent kisspeptin systems derived from evolutionary-ancient kiss genes in the brain of zebrafish. *Endocrinology* 2011;152(4):1527–1540.

36. **Yosten GLC, Lyu RM, Hsueh AJW, Avsian-Kretchmer O, Chang JK, Tullock CW, Dun SL, Dun N, Samson WK.** A Novel Reproductive Peptide, Phoenixin. *J. Neuroendocrinol.* 2013;25(2):206–215.

37. **Treen AK, Luo V, Belsham DD.** Phoenixin Activates Immortalized GnRH and Kisspeptin Neurons Through the Novel Receptor GPR173. *Mol. Endocrinol.* 2016;30(8):872–888.

CHAPTER 4: DESCRIPTION OF HYPOTHALAMIC EXPRESSION OF *PHOENIXIN/SMIM20* IN ADULT ZEBRAFISH.

INTRODUCTION

Regulation of reproduction in vertebrates via the hypothalamus-pituitary-gonadal axis is controlled by hypothalamic Gonadotropin-Releasing Hormone (GnRH1). The GnRH1 peptide is secreted by neurons that reside in the preoptic area in the hypothalamus (reviewed in Stevenson et al., 2013). GnRH1 allows the synthesis of gonadotropic hormones from the anterior pituitary, stimulating the gametogenesis as well as the synthesis of the gonadal steroid hormones (reviewed in Hrabovszky and Liposits, 2013). The control of reproduction via GnRH peptide is highly conserved across vertebrate species (reviewed in Gorbman and Sower, 2003; Okubo and Nagahama, 2008).

Surprisingly in zebrafish, *gnrh1* is lost in zebrafish (Whitlock et al., 2019). Additionally, knock-outs of *gnrh2* and *gnrh3* (Spicer et al., 2016) (Liu et al., 2017) and double knock-out *gnrh2*$^{-/-}$/*gnrh3*$^{-/-}$ (Marvel et al., 2018) in zebrafish did not result in defects in fetility or reproduction. These findings are supported by our protein analyses (MALDI-TOF; OrbiTrap) suggesting that all isoforms of GnRH (GnRH1 GnRH2, and GnRH3) are absent from the hypothalamus of adult zebrafish (Ceriani, PhD Thesis; Whitlock et al., 2019). Thus, these results suggest that another mechanism, independent of GnRH and Kiss, exists for the control of reproduction in zebrafish. In considering possible candidates that may replace GnRH in the control of the hypothalamus-pituitary-gonadal axis in zebrafish, kisspeptin, a critical neuropeptide in the control of reproduction in mammals (Dungan et al., 2006), was suggested. but single or multiple knockouts of *gnrh3*-, *kiss1*, and *kiss2* did not affect fertility/reproduction (Tang et al., 2015) (Liu et al., 2017).

The recent discovery of a soluble peptide Phoenixin (PNX)/Small Integral Membrane Protein 20 (SMIM20) has shown that this peptide has the potential to regulate reproduction and is highly conserved in vertebrates including in zebrafish (Yosten et al., 2013). PNX/SMIM20 is a prohormone where two major isoforms having similar biological activity have been identified: 20 (PNX-20) and 14 (PNX-14) amino acids found in the hypothalamus and heart, respectively (Yosten et al., 2013). These isoforms are generated product of the cleavage of the C-terminal to form a pro-hormone protein call small integral membrane protein 20 (Yosten et al., 2013).

Although PNX/SMIM20 is located in several non-central nervous system (CNS) tissues, the highest peptide level was found in the hypothalamus (Yosten et al., 2013), in agreement with its potential controlling reproductive functions. PNX/SMIM20 together with its orphan G protein-coupled receptor (Gpr173) stimulate the released of luteinizing hormone (LH) (Stein et al., 2016). Intracerebroventricular injection of PNX/SMIM20 increased the plasma LH level in diestrous female rat and the LH level decrease when the Gpr173 expression was compromised (Stein et al., 2016). The increase of the LH level is through the modulation of the GnRH receptor by PNX/SMIM20 in pituitary gonadotroph cells (Yosten et al., 2013). Moreover an *in vitro* study demonstrated that the PNX/SMIM20 controls the expression of *gnrh* and *kiss* (Treen et al., 2016).

According to these results PNX/SMIM20 is a potential candidate to replace GnRH and Kiss in the control of reproduction in zebrafish. We have shown for the first time that *pnx/smim20* is expressed in the brain including the hypothalamus, thus supporting its potential role in controlling reproduction in zebrafish.

MATERIALS AND METHODS

Animals

Valparaiso wild-type fish (Whitlock lab) and Cornell wild-types strains, derived from the AB genetic background was used for all base line studies. Zebrafish were generated in Whitlock laboratory and maintained in a re-circulating system (Aquatic Habitats Inc, Ap-opka, FL) at 28°C on a light-dark cycle of 14 and 10 hours respectively. All protocols and procedures employed were reviewed and approved by the Institutional Committee of Bioethics for Research with Experimental Animals, University of Valparaiso (#BA084-2016).

Cloning of zebrafish *pnx*/*smim20*

RNA from total adult brain of zebrafish were isolated using with 1mLTrizol (Invitrogen) according to the manufacturer's instructions. RNA was treated with DNAse I Amplification grade (Invitrogen) and concentration was measured using Quant-it RNA BR Assay Kit (Invitrogen). The cDNA was synthesized according to the manufacturer's instructions from 1 µg of total RNA using SuperScript II reverse transcriptase (Invitrogen), Oligo dT (Invitrogen), RNAse Out (Invitrogen), and dNTP mix, in a final volume of 20 µL. For PCR analysis, 1 µL of cDNA was used, 10 µmol of primers forward primer, 5'- GTCCTCGAGTGAGGTGAAA -3'; reverse primer, 5' - CGGCAAAACAAAGTTACTCC- 3' (NCBI Reference Sequence: NM_001302624.1) and DreamTaq Green PCR Master Mix (Thermo Fisher Scientific), in a final volume 25 µL. The samples were incubated at 95°C for 2 min followed by 35 cycles of 30 s at 95°C, 30 s at 56°C, and 1 min. at 72°C and a final extension of 10 min at 72°C. Products were

visualized using a 3% agarose gel in TAE buffer. The amplicon was sequenced in triplicate. The deduced amino acid sequence was obtained using the online software ExPASy translate tool (https://web.expasy.org/translate/). The alignment of the sequences was performed by ClustalX2.0.

Reverse transcription-polymerase chain reaction (RT-PCR)

The procedure was previously described in "Cloning of Zebrafish smim20 protocol". RNA from total embryos 3 dpf, head of 7 dpf, head of 1 month and POA region of adult zebrafish were isolated using with 1mLTrizol (Invitrogen) according to the manufacturer's instructions. forward primer: 5'-CCTCGAGTGAGGTGAAACTGTCAA-3'; reverse primer, 5' 5'-ATCAGACCAGACCTTCACACCAAC-3´ (NCBI Reference Sequence: NM_001302624.1) were used. The samples were incubated at 95°C for 2 min followed by 35 cycles of 30 s at 95°C, 30 s at 56°C, and 1 min. at 72°C and a final extension of 10 min at 72°C. Products were visualized using a 3% agarose gel in TAE buffer.

In situ Hybridization

Adult females were sacrificed in ice water at 10 AM, decapitated and their heads were fixed in PFA 4% overnight at 4°C. The heads were decalcified in 0.2 M EDTA solution pH 7.6 for 48 h at 4°C, embedded in 1.5% agarose/5% sucrose blocks and submerged in 30% sucrose overnight at 4 °C. Blocks were frozen at -20°C with O.C.T. Compound (Tissue Tek®), then 20 µm cryostat sections were obtained. *In situ* hybridization was performed as described in Thisse et al., 1993 (Thisse et al., 1993b), using single-stranded RNA probes labeled with digoxigenin-UTP (Roche,Mannheim, Germany). The *pnx/smim20* probe was generated as described previously (Whitlock et

al., 2005), using primers to the zebrafish *pnx*/*smim20* gen (NCBI Reference Sequence: NM_001302624.1) forward primer, 5'- GTCCTCGAGTGAGGTGAAA -3'; reverse primer, 5'- CGGCAAAACAAAGTTACTCC- 3'.

Immunohistochemistry

Females adult fish 1 year old were used. Fish were sacrificed at 10 AM. Heads were fixed in 4% paraformaldehyde in PBS for 24 h at 4°C and decalcified in 0.2 M EDTA solution pH 7.6 for 48 h at 4°C. The samples were embedded in 1.5% agarose/5% sucrose blocks and submerged in 30% sucrose overnight at 4 °C. Blocks were frozen at -25°C with O.C.T. Compound (Tissue Tek®). Tissues were sectioned to 40 µm thick with cryostat. Rabbit anti-PNX (1:200, Cat N°: G-079-01. Phoenix Pharmaceuticals, Inc.) was using. The labeling was visualized using VECTASTAIN elite ABC HRP kit (Rabbit IgG. VECTOR; PK-6101) and ImmPACT® DAB Peroxidase (HRP) Substrate (VECTOR; SK-4105) or Tyramide signal Amplification Kit (Invitrogen; T20914).

Pre-absorption essay

Pre-absorption protocol used was modification according to (Cowan et al., 2015; Prinz et al., 2017; Jones et al., 2001). Briefly, 10µg of phoenixin-14 amide or phoenixin-20 amide (Phoenix Pharmaceuticals Inc.) were incubated with anti-phoenixin-14 antibody (1:200) diluted in 1% DMSO in PBS for 2 hours at RT on a rotator. The pre-absortion solution was centrifuged for 15 min at 13,000 rpm and the supernatant was suplemented with goat serum (final concentration 5%) and BSA (final concentration 1%). The pre-absortion solution was used to immnunohistochemistry in adult brain sections.

Microscopy and images processed

Bright field images were obtained with a Leica DMR microscope (Leica Microsystems CMS GmbH, Wetzlar, Germany) and a Leica DFC 480 camera (Leica Microsystems Ltd, Heerbrugg, Switzerland and processed with the Leica Application Suite 2.3.3 software (Leica Microsystems Ltd).). Fluorescent images were taken using a Spinning Disc microscope Olympus BX-DSU (Olympus Corporation, Shinjuku-ku, Tokyo, Japan) and acquired with ORCA IR2 Hamamatsu camera (Hamamatsu Photonics, Higashi-ku, Hamamatsu City, Japan). Images were acquired using the Olympus Cell-R software (Olympus Soft Imaging Solutions, Munchen, Germany) processed using the deconvolution software AutoQuantX 2.2.2 (Media Cybernetics, Bethesda, MD, USA). All images were edit using ImageJ® software (National Institute of Health, Bethesda, Maryland, USA).

RESULTS

By bioinformatic algorithm *phoenixin/smim20* in zebrafish has been identified (Yosten et al., 2013), but its expression has not described. In order to analyze the zebrafish *phoenixin/smim20* precursor, the cDNA was obtained from adult zebrafish and aligned with zebrafish *smim20* sequence (Danio rerio: NM_001302624.1) acquired from NCBI database. The alignment showed a 99% identity between sequences, with a single nucleotide difference (G/T) at position 182, producing a silent substitution (Fig. 1, A, red, asterisk). We performed an alignment of deduced zebrafish SMIM20 amino acids sequence with other species. It showed an identity of 57%, 56%, 57% and 71% with *Homo sapiens* (NP_001138904.1), *Mus musculus* (NP_001138904.1), *Gallus gallus* (NP_001138902.1) and *Scatophagus argus* (AWM96408.1), respectively (Fig. 4.1, B). As expected the highest conservation of identity was between zebrafish and Scatophagus argus (Fig. 1, B, box area, blue). The Phoenixin/SMIM20 sequences of zebrafish not have amidation signal in the C-terminal unlike of other animals (Yosten et al., 2013; Wang et al., 2018) (Fig. 1, B, rectangles), and do not share all cleavage sites with those in previously described (Yosten et al., 2013), (Fig. 1, B).

A

```
Homo sapiens              TCGGCGGGTCAG---GGCAGCCCGGGGCCTGACGCCATGTCCCGGAACCTGCGCACCGCG  24
Mus musculus              TTCGCCGGCTCTGCTGCCCCCTTTCTCTCCATGGCAGCGGCCCGGAACCTGCGCACCGCG
Gallus gallus             GCTTCCGTCCCGGACGCGGGGCGTCCCTCCGCCGCCATGGCCAGGCTGTTCCGCACGCTC
Scatophagus argus         ---TGTGAGAGCGTTACATCCGATGCAACATTTAAAATGTCCAAAAACACTAGAATAGCT
Danio rerio               ------GTCCTCGAGTGAGGTGAAACTGTCAAAATCATGTCCAGTTCTAAGAGGATAACG
                                 *                                 * **          * *

Homo sapiens              CTCATTTTCGGCGGCTTCATCTCCCTGATCGGCGCCGCCTTCTATCCCATCTACTTCCGG  84
Mus musculus              CTCATATTCGGAGGCTTCATCTCCATGGTCGGCGCCGCCTTCTATCCCATCTACTTCCGG
Gallus gallus             GTCATCTTCGGCGGCTTCGCGGCCGTGGTGGGGGCCGCCTTCTACCCCATCTACTTCCGG
Scatophagus argus         TTCATATTTGGAGGCTTTGTAACGGCTGTTGCCGCTGCATTTTACCCCATATTCTTCTAC
Danio rerio               CTCATATTTGGAGGCTTCGTTGCAGCTGTTGCTGCAGCTTTTTATCCTATATTTTTTCAT
                           **** ** ** *****     *     * *  ** ** ** ** ** ** *  **

Homo sapiens              CCCCTAATGAGATTGGAGGAGTACAAGAAGGAACAAGCTATAAATCGGGCTGGAATTGTT  144
Mus musculus              CCCCTTATGCGGCTGGAGGAATACCAGAAGGAGCAGGCTGTAAATCGAGCTGGTATTGTC
Gallus gallus             CCGCTGCTGCTGCCCGAGGAGTACAAGAGAGAACAGTCAATAAACCGAGCTGGTATTGTT
Scatophagus argus         CCGCTCGCACACAAAAACGAGTACAGAGAAGTCCAAAAGATAAACCGGACAGGAATCGAC
Danio rerio               CCTCTCACACACTCTGAAGACTACAAGCAAGTGCAGAAGGTGAACCGGGCTGGAGTCAAT
                          ** **           * ** ***      *  **     * ** **  * **  *

Homo sapiens              CAAGAGGATGTGCAGCCACCAGGGTTAAAAGTGTGGTCTGATCCATTTGGCAGGAAATGA  204
Mus musculus              CAGGAAGATGTGCAACCGCCAGGGTTGAAAGTGTGGTCTGATCCATTTGGCAGGAAATGA
Gallus gallus             CAAGAGAATATCCAGCCTCCAGGGTTAAAAGTGTGGTCTGATCCATTTGGAAGAAAGTAA
Scatophagus argus         CAAGCAGACATTCAGCCTGTGGGTGTGAAAATATGGTCTGATCCATTCAAGCCTGCAGGC
Danio rerio               CAAGCAGACATACAGCCTGTTGGTGTGAAGGTCTGGTCGGATCCCTACAAGCCCAAATCA
                          ** *   *  * ** **    **  * **  * ***** ***** *
                                                                  *

Homo sapiens              GAGGGCTGTCATCAGCTCTGATTAAGAAAGGAGATTTCTTCATGCTTTCGATTCTGCATG  264
Mus musculus              GGCTGTCAGC---AAGTCTGATGAGGAAAGTGGACGTCTTTATCCTGTGCACTCCGCAGT
Gallus gallus             TGTTGCCAGCGTGGTGCATTTCAAGGTAGAACTGAAGATGAACT---TCAATTATTTCTT
Scatophagus argus         AAATGATGGCCAGTGACGGCTCACCCTTTCACTAAC-------------------------
Danio rerio               TGACTCCTGTGATTAACTTATGGATGAAAAGGACGAATGC--------------GTCC--
```

B

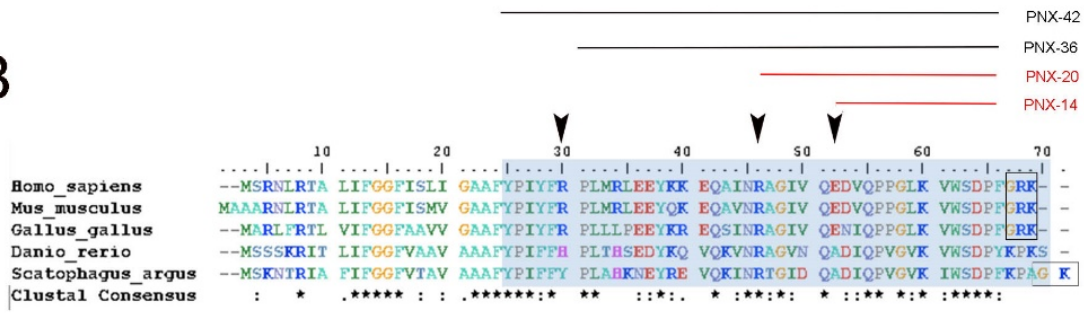

Figure 4.1. Characterization of *zebrafish phoenixin/smim20*. (A) cDNA sequence alignment of: *Homo sapiens*, *Mus musculus*, *Gallus gallus*, *Scatophagus argus*, and *Danio rerio phoenixin/smim20* indicating conservation of the start codon (orange box) and stop codon (green boxes) between zebrafish and other vertebrates. The zebrafish sequence obtained here differs at position 182 from the sequence deposited at NCBI (NM_001302624.1), where a (silent) substitution replaces the T with a G (red asterisk). **(B)** Corresponding amino acid sequence alignment of Phoenixin proteins is shown in blue. Homo sapiens, *Mus musculus*, *Gallus gallus*, and *Scatophagus argus* contain amidation sites (rectangles). Predicted (black) and confirmed (red) cleavage sites are indicated (arrowheads), produce peptides of varying amino acid lengths (top).

In order to determine whether *phoenixin/smim20* is expressed during development, we first performed RT-PCR analysis at 3 days post fertilization (dpf), 7 dpf, 1 month post fertilization (mpf) and adult hypothalamus. The *phoenixin/smim20* gene (predicted size: 214 bp) was detected the *phoenixin/smim20* transcript at four stages analyzed (Fig. 4.2). Which indicate that *phoenixin/smim20* is expressed in early in development and maintained through adulthood. To examine the distribution of *phoenixin/smim20* expression within the adult brain (n= 3 fish), *in situ* hybridization using a *phoenixin/smim20* mRNA probe in adult brain sections were performed. We found *phoenixin/smim20* expression throughout the brain including: olfactory bulb, telencephalon, tectum opticum and corpus cerebelli (Fig. 4.3, A-D). Also, the expression of *phoenixin/smim20* was localized to the periventricular hypothalamus including the ventral, caudal and dorsal zone, neurosecretory preoptic area (NPO) and pituitary (Fig. 4.3, E- H), whereas no signal was detected in brain section using *phoenixin/smim20* sense probe (Fig. 4.3, I). *In situ* hybridization performed in cross sections of the hypothalamus showed expression of *phoenixin/smim20* in NPO located mainly in magnocellular preoptic nucleus PM (Fig. 4.4, A), adjacent to the DiV (Fig. 4.4, B, arrow). As observed in sagittal sections, the *phoenixin/smim20* expression is found in periventricular hypothalamus (Fig. 4.4, C-D, arrow). Thus, our results demonstrate that the *phoenixin/smim20* is expressed in the several structures of the brain, including the hypothalamus and pituitary.

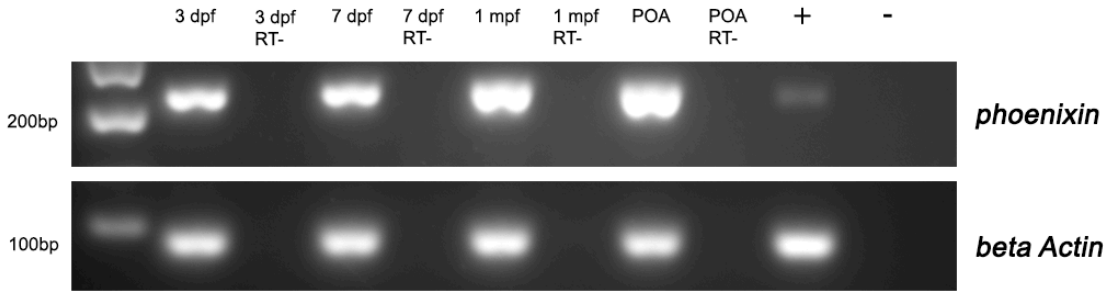

Figure 4.2. *phoenixin/smim20* is expressed in embryos and juvenile zebrafish. RT-PCR from cDNA samples of 3dpf, 7dpf, 1mpf and of the pre-optic area (POA) of adult fish. +, - : genomic DNA from POA of adult zebrafish. Housekeeping gene: *beta actin*.

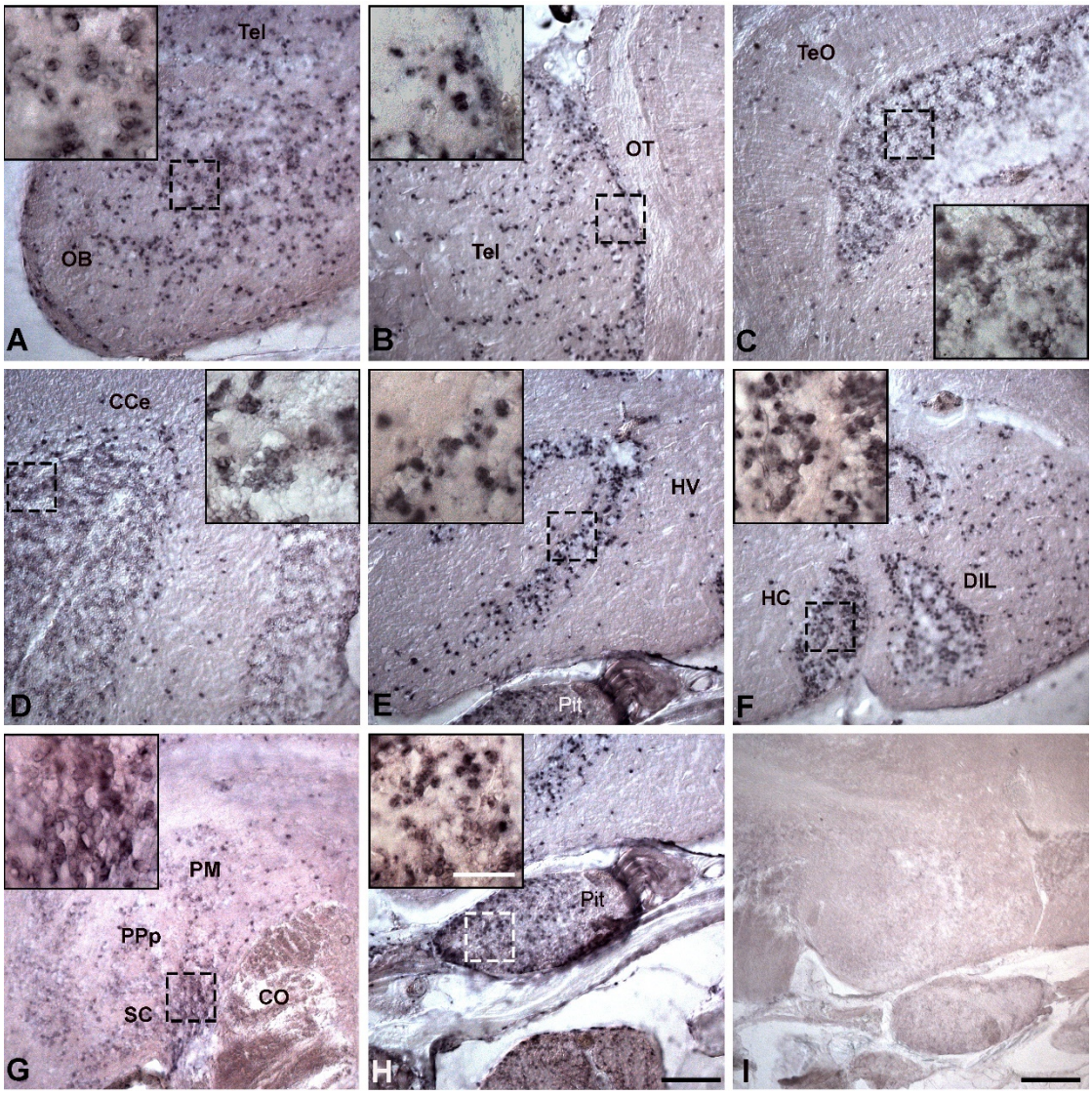
Tel
OB
A
OT
Tel
B
TeO
C
CCe
D
HV
Pit
E
HC
DIL
F
PM
PPp
SC
CO
G
Pit
H
I

Figure 4.3. *phoenixin*/*smim20* is expressed in the adult brain of zebrafish. (A-I) *In situ* hybridization using *phoenixin/smim20* probe on 20 um sagittal cryosections, anterior to the left. *phoenixin/smim20* is expressed in: **(A)** Olfactory Bulb (OB), **(B)** telencephalon (Tel), **(C)** tectum opticum (TeO), **(D)** corpus cerebelli (CCe), **(E)** ventral zone of the periventricular hypothalamus (HV), **(F)** caudal (HC) and dorsal (DIL) zones of periventricular hypothalamus, **(G)** magnocellular preoptic nucleus (PM) and parvocellular preoptic nucleus, posterior part (PPp) and suprachiasmatic nucleus (SC) and **(H)** pituitary. High-power views are shown (square). **(I)** *smim20* sense probe. High-power views are shown of box area (square). Scale bar: **(A-I)** 100 µm, box area 20 µm.

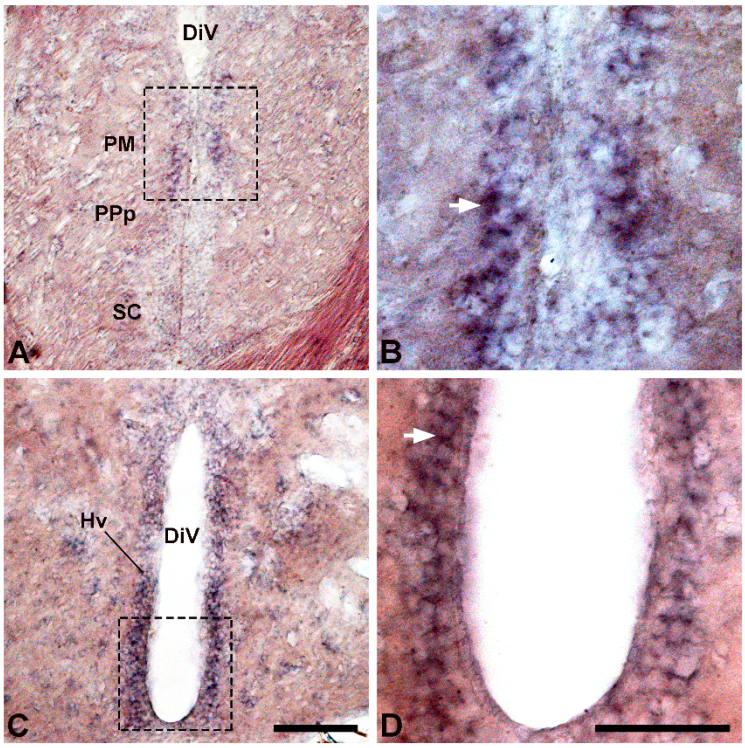

Figure 4.4. Expression of *phoenixin*/*smim20* in adult hypothalamus. (A-D) *phoenixin/smim20 expression* was found in **(A)** magnocellular nucleus (PM) of the POA (purple, box area), **(B)** magnification of box area in A, shown the cells positive to *smim20* (arrow) and **(C)** in the ventral zone of the periventricular hypothalamus (purple, boxed area), **(D)** magnification of box area in C (arrow). parvocellular preoptic nucleus, posterior part (PPp) and suprachiasmatic nucleus (SC) and diencephalic ventricle (DiV). All images are from 20 µm cryostat cross-sections of adult brain. Scale bar: **(C, D)** 50 µm.

To determine whether the protein expression replicated that of *pnx*/*smim20* expression, we used the commercially available antibody recognizing PNX in mammals (PHOENIX PHARMACEUTICALS, INC). The PNX antibody recognizes the last 14 amino acid (53-66) of the C-terminal of the human PNX, including the amide. This region is conserved across the mammals (Yosten et al., 2013), with a high identity (71%) and similarity (92%) between the region that recognizes the antibody and zebrafish sequence (Fig. 4.5). Phoenixin (PNX)-like immunoreactive cells were found NPO and pituitary (Fig. 4.6, A, arrows). In NPO, PNX-like immunoreactive cells are distributed in the magnocellular preoptic nucleus (PM), parvocellular preoptic nucleus, posterior part (PPp) and suprachiasmatic nucleus (SC) (Fig. 4.6, B, higher magnification shown in C, boxed area). The PNX-like immunoreactive cells are found adjacent to the diencephalic ventricle (DiV) (Fig. 4.6, higher magnification view shown in E, boxed area). Because the processes of PNX-like immunoreactive cells could not be discerned in brain sections processed with DAB, we performed an immunofluorescent labeling using amplified signal (TSA kit). Similar to the DAB method, we observed PNX-like immunoreactive cells in the NPO, adjacent to the DiV (Fig. 4.6, F) and PNX-like immunoreactive processes that projected towards ventral-lateral region (Fig. 4.6, F, higher magnification view shown in G, boxed area). Thus, these results show that the immunoreactivity of PNX antibody is restricted to the NPO and pituitary.

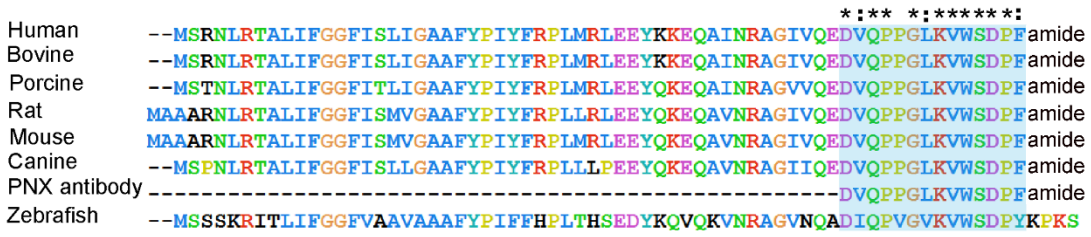

Figure 4.5. Alignment between mammals and zebrafish PNX sequence with region that recognize the PNX antibody. Commercial PNX antibody (PHOENIX PHARMACEUTICALS, INC) recognizes amidated PNX14 isoform.

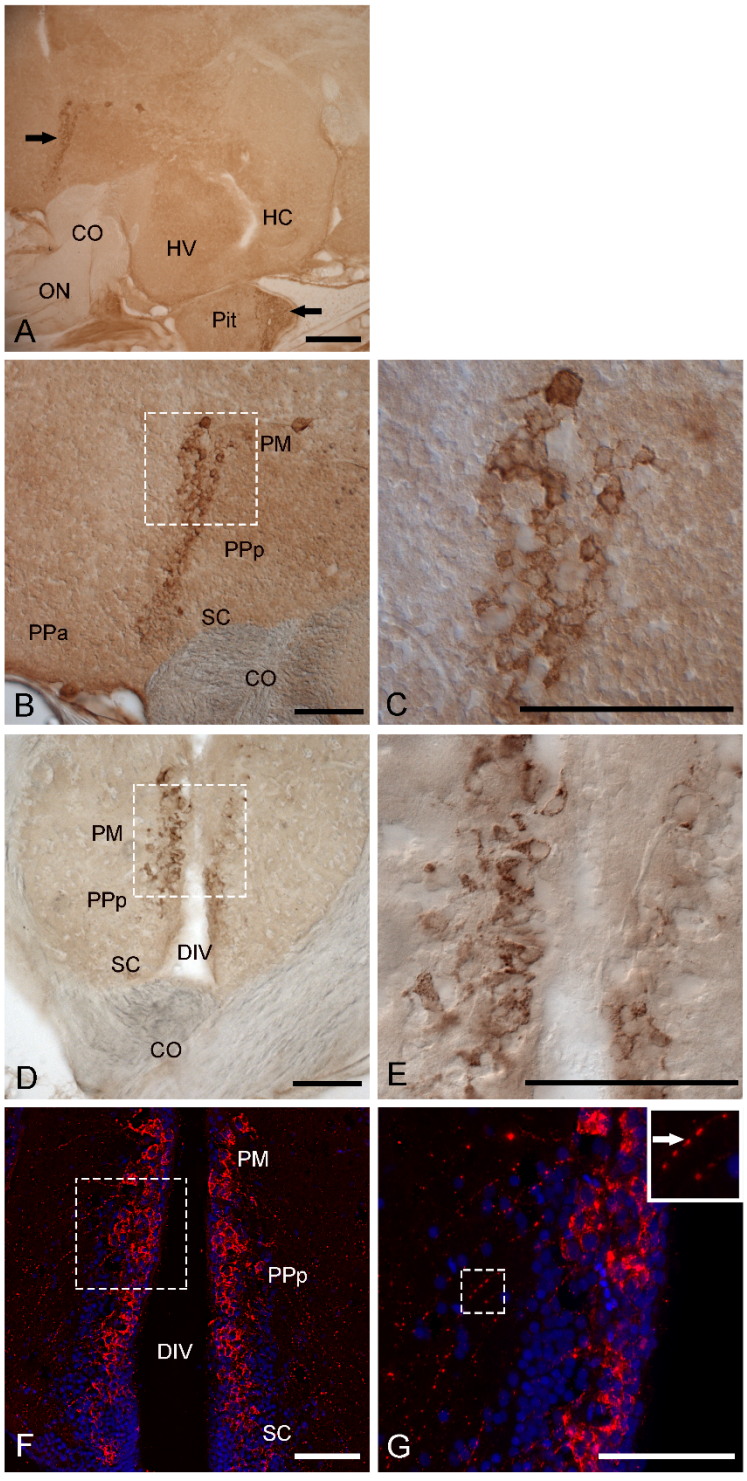
A
CO
HV
HC
ON
Pit
B
PM
PPp
PPa
SC
CO
C
D
PM
PPp
SC
DIV
CO
E
F
PM
PPp
DIV
SC
G

Figure 4.6. Phoenixin-like immunoreactive is restricted to the NPO and pituitary in the brain of adult zebrafish. (A-C) Sagittal cryosection of 40 µm of adult brain. **(A)** anti-PNX antibody expression was found in the pre-optic neurosecretory area (NPO) and pituitary (Pit) (arrows). **(B)** NPO, Phoenixin-like immunoreactive cells are located in magnocellular preoptic nucleus (PM) and parvocellular preoptic nucleus, posterior part (PPp) and suprachiasmatic nucleus (SC) (white boxed). **(C)** Magnification of the box of **(B)**. **(D, E)** Transverse section of the adult brain. **(F)** PNX-like immunoreactive cells are distribution adjacent to the diencephalic ventricle DiV and in the magnocellular preoptic nucleus PM and PPp (white arrow). **(E)** Magnification of white box of **(D)**. **(F, G)** Transversal sections were treated with TSA method. **(F)** PNX-like immunoreactive cells (red) with similar distribution as section processed with DAB. **(G)** Image from boxed region in **(F)**, show the axon of PNX-like immunoreactive cells (box). High-power views are shown (square, upper-left corner. arrow). **(F, G)** Sections were labeled with DAPI labeling (blue). Ventral zone of periventricular hypothalamus (HV), caudal zone of periventricular hypothalamus (HC), optic tract OT, optic nerve ON, chiasma opticum CO, parvocellular preoptic nucleus, anterior part (PPa). All images are from 20 um cryostat sections of adult brain. Scale bar: **(A)** 200 µm; **(B-E)** 100 µm; **(F, G)** 50 µm.

Although, PNX-like immunoreactive processes extending towards the pituitary were not observed, we detected immunoreactivity of PNX antibody in the pituitary (Fig. 4.6. A. arrow). In sagittal sections, the immunoreactivity of PNX antibody was observed in the proximal (Fig. 4.7, A, boxed 1; B arrow) and posterior (Fig. 4.7, A, boxed 2; B arrow) region of the pituitary. We found putative PNX-like immunoreactive in the structures call Hearing bodies that correspond neurosecretory terminal observed in the pituitary, have also been observed in fish (Kharat and Khillare, 2013; Ekici and Timur, 2013) (Fig. 4.7 D, E arrow), located in the neurohypophysis (NeH) as observed in section with tricromic staining (Fig. 4.7, F arrow). Similar to the proximal region, putative PNX-like immunoreactive was detected in the posterior region of the NeH (Fig. 4.7, G boxed) (Fig. 4.7, H arrow), although the hearing bodies were not observed through tricromic staining (Fig. 4.7, I), it possible that PNX-like immunoreactive correspond to hearing bodies. Therefore, this result showed that the Hearing bodies are immunoreactive to PNX antibody in the pituitary.

Due to the difference observed between *in situ* hybridization and PNX antibody, we performed antibody pre-absorption assay to determine whether the labeling was lost in pre-absorbed antibody. Sagittal sections of adult brain were incubated with antibody pre-absorbed with mammals PNX-14 and PNX-20 peptide respectively. Anti-PNX immunoreactivity was widely decreased in the NPO and the pituitary when the PNX antibody was pre-absorbed with PNX-14 (Fig. 4.8 A boxed, B boxed) and PNX-20 peptides (Fig. 4.8 C boxed, D boxed). Therefore, this result would support limited cross-reactivity of the anti-PNX antibody for zebrafish.

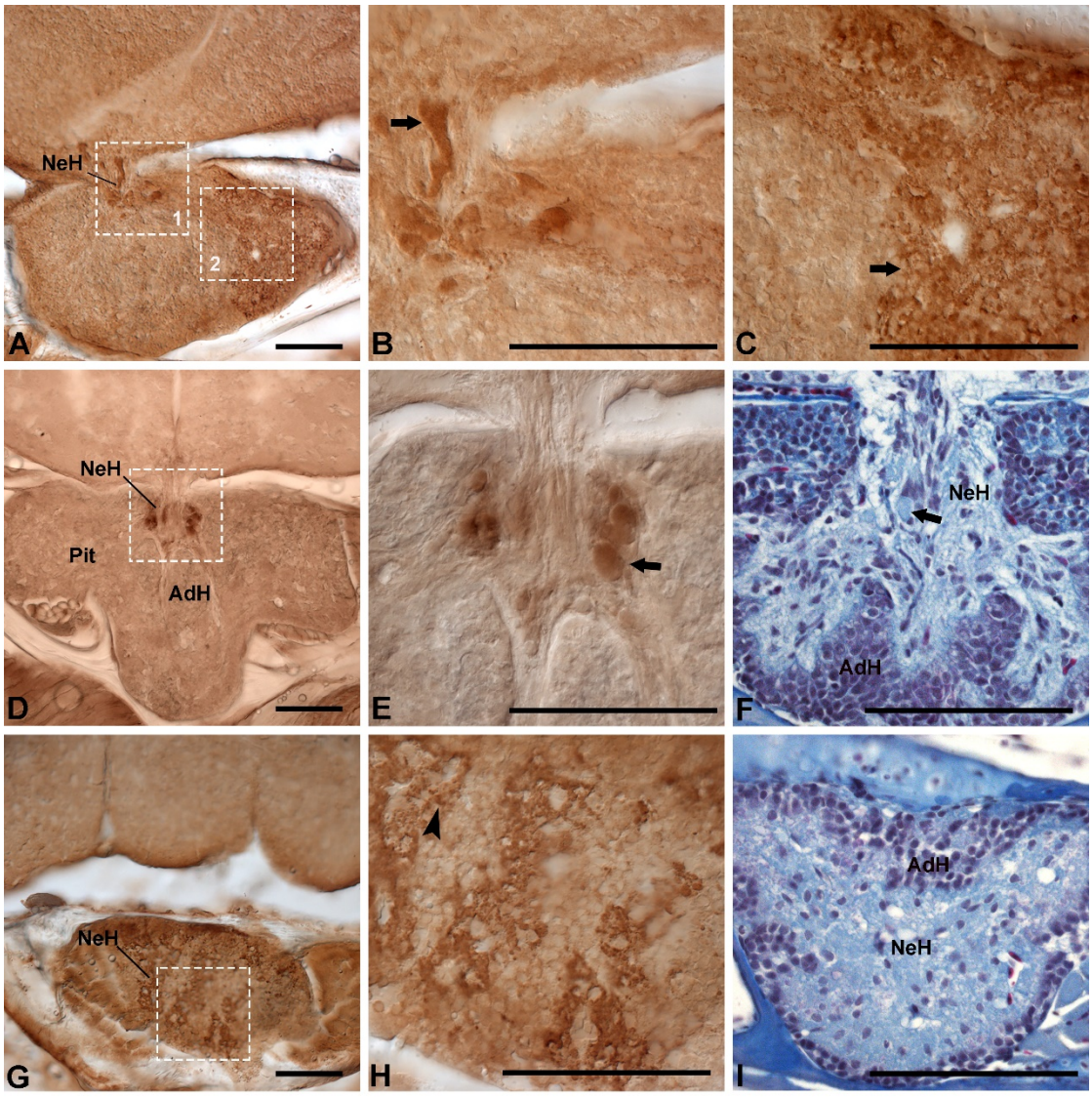
NeH
1
2
A
B
C
NeH
Pit
AdH
D
E
NeH
AdH
F
NeH
G
H
AdH
NeH
I

Figure 4.7. Phoenixin-like immunoreactive is found in the pituitary. (A-C) Sagittal section. **(A)** PNX-like immunoreactive is located in neurohypophysis (NeH) and adenohypophysis (AdH). **(B)** Magnification of boxed 1, show hearing bodies positives (arrow) and axons positive to anti-PNX antibody (arrowhead). **(C)** Magnification of box 2 demonstrates PNX-like immunoreactive in the axons and in the posterior region of the NeH. **(D-I)** Transverse view**. (D, E, G, H)** Cryosection of 20 µm **(D)** Hearing bodies positive to anti-PNX antibody are observed in the central portion of NeH and in **(E)** magnification of box of **(D)**. **(F)** Paraffin section dye with tricromic stain, shown the distribution of hearing bodies in the NeH. **(G)** PNX-like immunoreactivity is located in the posterior section of the pituitary. **(H)** Magnified image of boxed G shows vesicle positive for PNX-like immunoreactive. **(I)** Paraffin section dye with tricromic stain of the posterior section of the pituitary. Scale bar: 100 µm.

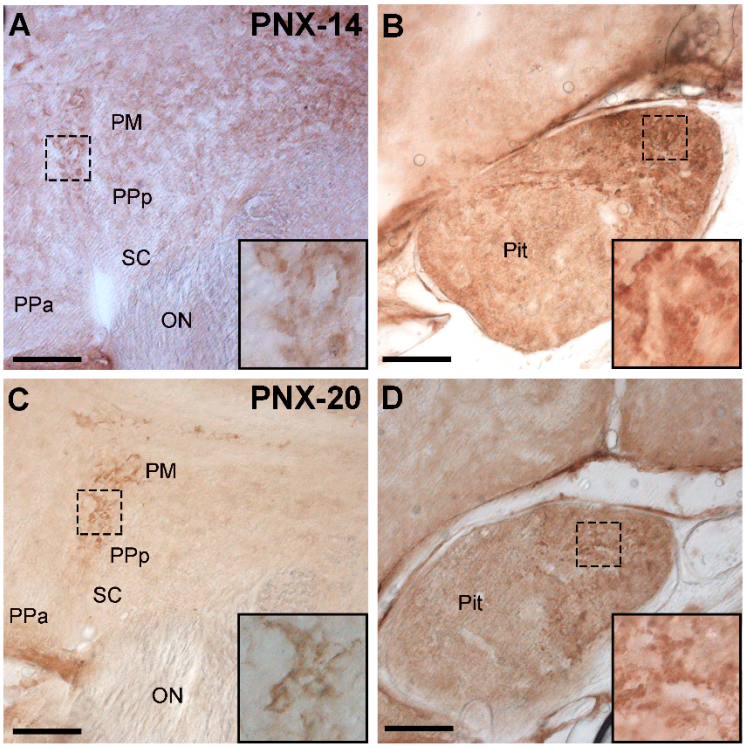

Figure 4.8. Anti-PNX pre-absorbed antibody decreased the immunolabeling in NPO and pituitary. Sagittal cryosection of 20 µm**. (A, B)** Anti-PNX antibody was pre-absorbed with PNX-14 peptide, **(A)** pre-optic neurosecretory area (NPO) and **(B)** pituitary (Pit). PNX-20 peptide was used, **(C)** pre-optic neurosecretory area (NPO) and **(D)** pituitary (Pit). High-power views are shown (boxed). magnocellular preoptic nucleus (PM) and parvocellular preoptic nucleus, posterior part (PPp), optic nerve and suprachiasmatic nucleus (SC). Scale bar: 100 µm.

DISCUSSION

In the present study, we characterized the expression of *phoenixin/smim20* in zebrafish brain. Due to its role in the regulation in GnRH, Kiss (Treen et al., 2016) and GnRH receptor (Yosten et al., 2013), triggering the release of LH in the mammals pituitary (Yosten et al., 2013), we propose that the PNX/SMIM20 could be a good candidate in the control of reproduction in zebrafish.

Although, two active isoforms PNX-14 and PNX-20 have been experimentally identified in rat (Yosten et al., 2013; Cowan et al., 2015), in zebrafish, these isoforms are still unknown. However, it has been described that intraperitoneal injection of PNX-14 and PNX-20 increase the expression of the *growth hormone-releasing hormone receptor* (*ghrhr*) and *growth hormone* (*gh*) in the pituitary and *growth hormone receptor 1* (*ghr1*) and *growth hormone receptor 2* (*ghr2*) in the liver of a teleost fish (Scatophagus argus) (Wang et al., 2018). This suggests, that both PNX isoforms could be in teleost, including in zebrafish.

Using the anti-PNX antibody, we observed immunoreactivity in the NPO (homologous to paraventricular and supraoptic nucleus in mammals) and pituitary. In the NPO, parvocellular, magnocellular, and gigantocellular neurons, these neurons release neuropeptides such as vasotocin and isotocin, that project axons directly to the neurohypophysis (Eaton et al., 2008; Almeida and Oliveira, 2015). According to its morphology and distribution in the POA, Phoenixin-like immunoreactive cells correspond to this type of neurons.

In teleost fish the neurohypophysis is localized in the distal part stalk and interdigitates with all regions of the adenohypophysis (Schreibman et al., 1973). Our results showed that anti-PNX labeling could be found in the bodies Herring located in

the neurohypophysis. These could be the neurosecretory terminal (Dellmann and Rodríguez, 1970) of hypothalamic magnocellular neurons that send axons to the neurohypophysis (Tweedle, 1983). Similar to mammals, studies have described the expression of Herring bodies in the neurohypophysis of teleost fish (Kharat and Khillare, 2013; Ekici and Timur, 2013). Based on our results, PNX/SMIM20 could also be controlling the release of LH by direct innervation of gonadotropic cells in the pituitary of zebrafish.

According to the expression differences found between the PNX antibody and *in situs* hybridization for *phoenixin/smim20*, we do not discard that the PNX antibody be unspecific, because the antibody was not made against a zebrafish protein and zebrafish PNX/SMIM20 is not amidated. Previously it has been shown by enzyme-linked immunoassay (EIA), that the anti-PNX antibody did not cross-react with the non-amidated forms of PNX-14 and PNX-20 (Yosten et al., 2013). A study performed in visceral pain in rat found that the non-amidated PNX does not have bioactivity unlike the amidated PNX (Lyu et al., 2013). While, amidation is required for the biological activity of over 50% of all peptides (Merkler, 1994) non-amidated peptides can have biological activity (Eipper et al., 1992; Kulathila et al., 1999).

In conclusion, we described the expression of *phoenixin/smim20* in developing and adult zebrafish. In the adult brain *phoenixin/smim20* is expressed in a variety of brain structures. Most importantly, *phoenixin/smim20* is expressed in hypothalamic structures: NPO, posterior hypothalamus and pituitary. Consistent with the potential role in regulating fertility and reproduction in zebrafish. This difference of expression observed between *in situ* hybridization and PNX antibody can be resolved in future studies through the generation of a zebrafish-specific anti-PNX antibody.

REFERENCES

1. **Stevenson TJ, Hahn TP, MacDougall-Shackleton SA and BG.** Gonadotropin-releasing hormone plasticity: A comparative perspective. *Front Neuroendocr.* 2013;33(3):287–300.
2. **Hrabovszky E, Liposits Z.** Afferent Neuronal Control of Type-I Gonadotropin Releasing Hormone Neurons in the Human. *Front. Endocrinol. (Lausanne).* 2013;4(September):130.
3. **Okubo K, Nagahama Y.** Structural and functional evolution of gonadotropin-releasing hormone in vertebrates. *Acta Physiol. (Oxf).* 2008;193(1):3–15.
4. **Gorbman A, Sower SA.** Evolution of the role of GnRH in animal (Metazoan) biology. *Gen. Comp. Endocrinol.* 2003;134(3):207–213.
5. **Whitlock KE, Postlethwait J, Ewer J.** Neuroendocrinology of reproduction: Is gonadotropin-releasing hormone (GnRH) dispensable? *Front. Neuroendocrinol.* 2019;(November 2018):0–1.
6. **Spicer OS, Wong TT, Zmora N, Zohar Y.** Targeted mutagenesis of the hypophysiotropic Gnrh3 in zebrafish (Danio rerio) reveals no effects on reproductive performance. *PLoS One* 2016;11(6):1–22.
7. **Liu Y, Tang H, Xie R, Li S, Liu X, Lin H, Zhang Y, Cheng CHK.** Genetic evidence for multifactorial control of the reproductive axis in zebrafish. *Endocrinology* 2017;158(3):604–611.
8. **Marvel M, Spicer OS, Wong T-T, Zmora N, Zohar Y.** Knockout of the Gnrh genes in zebrafish: effects on reproduction and potential compensation by reproductive and feeding-related neuropeptides†. *Biol. Reprod.* 2018;99(3):565–577.
9. **Dungan HM, Clifton DK, Steiner RA.** Minireview: Kisspeptin neurons as central processors in the regulation of gonadotropin-releasing hormone secretion. *Endocrinology* 2006;147(3):1154–1158.
10. **Tang H, Liu Y, Luo D, Ogawa S, Yin Y, Li S, Zhang Y, Hu W, Parhar IS, Lin H, Liu X, Cheng CHK.** The kiss/kissr systems are dispensable for zebrafish reproduction: Evidence from gene knockout studies. *Endocrinology* 2015;156(2):589–599.
11. **Yosten GLC, Lyu RM, Hsueh AJW, Avsian-Kretchmer O, Chang JK, Tullock CW, Dun SL, Dun N, Samson WK.** A Novel Reproductive Peptide, Phoenixin. *J.*

Neuroendocrinol. 2013;25(2):206–215.

12. **Stein LM, Tullock CW, Mathews SK, Garcia-Galiano D, Elias CF, Samson WK, Yosten GLC.** Hypothalamic action of phoenixin to control reproductive hormone secretion in females: importance of the orphan G protein-coupled receptor *Gpr173*. *Am. J. Physiol. - Regul. Integr. Comp. Physiol.* 2016;311(3):R489–R496.
13. **Treen AK, Luo V, Belsham DD.** Phoenixin Activates Immortalized GnRH and Kisspeptin Neurons Through the Novel Receptor GPR173. *Mol. Endocrinol.* 2016;30(8):872–888.
14. **Thisse C, Thisse B, Schilling TF, Postlethwait JH.** Structure of the zebrafish snail1 gene and its expression in wild-type, spadetail and no tail mutant embryos. *Development* 1993;119(4):1203–1215.
15. **Whitlock KE, Smith KM, Kim H, Harden M V.** A role for foxd3 and sox10 in the differentiation of gonadotropin-releasing hormone (GnRH) cells in the zebrafish Danio rerio. *Development* 2005;132(24):5491–502.
16. **Jones lW, Paul Bolam J, Wonnacott S.** Presynaptic localisation of the nicotinic acetylcholine receptor β2 subunit immunoreactivity in rat nigrostriatal dopaminergic neurones. *J. Comp. Neurol.* 2001;439(2):235–247.
17. **Prinz P, Scharner S, Friedrich T, Schalla M, Goebel-Stengel M, Rose M, Stengel A.** Central and peripheral expression sites of phoenixin-14 immunoreactivity in rats. *Biochem. Biophys. Res. Commun.* 2017;493(1):195–201.
18. **Cowan A, Lyu RM, Chen YH, Dun SL, Chang JK, Dun NJ.** Phoenixin: A candidate pruritogen in the mouse. *Neuroscience* 2015;310:541–548.
19. **Wang M, Deng SP, Chen HP, Jiang D neng, Tian CX, Yang W, Wu T li, Zhu CH, Zhang Y, Li GL.** Phoenixin participated in regulation of food intake and growth in spotted scat, Scatophagus argus. *Comp. Biochem. Physiol. Part - B Biochem. Mol. Biol.* 2018;226(August):36–44.
20. **Kharat S, Khillare YK.** Morphology and histology of pituitary gland of torrential stream fish Nemacheilus Mooreh (Sykes). *Int. J. Bioassays* 2013;2(8):1079–1084.
21. **Ekici A, Timur M.** An anatomical and histochemical examination of the pituitary gland of carp (Cyprinus carpio). *Turkish J. Vet. Anim. Sci.* 2013;37(4):399–403.
22. **Eaton JL, Holmqvist B, Glasgow E.** Ontogeny of vasotocin-expressing cells in zebrafish: Selective requirement for the transcriptional regulators orthopedia and single-minded 1 in the preoptic area. *Dev. Dyn.* 2008;237(4):995–1005.

23. **Almeida O, Oliveira RF.** Social status and arginine vasotocin neuronal phenotypes in a cichlid fish. *Brain. Behav. Evol.* 2015;85(3):203–213.
24. **Schreibman MP, Leatherland JF, Mckeown BA.** Functional morphology of the teleost pituitary gland. *Integr. Comp. Biol.* 1973;13(3):719–742.
25. **Dellmann HD, Rodríguez EM.** Herring bodies; an electron microscopic study of local degeneration and regeneration of neurosecretory axons. *Zeitschrift für Zellforsch. und Mikroskopische Anat.* 1970;111(3):293–315.
26. **Tweedle CD.** Ultrastructural Manifestations of Increased Hormone Release in the Neurohypophysis. *Prog. Brain Res.* 1983;60(C):259–272.
27. **Lyu R, Huang X, Zhang Y, Dun SL, Luo JJ, Chang J, Dun NJ.** Phoenixin: a Novel Peptide in Rodent Sensory Ganglia. *Neuroscience* 2013;250:622–631.
28. **Merkler DJ.** C-Terminal amidated peptides: Production by the in vitro enzymatic amidation of glycine-extended peptides and the importance of the amide to bioactivity. *Enzyme Microb. Technol.* 1994;16(6):450–456.
29. **Eipper BA, Stoffers DA, Mains RE.** The Biosynthesis of Neuropeptides: Peptide alpha-Amidation. *Annu. Rev. Neurosci.* 1992;15(1):57–85.
30. **Kulathila R, Merkler KA, Merkler DJ, Kulathila R.** Enzymatic formation of C-terminal amides. *Nat. Prod. Rep.* 1999;16(2):145–154.